

**THE UNIVERSITY OF CALGARY**

**Involvement of purinergic receptors in spreading depression**

**by**

**Bradley David Hampel**

**A THESIS**

**SUBMITTED TO THE FACULTY OF GRADUATE STUDIES**

**IN PARTIAL FULFILLMENT OF THE REQUIREMENTS FOR THE**

**DEGREE OF MASTER OF SCIENCE**

**DEPARTMENT OF NEUROSCIENCE**

**CALGARY, ALBERTA**

**JUNE, 1997**

**© Bradley David Hampel 1997**



National Library  
of Canada

Bibliothèque nationale  
du Canada

Acquisitions and  
Bibliographic Services

Acquisitions et  
services bibliographiques

395 Wellington Street  
Ottawa ON K1A 0N4  
Canada

395, rue Wellington  
Ottawa ON K1A 0N4  
Canada

*Your file* *Votre référence*

*Our file* *Notre référence*

The author has granted a non-exclusive licence allowing the National Library of Canada to reproduce, loan, distribute or sell copies of this thesis in microform, paper or electronic formats.

The author retains ownership of the copyright in this thesis. Neither the thesis nor substantial extracts from it may be printed or otherwise reproduced without the author's permission.

L'auteur a accordé une licence non exclusive permettant à la Bibliothèque nationale du Canada de reproduire, prêter, distribuer ou vendre des copies de cette thèse sous la forme de microfiche/film, de reproduction sur papier ou sur format électronique.

L'auteur conserve la propriété du droit d'auteur qui protège cette thèse. Ni la thèse ni des extraits substantiels de celle-ci ne doivent être imprimés ou autrement reproduits sans son autorisation.

0-612-24667-1

Canada

## Abstract

Intrinsic optical signals (IOS), associated with the change in light transmittance, and correlated with changes in cell volume, were imaged during ouabain-induced (100  $\mu\text{M}$ ) spreading depression (SD) in hippocampal slices. The kinetics of the change in IOS varied remarkably in st. radiatum (st. rad) and st. pyramidale (st. pyr): increasing to peak then decaying to baseline in st. rad., and increasing to a plateau with no decay in st. pyr. The propagation rate in CA1 averaged  $\sim 100 \mu\text{m/s}$ . The role of different neurotransmitters were determined with several antagonists. The falling phase of SD in st. rad of CA1 was delayed by  $\text{P}_{2\text{y}}$  antagonists RB-2 and suramin (concentration-dependent), and occurred independent of extracellular calcium. Therefore, during the falling phase of SD there is a calcium-influx-independent release of ATP, activation of the metabotropic  $\text{P}_{2\text{y}}$  receptor, and a subsequent decrease in the IOS correlated with a reduction in cell volume.

## **Acknowledgments**

I would like to thank Dr. Brian MacVicar for his patience, outstanding supervision, and support of my career he has provided me over the course of this project and the last two years. I also wish to thank my supervisory committee, Drs. Richard Hawkes and Ray Turner, for their valuable time, support and assistance throughout my program. In addition, I would like to thank Dr. Brian Bland for serving as an external examiner on my thesis committee.

Throughout the last two years and as a summer student I have had the pleasure of working with many talented and successful people. I wish to thank Dr. Trent Basarsky, Mr. Spencer Borg, Dr. Dennis Churchill, Dr. Valérie Crépel, Mr. Dan Doll, Dr. Steven Duffy, Dr. Paolo Federico, Dr. Douglas Fraser, Ms. Denise Feighan, Dr. Cathryn Jarvis, Mr. Michael Johns, Dr. Mel Kelly, Mr. Bill Panenka, Ms. Shelley Rybachuk, Mr. Arunas Salkauskas, Ms. Laurie Schoonveld and Dr. Sylvain Williams. I will not soon forget the insight, humour and friendship I have shared with these people. I would also like to express my sincerest thanks to Dr. Steven Duffy for his work in laying the groundwork for the imaging techniques, to Dr. Trent Basarsky for his critical comments on my thesis proposal and presentation of data, and to Mr. Michael Johns for his help in editing this manuscript.

## **Dedication**

To my parents David and Vera, and my siblings Craig and Kyla, and to little P, who have always been inspirational. A special thanks to Steffany Dupuis, who gave me unbelievable support, encouragement, and dedication so vital to the success of this project. This thesis was successfully defended on my dad's 52<sup>nd</sup> birthday, as my parents celebrate twenty-nine years of marriage. To all of those who instilled in me the passion for scientific discovery, thank you.

# Table of Contents

APPROVAL PAGE .....	ii
ABSTRACT .....	iii
ACKNOWLEDGMENTS .....	iv
DEDICATION .....	v
TABLE OF CONTENTS .....	vi
LIST OF TABLES .....	x
LIST OF FIGURES .....	xi
ABBREVIATIONS USED .....	xiv
HYPOTHESIS AND OBJECTIVES .....	xvi
<b>1 INTRODUCTION .....</b>	<b>1</b>
1.1 Features of Spreading Depression .....	1
1.2 Membrane Changes During Spreading Depression .....	2
1.3 Ionic Mechanism of Spreading Depression .....	2
1.4 Propagation of Spreading Depression .....	3
1.5 Neuroanatomy of the Hippocampal Formation .....	4
1.6 Propagation of Spreading Depression in Rat Hippocampus .....	9
1.7 Imaging of Intrinsic Optical Signals .....	9
1.8 Imaging Spreading Depression in a Submerged Imaging Chamber .....	10
1.9 Cellular Mechanisms of Intrinsic Optical Signals .....	14
1.10 Source of Intrinsic Optical Signals In a Submerged Hippocampal Slice.....	16
1.11 Structure and Function of Na <sup>+</sup> ,K <sup>+</sup> -ATPase: Binding of Ouabain .....	17
1.12 Initiation of Spreading Depression by Ouabain .....	21
1.13 Purinergic Receptors .....	27
1.14 NMDA, AMPA and Kainate Receptors: Inhibition by Selective Antagonists .....	30
1.15 Regulation of Cell Volume .....	32

1.16	Clinical Significance .....	33
	Spreading Depression as a Pathological Model for Migraines.....	33
<b>2</b>	<b>MATERIALS AND METHODS .....</b>	<b>38</b>
2.1	Tissue Preparation .....	38
2.2	Drug Application.....	38
2.3	Experimental Protocol .....	39
2.4	Imaging Techniques .....	40
2.5	Statistical Analysis and parameters of ouabain-induced spreading depression .....	41
<b>3</b>	<b>RESULTS .....</b>	<b>45</b>
3.1	Characteristics of ouabain-induced SD in the hippocampal slice .....	45
3.2	Ouabain-induced SD occurs in low calcium conditions .....	48
3.3	Suramin effects both the onset and falling phases of spreading depression .....	49
3.4	Suramin effects both the onset and falling phases of SD in 0 Ca <sup>2+</sup> conditions.....	59
3.5	Suramin in the presence of glutamatergic and GABA receptor antagonists effects the falling phase of SD .....	63
3.6	Suramin demonstrates a dose-dependent inhibition of both the onset and falling phases of spreading depression .....	69
3.7	PKC inhibition with H-7 does not effect the onset or falling phases of spreading depression .....	72
3.8	Reactive Blue 2 effects the falling phase of spreading depression, but not in the presence of NMDA, non-NMDA, and GABA receptor antagonists .....	73
3.9	PPADs effects the onset phase of spreading depression, but not in the presence of NMDA, non-NMDA and GABA receptor antagonists .....	81

3.10	Ecto-nucleotidase inhibition with AMP-PNP does not effect the onset or falling phases of spreading depression .....	89
3.11	Glibenclamide has an effect on the onset and falling phases of SD .....	92
3.12	Glibenclamide effects only the falling phase of SD in low calcium conditions .....	98
3.13	Tolbutamide does not have an effect on the onset or falling phases of SD .....	101
3.14	A slow spreading depression-like process occurs in low Na <sup>-</sup> conditions .....	101
3.15	Amiloride effects the onset phase of spreading depression .....	109
3.16	Benzamil effects the onset phase of spreading depression .....	110
3.17	P <sub>2</sub> -purinergic receptor agonists: inconclusive results.....	116
<b>4</b>	<b>DISCUSSION</b> .....	<b>119</b>
4.1	A novel mechanism for the recovery of cell volume during the falling phase of ouabain-induced spreading depression .....	119
4.2	Imaging intrinsic optical signals in the hippocampal slice: changes in cell volume .....	122
4.3	Ouabain-induced spreading depression in the hippocampal slice .....	123
4.4	P <sub>2x</sub> -purinergic receptor involvement in the onset phase of SD .....	127
4.5	P <sub>2</sub> antagonists do not slow the falling phase of SD by inhibiting ecto-nucleotidases nor by blocking GABA- and glutamate receptors .....	128
4.6	Purinergic antagonists slow the falling phase of SD by P <sub>2y</sub> -purinergic receptor blockade .....	129
4.7	Interaction of the glutamatergic and purinergic systems during SD: release of ATP or related compound .....	133
4.8	Origin of extracellular ATP: release during spreading depression .....	135
4.9	Activation of purinergic receptors and regulatory volume decrease .....	137

4.10	Role of sodium influx in SD: Implication of $\text{Na}^+/\text{Ca}^{2+}$ exchanger in the onset phase .....	140
4.11	Ouabain-induced spreading depression may lead to cell death .....	142
4.12	Decreased activity of $\text{Na}^+/\text{K}^+$ -ATPase by ouabain may result in cell death .....	143
<b>5</b>	<b>SUMMARY CONCLUSIONS</b> .....	<b>145</b>
5.1	Future Experiments .....	145
<b>6</b>	<b>LITERATURE CITED</b> .....	<b>147</b>

## List of Tables

<b>Table 1.</b>	The propagation velocities of ouabain-induced spreading depression in the hippocampus in <i>st. radiatum</i> and <i>st. oriens</i> of the CA1 .....	50
-----------------	---	----

## List of Figures

<b>Figure 1.</b>	Neuroanatomy and circuitry of the transverse hippocampal slice .....	5
<b>Figure 2.</b>	Diagram of the imaging equipment .....	12
<b>Figure 3.</b>	A schematic representation of a model for Na <sup>+</sup> ,K <sup>+</sup> -ATPase .....	18
<b>Figure 4.</b>	A model of the regenerative processes assumed to occur during ouabain-induced spreading depression .....	23
<b>Figure 5.</b>	A schematic diagram based on a theory that migraine attacks are initiated by a wave of cortical spreading depression .....	35
<b>Figure 6.</b>	A tissue transmittance profile for a control response during ouabain-induced spreading depression as measured in st. radiatum of the CA1 .....	42
<b>Figure 7.</b>	Ouabain-induced spreading depression in the hippocampal slice in control conditions .....	46
<b>Figure 8.</b>	Low extracellular calcium slows the onset phase but not the falling phase in st. radiatum of the CA1 during ouabain-induced spreading depression .....	52
<b>Figure 9.</b>	Ouabain-induced spreading depression in the hippocampal slice in the presence of suramin .....	55
<b>Figure 10.</b>	Suramin slows both the onset and falling phases in st. radiatum of the CA1 during ouabain-induced spreading depression .....	57
<b>Figure 11.</b>	A comparison of the changes in tissue transmittance during ouabain-induced spreading depression in 0 Ca <sup>2+</sup> conditions and in the presence of suramin .....	61
<b>Figure 12.</b>	Suramin slows both the onset and falling phases in st. radiatum of the CA1 during ouabain-induced spreading depression in low calcium conditions .....	64
<b>Figure 13.</b>	A comparison of the tissue transmittance during ouabain-induced spreading depression in control conditions and in MK-801, CNQX, and bicuculline, with and without suramin .....	67

<b>Figure 14.</b> Suramin in the presence of MK-801, CNQX, and bicuculline slowed both the onset and falling phases of ouabain-induced SD in a concentration-dependent manner .....	70
<b>Figure 15.</b> H-7 does not effect the falling phase in st. radiatum of the CA1 during ouabain-induced spreading depression in the presence of GABA- and glutamatergic antagonists .....	74
<b>Figure 16.</b> Ouabain-induced spreading depression in the hippocampal slice in the presence of RB-2 .....	76
<b>Figure 17.</b> RB-2 slows the falling phase but not the onset phase of ouabain-induced spreading depression in st. radiatum of the CA1 .....	79
<b>Figure 18.</b> RB-2 in the presence of GABA- and glutamatergic antagonists, does not effect the falling phase of ouabain-induced spreading depression in st. radiatum of the CA1 .....	82
<b>Figure 19.</b> Ouabain-induced spreading depression in the hippocampal slice in the presence of PPADs .....	84
<b>Figure 20.</b> PPADs slows the onset phase, but not the falling phase of ouabain-induced spreading depression in st. radiatum of the CA1 .....	87
<b>Figure 21.</b> PPADs, in the presence of GABA- and glutamatergic antagonists, does not effect the onset phase of ouabain-induced spreading depression in st. radiatum of the CA1 .....	90
<b>Figure 22.</b> AMP-PNP does not effect either the onset or falling phase of ouabain-induced spreading depression in st. radiatum of the CA1 .....	93
<b>Figure 23.</b> Glibenclamide slows both the onset and falling phases in st. radiatum of the CA1 during ouabain-induced spreading depression .....	96
<b>Figure 24.</b> Glibenclamide slows the falling phase in st. radiatum of the CA1 during ouabain-induced spreading depression in low calcium conditions .....	99
<b>Figure 25.</b> Tolbutamide does not effect either the onset or falling phases of ouabain-induced spreading depression in st. radiatum of the CA1 .....	102
<b>Figure 26.</b> Low sodium conditions slows both the onset and falling phases in st. radiatum of the CA1 during ouabain-induced spreading depression .....	105

<b>Figure 27.</b> Ouabain-induced spreading depression in the hippocampal slice in low sodium conditions .....	107
<b>Figure 28.</b> Amiloride slows the onset phase but not the falling phase of ouabain-induced spreading depression in st. radiatum of the CA1 .....	111
<b>Figure 29.</b> Benzamil slows the onset phase but not the falling phase of ouabain-induced spreading depression in st. radiatum of the CA1 .....	114
<b>Figure 30.</b> A novel mechanism proposed to describe the cell volume recovery during the falling phase in st. radiatum of the CA1 during ouabain-induced spreading depression .....	120
<b>Figure 31.</b> A simplistic model to describe the series of events which contributes to cellular swelling during the onset phase of ouabain-induced spreading depression .....	124

## Abbreviations Used

aCSF	artificial cerebrospinal fluid
ADP	adenosine 5'-diphosphate
ADP $\beta$ S	adenosine 5'-O-(2-thiodiphosphate)
AMPA	$\alpha$ -amino-3-hydroxy-5-methyl-4-isoxazolepropionic acid
AMP-PNP	adenylyl-imidodiphosphate
AP5	2-amino-5-phosphonopentanoic acid
APV	L-2-amino-5-phosphonovaleric acid
ATP	adenosine 5'-triphosphate
$^{\circ}\text{C}$	degrees centigrade
CA	cornu Ammonis
$[\text{Ca}^{2+}]_o$	extracellular calcium
cAMP	cyclic adenosine monophosphate
$[\text{Cl}^-]_o$	extracellular chloride
CCD	charge coupled device
CNQX	6-cyano-7-nitroquinoxaline-2,3-dione
CNS	central nervous system
CPP	( $\pm$ )-3-(2-Carboxypiperazin-4-yl)-propyl-1-phosphonic acid
CSD	cortical spreading depression
DMSO	dimethyl sulfoxide
EGTA	ethyleneglycol-bis( $\beta$ -aminoethylether)-N,N,N',N'-tetra-acetate
GABA	$\gamma$ -aminobutyric acid
Hz	hertz
IOS	intrinsic optical signal
$[\text{K}^+]_o$	extracellular potassium
$[\text{K}^+]_i$	intracellular potassium
LT	light transmittance
MK-801	(+)-5-methyl-10,11-dihydro-5H-dibenzo[a,d]cyclo-hepten-5,10-imine maleate
min	minute
ml	millilitre
mm	millimeter
mM	millimolar
ms	millisecond
mV	millivolt
$[\text{Na}^+]_i$	intracellular sodium
$[\text{Na}^+]_o$	extracellular sodium
nm	nanometer
nM	nanomolar
NMDA	N-methyl-D-aspartate
NMDG	N-methyl-D-glucamine

NPPB	5-Nitro-2-(3-phenylpropylamino)benzoic acid
μm	micrometre
μM	micromolar
P <sub>1</sub>	purinergic receptor
P <sub>2x</sub>	ionotropic purinergic receptor
P <sub>2y</sub>	metabotropic purinergic receptor
P <sub>2u</sub>	metabotropic purinergic receptor
PCP	phencyclidine
PKC	protein kinase C
PLC	phospholipase C
PPADs	pyridoxal phosphate 6-azophenyl-2'-4'-disulphonic acid
RB-2	reactive blue 2
rCBF	regional cerebral blood flow
RVD	regulatory volume decrease
RVI	regulatory volume increase
s	second
SD	spreading depression
st.	stratum
TTX	tetrodotoxin

## Hypothesis and Objectives

Previous work in our laboratory has demonstrated that spreading depression (SD) is associated with a propagating wave-like transient increase in light transmittance that can be initiated spontaneously with the application of ouabain. The release of ATP has been demonstrated following Schaffer collateral stimulation in the hippocampal slice, and therefore the hypothesis of this thesis was:

**Hypothesis:** During ouabain-induced spreading depression (SD) in the rat hippocampal slice, there is a release of ATP, resulting in P<sub>2</sub> purinergic receptor activation during the wave of SD.

Preliminary experiments utilizing suramin, a non-selective P<sub>2x</sub> and P<sub>2y</sub> antagonist, in the presence of ouabain-induced SD, indicated that P<sub>2</sub> purinergic receptors may play a role in SD. Thus, the objectives of this thesis were:

- Objectives:**
- 1) To determine if purinergic receptors play a role in ouabain-induced SD
  - 2) To determine if the removal of extracellular calcium effects ouabain-induced SD
  - 3) To investigate possible mechanisms of Na<sup>+</sup> influx during the onset phase of SD

# 1 INTRODUCTION

## 1.1 Features of Spreading Depression

Spreading depression (SD) was first observed and described in detail in the rabbit cerebral cortex (Leão, 1944, 1947). Cortical spreading depression (CSD) has since been induced in the cortex, hippocampus and retina (Van Harreveld, 1978) of a variety of species (Bures *et al.*, 1974; Snow *et al.*, 1983). SD has been found to be more easily initiated in rodents than in primates, although no class of mammal is “immune”. Among regions of the central nervous system (CNS), susceptibility to SD decreases in the following order: hippocampus (primarily CA1), neocortex, subcortical nuclei, brainstem gray matter, cerebellar cortex (Bures *et al.*, 1974) and spinal cord (Czéh and Somjen, 1990; Somjen *et al.*, 1992).

Spreading depression is a chain of events which can be initiated by a number of mechanical, electrical and chemical stimuli (Bures *et al.*, 1974; Somjen *et al.*, 1992). SD, as its name suggests, is a slowly propagating wave of cortical depolarization, which “spreads” or propagates from its initiation site as a concentric wave. The initial wave of depolarization leads to depression of neuronal activity, and propagates in all directions without relation to neuronal pathways (Leão, 1944; Moskowitz, 1984). SD propagates at a rate of 1.5-7.5 mm/min, although slightly faster in hippocampus relative to neocortex, and moves through gray matter exclusively (Somjen *et al.*, 1992). SD usually halts at the border of white matter and does not penetrate glial scar tissue (Somjen *et al.*, 1992).

## 1.2 Membrane Changes During Spreading Depression

One of the earliest discoveries was that there is a negative shift of extracellular potential with spreading depression (Leão, 1947). The amplitude of this shift, determined to be at least 10 mV (Hansen, 1985) and typically 15-35 mV, is far greater than other extracellular signals which rarely exceed 2 mV. For this reason, it was hypothesized that a voltage of that magnitude would only be generated by the simultaneous depolarization of many cells at or near the recording electrode. Intracellular recordings confirmed a depolarization of both neurons and glial cells (Collewijn and Van Harreveld, 1966; Higashida *et al.*, 1974; Sugaya *et al.*, 1975). Additionally, the input resistance of depolarizing neurons decreased to or below the detection limit of the method (Mody *et al.*, 1987; Haglund and Schwartzkroin, 1990).

Electrical impedance of the tissue during SD was found to increase, as measured with extracellular electrodes (Van Harreveld and Ochs, 1957; Marshall, 1959). This increase in tissue impedance during SD has been attributed to cell swelling (Van Harreveld and Khattab, 1967). In addition, there is a loss of neuronal membrane resistance (Somjen *et al.*, 1992), which is in itself consistent with the depolarization of neurons and redistribution of ions (Reviewed in Somjen *et al.*, 1992).

## 1.3 Ionic Mechanism of Spreading Depression

Intracellular recordings have shown that during SD neuronal and glial membranes depolarize to ~0 mV and then slowly recover within 1-3 min (Collewijn and Van Harreveld, 1966; Higashida *et al.*, 1974; Sugaya *et al.*, 1975). During the peak of SD depolarization, neuronal action potentials are completely inactivated (Snow *et al.*, 1983). However, intense transient spike activity occurs both before and afterward (Sugaya *et al.*, 1975; Snow *et al.*, 1983).

The depolarization during spreading depression results in a change in the distribution of ions between the intra- and extracellular compartments. Sodium, calcium and chloride enter together with water, resulting in a decrease in the size of the

extracellular space to approximately half, while potassium and hydrogen ions leave the cell (Kraig and Nicholson, 1978; Hansen, 1985). During SD there is a rapid rise of extracellular potassium,  $[K^+]_o$ , from 3 to as high as 60 mM (Hansen, 1985). In addition, the decrease in extracellular sodium  $[Na^+]_o$ , chloride  $[Cl^-]_o$  and calcium  $[Ca^{2+}]_o$  is similar to that observed during anoxia (Hansen, 1985). Most ion concentrations (Kraig and Nicholson, 1978) and the size of the extracellular space recover spontaneously after 30-60 s, but the calcium and pH levels may take a few more minutes to recover.

#### 1.4 Propagation of Spreading Depression

One of the earliest discoveries of spreading depression was that it could be initiated by glutamate (Van Harreveld, 1959). In addition to glutamate, aspartate, and agonists of the glutamate subtype receptors (N-methyl-D-aspartate (NMDA), quisqualate, and kainate) also trigger CSD (Van Harreveld, 1959; Curtis and Watkins, 1963; Bures *et al.*, 1974; Lauritzen *et al.*, 1988). NMDA was determined to be 100 times more potent than glutamate in initiating SD (Curtis and Watkins, 1963). The cortex is known to release excitatory amino acids, including glutamate (Van Harreveld and Fifková, 1971; Fabricius *et al.*, 1993), during spreading depression, but typically the increase is brief, lasting for only approximately one minute (Van Harreveld and Kooiman, 1965).

Propagation of CSD is independent of the vascular system, as cortical, hippocampal, cerebellar and retinal nervous tissues support CSD *in vitro* (Bures *et al.*, 1974). Cortical SD is blocked by various competitive and non-competitive NMDA antagonists (Hernández-Cáceres *et al.*, 1987; Mody *et al.*, 1987; Lauritzen *et al.*, 1988; Marrannes *et al.*, 1988, Avoli *et al.*, 1991; Lauritzen and Hansen, 1992) but not by antagonists of non-NMDA glutamate receptors (Lauritzen and Hansen, 1992). Specifically, the NMDA antagonists kynurenic acid, MK-801, and AP5 (2-amino-5-phosphonopentanoic acid) have been shown to block SD (Lauritzen and Hansen, 1992; Sheardown, 1993; Nedergaard *et al.*, 1995).

Additionally, action potentials blocked with a local application of tetrodotoxin (TTX) do not affect the propagation of SD (Sugaya *et al.*, 1975).

There is currently no explanation of the spreading mechanism of SD, but it has been hypothesized that the spread most likely involves the diffusion of one or more chemical mediators, perhaps  $K^+$  or glutamate in the extracellular compartment (Van Harreveld, 1978). It has been observed that the propagation of calcium waves mediated by gap junctions in glial cell cultures is similar to the spread of SD (Charles *et al.*, 1990; Cornell-Bell *et al.*, 1990; Nedergaard *et al.*, 1995). In a recent study, SD was examined in the isolated chicken retina, a preparation in which the rate and extent of propagation is analogous to that of cortical gray matter (Martins-Ferreira and de Oliveira-Castro, 1966; Nedergaard *et al.*, 1995). It was demonstrated, in this preparation, that waves of SD are blocked by inhibitors of gap junctions (Nedergaard *et al.*, 1995). For this reason it has been hypothesized that gap junction-mediated intercellular diffusion is necessary for the generation of SD (Nedergaard *et al.*, 1995). Previous findings in our laboratory have combined optical imaging with calcium imaging using the intracellular calcium-sensitive dye, Fura-2, in hippocampal slices. It was found that there is a calcium wave propagating slightly ahead in time of the intrinsic SD wavefront. This calcium wave has been postulated to occur in glial cells, and may in fact underlie SD (Duffy and MacVicar, personal communication).

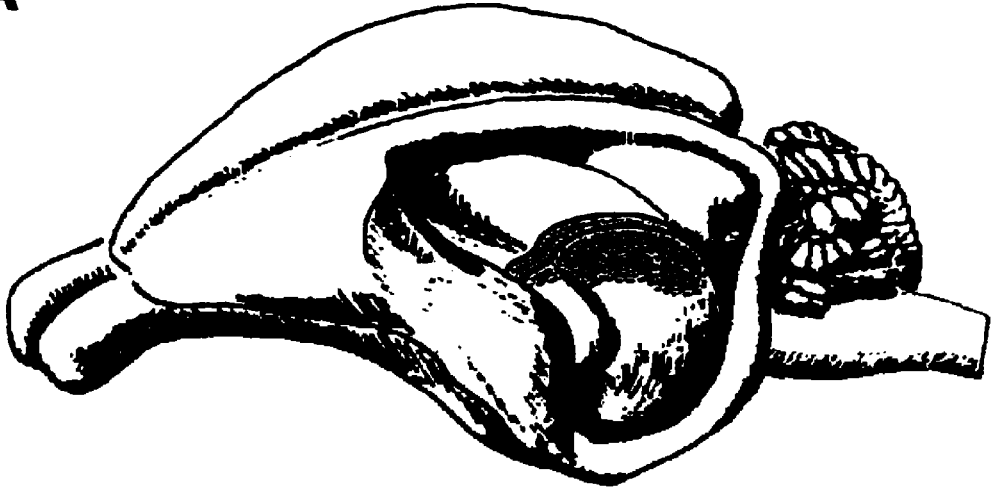
## 1.5 Neuroanatomy of the Hippocampal Formation

'Hippocampus' means 'seahorse', and over four-hundred years ago, in 1587, the medieval anatomist Arantius named the hippocampus because of its resemblance in gross anatomical terms to the sea creature (Rosene and Van Hoesen, 1987). Figs. 1A and 1B (Andersen *et al.*, 1971) are lateral views of the brain with the parietal and temporal neocortex removed to expose the hippocampal formation. The hippocampal formation in rodents is C-shaped, curving both laterally and ventrally (Fig. 1A). The hippocampal formation contains six cytoarchitecturally distinct regions.

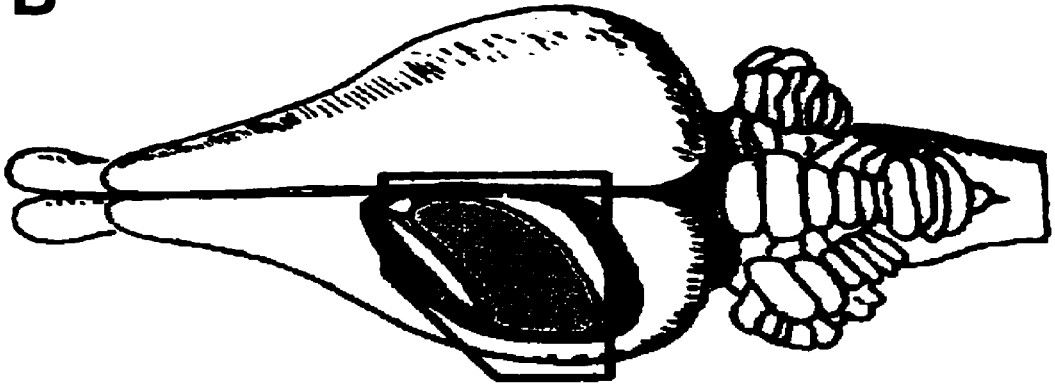
**Figure 1.** Neuroanatomy and circuitry of the transverse hippocampal slice (modified from Andersen *et al.*, 1971, inset from MacVicar and Hochman, 1991).

**A)** The grayed C-shaped hippocampus is exposed in a lateral view of the brain with the parietal and temporal neo-cortex removed. **B)** A diagram of the brain as viewed from above with the neo-cortex removed to expose the left hippocampal formation. **C)** A diagram of an enlarged hippocampal slice revealing the intrinsic circuitry in the CA1 and CA3 fields. The trisynaptic circuit is shown with the perforant pathway (PP) input to a granule cell (GC) in the dentate gyrus; mossy fiber (MF) input to a pyramidal cell in the CA3 region; and Schaffer collateral (Sch.) input to a pyramidal cell in the CA1 region. The CA1 region is demarcated by a box and is shown in expanded scale in the inset, demonstrating the stratum oriens, pyramidale, radiatum, and lacunosum-moleculare.

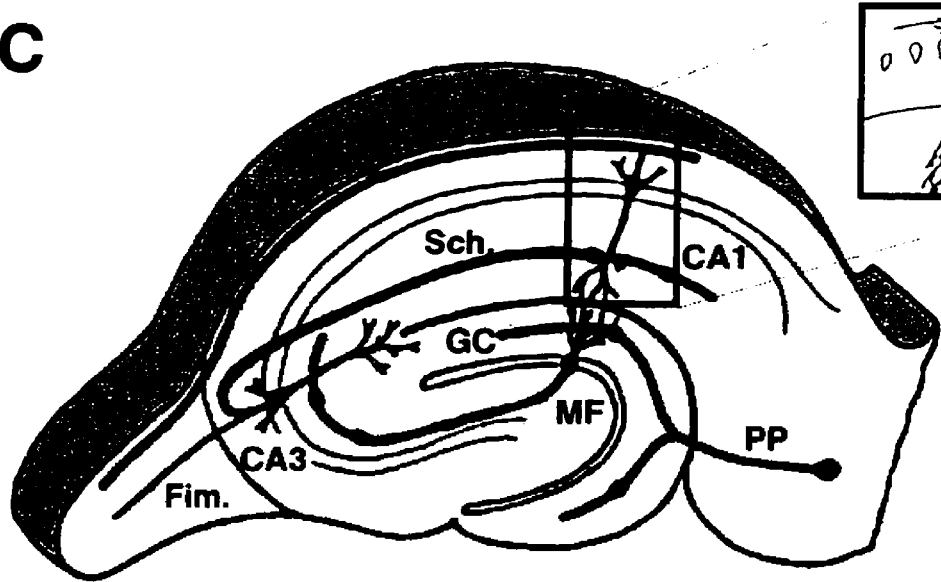
**A**



**B**



**C**



Oriens  
Pyramid  
Radiatur  
Lacunos  
Molecul

These include the hippocampus (or hippocampus proper), the dentate gyrus, subiculum, presubiculum, parasubiculum, and entorhinal cortex. The subiculum, presubiculum and parasubicular regions together constitute the subicular complex.

The hippocampus, or hippocampus proper, can be subdivided into two major regions: a large-celled proximal region and smaller-celled distal region. These two regions, regio inferior and regio superior, were named in pioneering studies in 1911 by Ramón y Cajal (Amaral and Witter, 1995). However, they will be referred to in this thesis by the more common terminology proposed by Lorente de Nó in 1933 (Amaral and Witter, 1995). de Nó divided the hippocampus into three cornu Ammonis (CA) fields; the CA1, CA2, and CA3. The CA1 field is equivalent to the regio superior, and the CA3 and CA2 fields are equivalent to the regio inferior (Amaral and Witter, 1995).

Sectioning the hippocampus perpendicular to the long axis reveals three major regions of the hippocampal formation: the hippocampus proper, dentate gyrus and subicular complex (Fig. 1C). The circuitry is organized on a plane perpendicular to the long axis and thus displays a laminar organization. The hippocampus proper is defined by a single layer of pyramidal neurons, termed stratum pyramidale. The primary neuronal cell in the hippocampus is the pyramid-shaped pyramidal cell. These cells vary in size and are characterized by a basal dendritic tree, an axon which extends into stratum oriens, and an apical dendritic tree which extends to the hippocampal fissure. The various sizes of this cell type define the subregions of cornu Ammonis. There are two regions on either side of stratum pyramidale which contain the apical and basal pyramidal cell dendrites: stratum oriens in the basal zone, and stratum radiatum in the apical zone. Proximal to stratum oriens is the alveus, followed by a layer of myelinated axons named the fimbria. Distal to stratum pyramidale and proximal to stratum radiatum is stratum lacunosum-moleculare.

The dentate gyrus is composed of three layers: proximal to the hippocampal fissure is the relatively cell-free molecular layer (stratum moleculare), then the principal cell layer, the granular cell layer (stratum granulosum) and finally the polymorphic layer (hilus). The principal cell type of the dentate gyrus is the granule cell.

These cells have an elliptical body, and a characteristic cone-shaped tree of spiny dendrites with branches directed towards the molecular layer.

Traditionally, the intrinsic connectivity of the hippocampal formation has been described as a trisynaptic circuit, although this disregards many of the longitudinal and local circuit interactions. The major intrinsic connections of the hippocampus are illustrated in Fig. 1C. There are reciprocal connections from the entire cortical region to the entorhinal cortex (Swanson and Köhler, 1986). The entorhinal cortex in turn provides the dentate gyrus with its major input via the perforant pathway (Fig. 1C). The granule cells of the dentate gyrus give rise to distinctive unmyelinated axons, which Ramón y Cajal named mossy fibers (Amaral and Witter, 1995). These fibers form the mossy fiber pathway and project from the dentate gyrus to the CA3 field of the hippocampus.

The CA3 and CA2 pyramidal cells give rise to projections to all portions of the hippocampus (Ishizuka *et al.*, 1990). The projections from CA3 to CA1 are called Schaffer collaterals, and from CA3 to CA2 are called associational connections. Another connection arises from the entorhinal cortex and innervates the CA1 field of the hippocampus. In addition, connections from the entorhinal cortex innervate the entire length of the dentate gyrus and CA1 (O'Mara, 1995). There are also projections from CA3 to CA1, and recurrent collaterals from CA3 (O'Mara, 1995), and a strong cross-commissural connection to the contralateral CA3 field.

The CA1 field in addition to projecting back to the entorhinal cortex also projects to the subiculum, from which further projections travel to the entorhinal cortex and the rest of the cortical region. One of the major extrinsic projections of the hippocampus, the fornix, arises from projections from both the CA1 and subiculum. This fiber bundle travels on to midline thalamic structures such as the mammillary bodies. There are also reciprocal connections from these structures back onto the CA1 and subiculum.

## 1.6 Propagation of Spreading Depression in Rat Hippocampus

Recurrent waves of spreading depression in the CA1 region of the rat hippocampus have been induced by microdialysis of high-K<sup>+</sup> solution. Waves emanated from the high-K<sup>+</sup> focus and traveled the length of the hippocampus in both rostral and caudoventral directions (Somjen *et al.*, 1992). The propagation velocity of SD waves was measured simultaneously in stratum radiatum and stratum pyramidale of the CA1 by two sets of double microelectrodes (Somjen *et al.*, 1992). SD appears to move semi-independently in the two layers even though stratum pyramidale and stratum radiatum contain the somata and dendrites of the same pyramidal cells (Somjen *et al.*, 1992).

The velocity of propagation was not the same in the two layers and varied from trial to trial (Somjen *et al.*, 1992). Additionally, when SD was initiated electrically in the CA3 field, the wave occasionally moved in opposite directions in the two adjacent layers (Somjen *et al.*, 1992).

Finally, in the presence of CPP (an NMDA receptor antagonist), propagation occurred in one layer and not the other (Somjen *et al.*, 1992). For these reasons, it is clear that SD can propagate among parts of the same cell, and in addition can move from dendrite to dendrite without involving somata, or from soma to soma independently of the dendrites (Somjen *et al.*, 1992).

## 1.7 Imaging of Intrinsic Optical Signals

Optical recordings of voltage-sensitive dyes have been employed in a variety of studies (Blasdel and Salama, 1986; Gainer *et al.*, 1986; Grinvald *et al.*, 1986; Frostig *et al.*, 1990). The imaging of changes in membrane potential in CNS preparations with fast voltage sensitive dyes was found to be distorted by much slower intrinsic signals (Grinvald *et al.*, 1982; Salzberg *et al.*, 1985). In fact, a study by Blasdel and Salama (1986) observed an intrinsic optical signal which they did not find useful, and as a consequence they attributed their findings to changes in the voltage-sensitive dye (Grinvald *et al.*, 1986).

This was disputed by Grinvald *et al.* (1986), who found evidence for a large intrinsic optical signal generated in the absence of any dye.

Imaging with voltage-sensitive dyes poses two major disadvantages. The first is that voltage-sensitive dyes can be potentially toxic to the tissue, and the second is that dye-photobleaching can occur to the extent that the tissue is not sufficiently stained.

Intrinsic changes in optical properties during activity in excitable tissues were first described several decades ago (Hill and Keyens, 1949). Such activity-dependent changes in intrinsic optical signals (IOS) have been employed in numerous preparations, such as crab nerves (Hill and Keyens, 1949), olfactory nerves (Kauer, 1991), cerebral cortical slices (Lipton, 1973; Holthoff *et al.*, 1994), hippocampal slices (MacVicar and Hochman, 1991; Andrew and MacVicar, 1994; Kreisman *et al.*, 1995), isolated whole brain preparations (Federico *et al.*, 1994) and *in vivo* in both animals (Grinvald *et al.*, 1986) and humans (MacVicar *et al.*, 1990; Haglund *et al.*, 1992). Imaging changes in IOS has several advantages when compared to imaging optical signals from voltage-sensitive dyes. The first is that the measurement of IOS is less invasive and the second is that problems of dye bleaching do not exist (Grinvald *et al.*, 1986; Lieke *et al.*, 1989; Frostig *et al.*, 1990). The major disadvantage of intrinsic optical imaging is that more time is required to generate optical signals. Voltage-sensitive dyes require a time resolution of often less than 1 ms (Grinvald *et al.*, 1986), while imaging intrinsic optical signals may require a longer time depending on the wavelength (Grinvald *et al.*, 1986; Lieke *et al.*, 1989; Frostig *et al.*, 1990).

### **1.8 Imaging Spreading Depression in a Submerged Imaging Chamber**

Hippocampal brain slices were introduced in the 1960's (Yamamoto and McIlwain, 1966) and because of their unique neuronal circuitry proved to be an ideal model for studying neurophysiological and biophysical neuronal properties, membrane excitability, and ion channel regulation (Skrede and Westgaard, 1971; Dingledine *et al.*, 1980). The hippocampal formation can be cut into thin slices (250-500  $\mu\text{m}$ ) in a manner

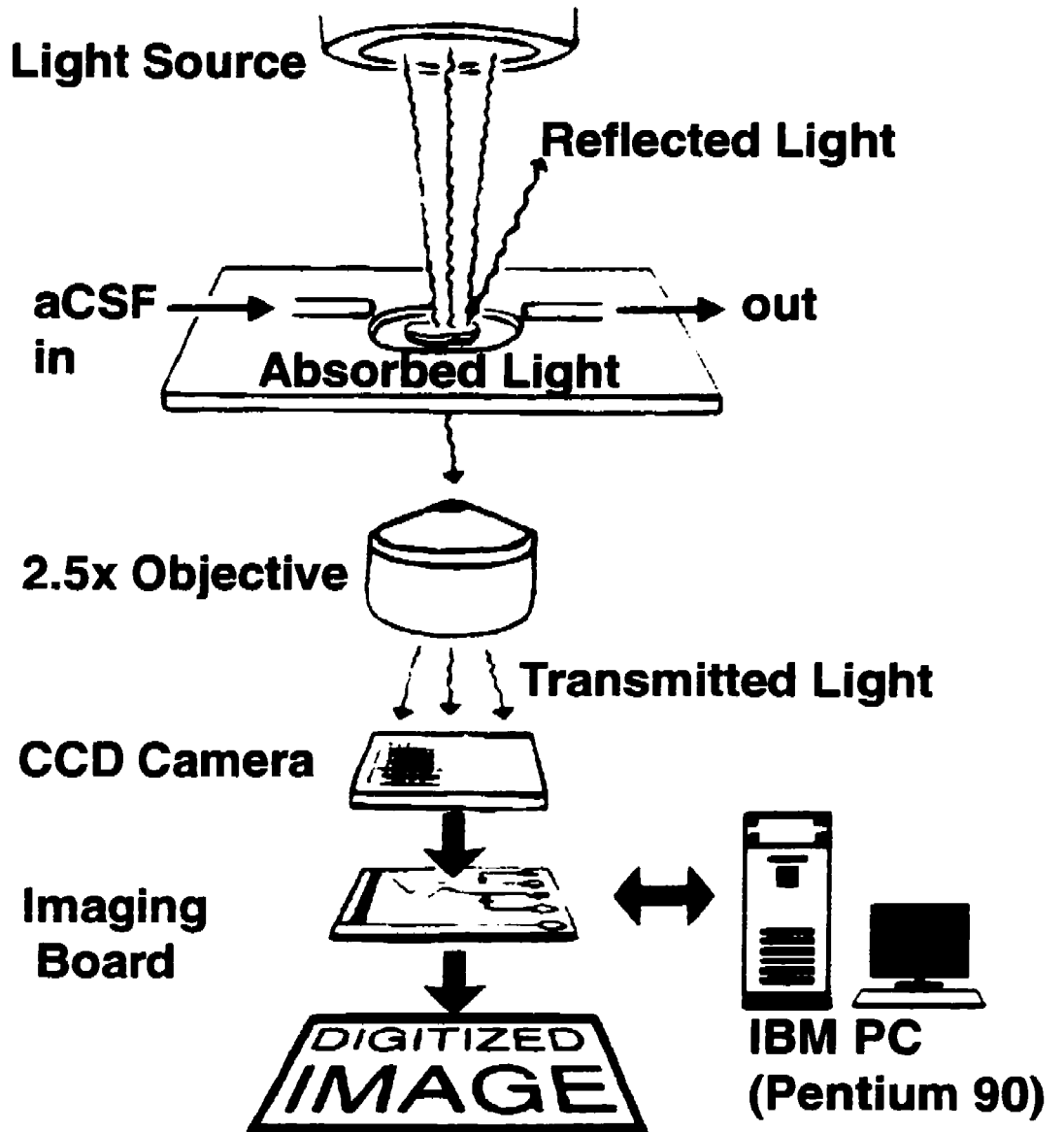
which both preserves the anatomical organization of the tissue and produces 5-7 analogous slices (Skrede and Westgaard, 1971; Dingledine *et al.*, 1977), shown in Fig. 1C. The hippocampal slice was characterized as an *in vitro* model for future studies on SD (Snow *et al.*, 1983).

There are two general methods of imaging the changes in IOS in a hippocampal slice: i) interfaced slices in an interface chamber and ii) submerged slices in an imaging chamber. SD has been imaged in both submerged (Martins-Ferreira and de Oliveira Castro, 1966; Lipton, 1973) and interface chambers (Snow *et al.*, 1983), and light transmittance changes consistently but in the opposite direction in the two preparations. These changes in light scattering were attributed to increased cellular volume and decreased extracellular space during SD (Van Harreveld, 1958; Van Harreveld and Khattab, 1967; Phillips and Nicholson, 1979), as light scattering is altered in several preparations by conditions known to change cell volume (Martins-Ferreira and de Oliveira Castro, 1966; Lipton, 1973; McManus *et al.*, 1993).

A relatively recent study examined the differences in the *direction* of IOS change between the interface chamber and submerged preparations, and determined that the direction of optical responses depends on the position of the slice relative to the surface of the bathing medium (Kreisman *et al.*, 1995). In slices positioned at the interface, a decrease in light transmittance in hypo-osmotic medium is observed and using submerged slices, an increase in light transmittance is observed, consistent with the findings of several studies (Martins-Ferreira and de Oliveira Castro, 1966; Lipton, 1973; Andrew and MacVicar, 1994). In addition, it was shown with spectrophotometric measurements that light absorbance by intrinsic chromophores does not contribute to the optical signals induced by changes in cell volume (Kreisman *et al.*, 1995).

A diagram of the imaging equipment for a submerged slice preparation is presented in Fig. 2 (adapted from Andrew *et al.*, 1997). Light emitted from the light source is either reflected, absorbed, or transmitted by the tissue. The transmitted light is collected through the objective and digitized using a CCD camera. Two factors affect the transmittance of

**Figure 2.** A diagram of the imaging equipment (Adapted from Andrew *et al.*, 1997). The light emitted from the light source will either be reflected, absorbed or transmitted. The transmitted light passes through the objective and is digitized by a CCD camera. The digital signal passes to the imaging board and into the IBM-PC compatible P90 computer for display on the monitor and storage on the hard drive.



light through tissue: absorbance and scattering. In a submerged slice preparation, tissue absorbance can be assumed to be negligible, as the spectral transmittance is unaffected by intrinsic chromophores (Kreisman *et al.*, 1995).

The remaining factors affecting light transmittance are presented in the equation:

$$\Delta T_{\text{net}} = \Delta T_{\text{scatter}} - \Delta T_{\text{reflection/refraction}}$$

where  $\Delta T_{\text{net}}$  is the net change in transmittance of light through the tissue during ouabain-induced SD,  $\Delta T_{\text{scatter}}$  is the change in transmittance due to light scattering by the tissue, and  $\Delta T_{\text{reflection/refraction}}$  is the change due to changes in reflection/refraction of the bath level in the imaging chamber (Kreisman *et al.*, 1995). The influx of water into cells during ouabain-induced SD would decrease the scattering of light by bringing the transparency of cells closer to that of the aqueous medium (Martins-Ferreira and de Oliveira Castro, 1966; Lipton, 1973; MacVicar and Hochman, 1991). Therefore, transmittance ( $\Delta T_{\text{scatter}}$ ) would increase during ouabain-induced SD. Consequently, for a net increase ( $\Delta T_{\text{net}}$ ) to occur,  $\Delta T_{\text{reflection/refraction}}$  should not change, as  $\Delta T_{\text{reflection/refraction}}$  is dependent on the shape of the meniscus and level of the bath in the imaging chamber. If these parameters remain constant, the optics of the system will not change, and the net change in transmittance will depend solely on the change in transmittance due to light scattering by the tissue.

## 1.9 Cellular Mechanisms of Intrinsic Optical Signals

The cellular mechanisms underlying intrinsic optical signals are not precisely understood. Intrinsic optical signals are activity-dependent optical changes in neuronal tissue and are postulated to result from three main sources (Ebner and Chen, 1995): i) activity-induced changes in light scattering, ii) alterations in the absorption or fluorescence by intrinsic chromophores, iii) changes in blood flow volume and oxygen delivery.

Activity-induced changes in light scattering have been attributed to cellular swelling (Cohen, 1973; La Manna *et al.*, 1987; MacVicar and Hochman, 1991). In the hippocampal slice, MacVicar and Hochman (1991) postulated that astrocyte swelling resulting from the uptake of  $K^+$  released extracellularly from neurons may make a major contribution to the intrinsic optical signal. The increased cell size would decrease light scattering and reflectance (Ebner and Chen, 1995) and increase light tissue transmittance (Cohen, 1973; Lipton, 1973). In the neurohypophysis, neurosecretion has been related to changes in light scattering since  $Ca^{2+}$  antagonists block these optical signals (Salzberg *et al.*, 1985; Obaid *et al.*, 1989). Additionally, rapid changes in orientation of membrane dipoles during action potentials in *Aplysia* neurons in culture (Stepnoski *et al.*, 1991) may underlie fast light scattering changes.

Alterations in the absorption or fluorescence by intrinsic chromophores may contribute to the generation of intrinsic optical signals (Jöbsis, 1977; Jöbsis *et al.*, 1977; La Manna *et al.*, 1987). Chromophores such as hemoglobin, cytochromes, and the reduced form of nicotinamide adenine dinucleotide may be involved (Jöbsis, 1977; Jöbsis *et al.*, 1977; La Manna *et al.*, 1987). Federico *et al.* (1994) found evidence that cytochrome-related signals may contribute significantly to reflectance changes in the isolated guinea pig brain *in vivo*. Additionally, in the hippocampal slice, cytochrome absorption maxima were observed when reflectance changes were measured by spectrophotometry (Fujii, 1991). In contrast, no similar wavelength dependence was observed in the hippocampal slice when transmittance changes were measured (MacVicar and Hochman, 1991; Kreisman *et al.*, 1995).

Changes in blood flow and or oxygen delivery will not contribute to the generation of an intrinsic optical signal in an isolated hippocampal slice, although they may contribute to the generation of intrinsic optical signals *in vivo* (Grinvald *et al.*, 1986; Frostig *et al.*, 1990).

### 1.10 Source of the Intrinsic Optical Signals In a Submerged Hippocampal Slice

Several studies have imaged intrinsic optical signals in submerged rat hippocampal slices (MacVicar and Hochman, 1991; Andrew and MacVicar, 1994; Kreisman *et al.*, 1995; Andrew *et al.*, 1996; Polischuk and Andrew, 1996b; Andrew *et al.*, 1997). In an early study, a change in light transmittance was observed during synaptic activation of Schaffer collaterals of the CA1. It was found that repetitive synaptic activity resulted in an increase in light tissue transmittance in CA1 stratum radiatum (MacVicar and Hochman, 1991). The optical changes were inhibited by blocking synaptic transmission with a  $\text{Ca}^{2+}$ -free EGTA perfusate, furosemide (an anion transport inhibitor), or by reducing extracellular  $\text{Cl}^-$  (MacVicar and Hochman, 1991). As a result, it was suggested that increased  $\text{Cl}^-$  transport may generate the optical signals due to refractive decreases associated with cell swelling (MacVicar and Hochman, 1991).

In another study, a brief exposure to hypo-osmotic aCSF elevated tissue transmittance consistently and reversibly in most regions of the hippocampal slice, most notably in the dendritic region (radiatum) of the CA1 (Andrew and MacVicar, 1994). To test the hypothesis that the increase in tissue transmittance can be attributed to cellular swelling and hence correlated with cell volume, the response of the hippocampal slice to hypo-osmotic saline was studied in the presence of TTX and  $0\text{-Ca}^{2+}$  aCSF (Andrew and MacVicar, 1994). Neither treatment altered the change in transmittance, suggesting a process independent of both synaptic transmission and neuronal activity. In addition, hyper-osmotic aCSF consistently lowered light transmittance, and glycerol, which is cell permeant, did not have an effect (Andrew and MacVicar, 1994).

Changes in tissue transmittance in the hippocampal slice were also observed in response to NMDA, kainate (Andrew *et al.*, 1996), and domoate, an excitatory amino acid with structural similarities to glutamate (Polischuk and Andrew, 1996b). The largest changes in light tissue transmittance were observed in st. radiatum and st. oriens of the CA1 (Andrew *et al.*, 1996), suggesting that in regions with high numbers of NMDA and

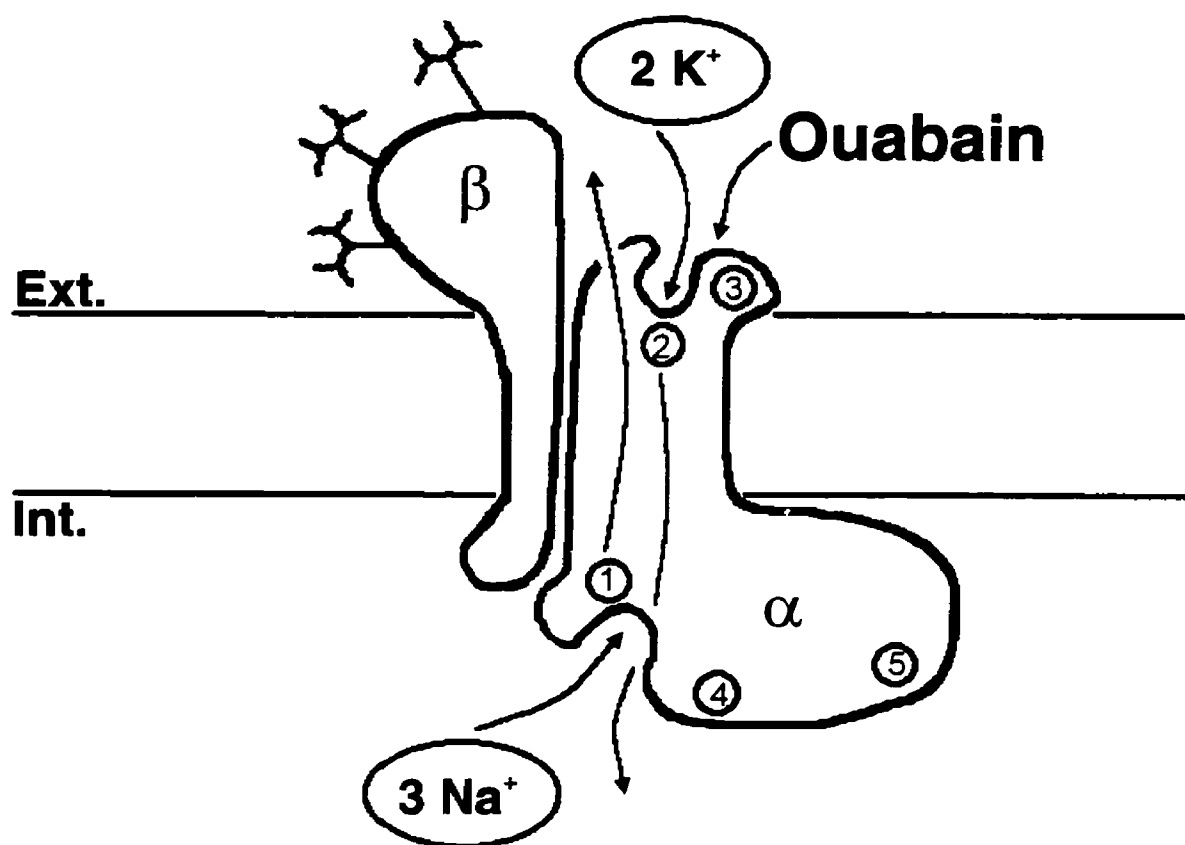
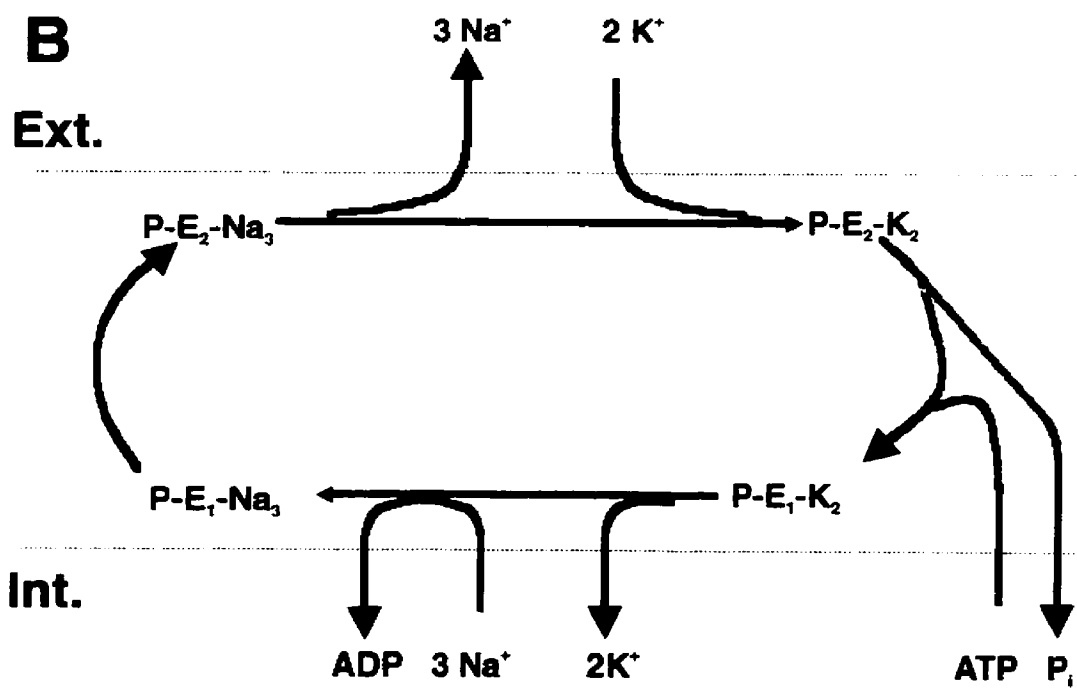
AMPA receptors, activation leads to  $\text{Na}^+$  influx, followed by  $\text{Cl}^-$  and water, causing significant swelling and corresponding changes in light tissue transmittance (Andrew *et al.*, 1996; Polischuk and Andrew, 1996b). Increased light tissue transmittance across the submerged brain slice directly correlates with cell swelling (Andrew and MacVicar, 1994; Andrew *et al.*, 1996; Holthoff and Witte, 1996) consistent with the findings of several other studies (MacVicar and Hochman, 1991; McManus *et al.*, 1993; Kreisman *et al.*, 1995).

### 1.11 Structure and Function of $\text{Na}^+, \text{K}^+$ -ATPase: Binding of Ouabain

One of the most important and ubiquitous ion pumps in animal tissues, including the brain, is the ouabain-inhibitable sodium/potassium pump (Lees, 1991; Kanzaki *et al.*, 1992; Lees and Leong, 1994). This membrane-bound enzyme couples the free energy found within the ATP molecule to the translocation of  $\text{Na}^+$  and  $\text{K}^+$  across the cellular membrane ( $\text{Na}^+, \text{K}^+$ -ATPase) (Horisberger *et al.*, 1991; Lees, 1991). The stoichiometry of the Na/K exchange is  $3 \text{Na}^+ : 2 \text{K}^+$ , and hence the Na,K-pump is termed electrogenic. In neurons,  $\text{Na}^+, \text{K}^+$ -ATPase is critical for the maintenance of the ionic gradients underlying the regulation of resting membrane potential (Horisberger *et al.*, 1991; Lees, 1991; Lees, 1993) and the restoration of transmembrane gradients following neuronal excitation. In addition, the sodium gradient maintained by the pump is used as a source of energy for other mechanisms such as the sodium/calcium exchange and the uptake of organic compounds (Horisberger *et al.*, 1991; Lees, 1993).  $\text{Na}^+, \text{K}^+$ -ATPase is also important in the regulation of transmembrane ion fluxes and cell volume (Horisberger *et al.*, 1991; Lees, 1991; Lees 1993).

A general model for  $\text{Na}^+, \text{K}^+$ -ATPase is presented in Fig. 3A, with the extracellular ouabain-binding site indicated. The enzyme consists of a heterodimer of  $\alpha$  and  $\beta$  subunits (Fig. 3A) with isoenzyme forms composed of three different  $\alpha$  ( $\alpha 1$ ,  $\alpha 2$ ,  $\alpha 3$ ) and three different  $\beta$  ( $\beta 1$ ,  $\beta 2$ ,  $\beta 3$ ) subunits (Horisberger *et al.*, 1991).

**Figure 3.** A schematic representation of a model for the  $\text{Na}^+$ ,  $\text{K}^+$ -ATPase. **A)** The  $\alpha,\beta$  heterodimer is presented with binding sites for  $\text{Na}^+$  (1),  $\text{K}^+$  (2), ouabain (3), phosphorylation (4) and the ATP binding site (5). **B)** A simplified scheme for the  $\text{Na}^+$ ,  $\text{K}^+$ -ATPase cycle. In the  $E_1$  conformation, the cation-binding sites face the cytoplasm, whereas in the  $E_2$  conformation they face the extracellular space. Ouabain binds only to the  $E_2$  state, preferentially to the  $P-E_2\text{-Na}_3$  state.

**A****B**

The  $\text{Na}^+/\text{K}^+$ -ATPase cycle is illustrated in Fig. 3B. This reaction involves a series of interconversions between two main enzyme conformations:  $E_1$  with a high affinity for ATP and  $\text{Na}^+$ , and  $E_2$  with a high affinity for  $\text{K}^+$ . In the  $E_1$  conformation of the enzyme, the cation-binding sites face the cytoplasm, whereas in the  $E_2$  conformation they face the extracellular space (Horisberger *et al.*, 1991). Ouabain binds preferentially to the  $E_2$  state, probably more specifically to the  $\text{P-E}_2\text{-Na}_3$  state (Yoda and Yoda, 1982; Swann, 1983). The combination of an  $\alpha$  and  $\beta$  subunit can hydrolyze ATP and undergo  $E_1$ - $E_2$  transition (Fig. 3B). Although both glial and neuronal cells have the  $\text{Na}^+/\text{K}^+$ -ATPase, they may differ in their expression of the isoenzymes.

Differences in ouabain sensitivity between different tissue types, for example the kidney and brain, have been described (Horisberger *et al.*, 1991). In rats and mice, so-called ouabain-insensitive species, the brain enzyme has a high affinity ( $\sim 10$  nM), similar to that observed in other ouabain-sensitive species (Horisberger *et al.*, 1991). The existence of several different isoenzymes, and range of sensitivity in different tissues and cell types to inhibitors such as ouabain, have led to the hypothesis that glycoside sensitivity is determined by the  $\alpha$  subunit isoform.

The dose-inhibition curve for ouabain in the rat brain is biphasic, suggesting two levels of inhibition and two types of binding sites with different affinities (Horisberger *et al.*, 1991). Using dose-response curves and binding assays with rat brain membranes, three components of ouabain inhibition with  $K_i$ s of 0.02, 0.5, and 320  $\mu\text{M}$  were determined (Berrebi-Bertrand *et al.*, 1990), indicating two high affinity and one low affinity site (Horisberger *et al.*, 1991).

The isoenzymes containing the high-affinity ouabain binding sites ( $\alpha_2$  and  $\alpha_3$  forms) are the most prevalent in neurons (Lees, 1991), and complete neuronal tissue demonstrated both low and high affinity ouabain sensitivity, while cultured glial cells, which express only the  $\alpha_1$  isoform, had only the low affinity component (Marks and Seeds, 1978). The isoenzyme  $\alpha_1$ , with between 100 and 1000 times lower affinity for ouabain, is present in both neuronal and glial cells (Marks and Seeds, 1978; Sweadner, 1979; Hauger

*et al.*, 1985; Antonelli *et al.*, 1989; Guillaume *et al.*, 1990; McGrail *et al.*, 1991). The high-affinity  $\alpha 3$  isoenzyme may be specific for neurons, and it has been suggested that glial cells under certain conditions can express the high-affinity isoenzyme  $\alpha 2$  (Atterwill *et al.*, 1984; McGrail *et al.*, 1991).

$\text{Na}^+/\text{K}^+$ -ATPase has a ubiquitous distribution in neurons throughout the brain, although regional differences in concentration do exist (Lees, 1991). Glial cells throughout the brain have been demonstrated to contain high levels of  $\text{Na}^+/\text{K}^+$ -ATPase (Stahl, 1986). In the hippocampus, the CA3 region has higher  $\text{Na}^+/\text{K}^+$ -ATPase activity than the CA1 region (Haglund *et al.*, 1985).

### 1.12 Initiation of Spreading Depression by Ouabain

Ouabain (3-[(6-Deoxy- $\alpha$ -L-mannopyranosyl)oxy]-1,5,11, $\alpha$ ,14,19-pentahydroxycard-20(22)-enolide) is a selective  $\text{Na}^+/\text{K}^+$ -ATPase inhibitor obtained from the seeds of *Strophanthus gratus* (Merck Index 11th Ed., No. 6854). A ouabain-like compound has been found endogenously within animal tissues (Hamlyn *et al.*, 1991). As a result of brain insults such as ischaemia, hypoglycemia, and seizure activity, there is the production or release of compounds inhibiting  $\text{Na}^+/\text{K}^+$ -ATPase (Lees, 1991). Ouabain binds specifically to  $\text{Na}^+/\text{K}^+$ -ATPase and is a potent inhibitor of its activity (Albers *et al.*, 1968; Kanzaki *et al.*, 1992).

The *in vitro* hippocampal slice allows an opportunity to study two distinct cell populations. The first, the CA1 region, is relatively prone to SD, and the second, the CA3, is relatively SD-resistant (Haglund and Schwartzkroin, 1990). The differences between the two regions in their resistance to SD can be attributed to differences in the  $\text{Na}^+/\text{K}^+$ -ATPase activity. It has been demonstrated that  $\text{Na}^+/\text{K}^+$ -ATPase activity is higher in the CA3 than in the CA1 (Haglund and Schwartzkroin, 1984, 1990; Haglund *et al.*, 1985). For this reason, it has been suggested that  $\text{Na}^+/\text{K}^+$ -ATPase plays a role in preventing SD in the CA3 region (Haglund and Schwartzkroin, 1990). In addition, there is a tendency for  $[\text{K}^+]_o$  to rise higher in the CA1 than in other regions of the hippocampal slice (Kawasaki *et al.*,

1990), making this region of the hippocampus more vulnerable to spreading depression (Kreisman and Smith, 1993).

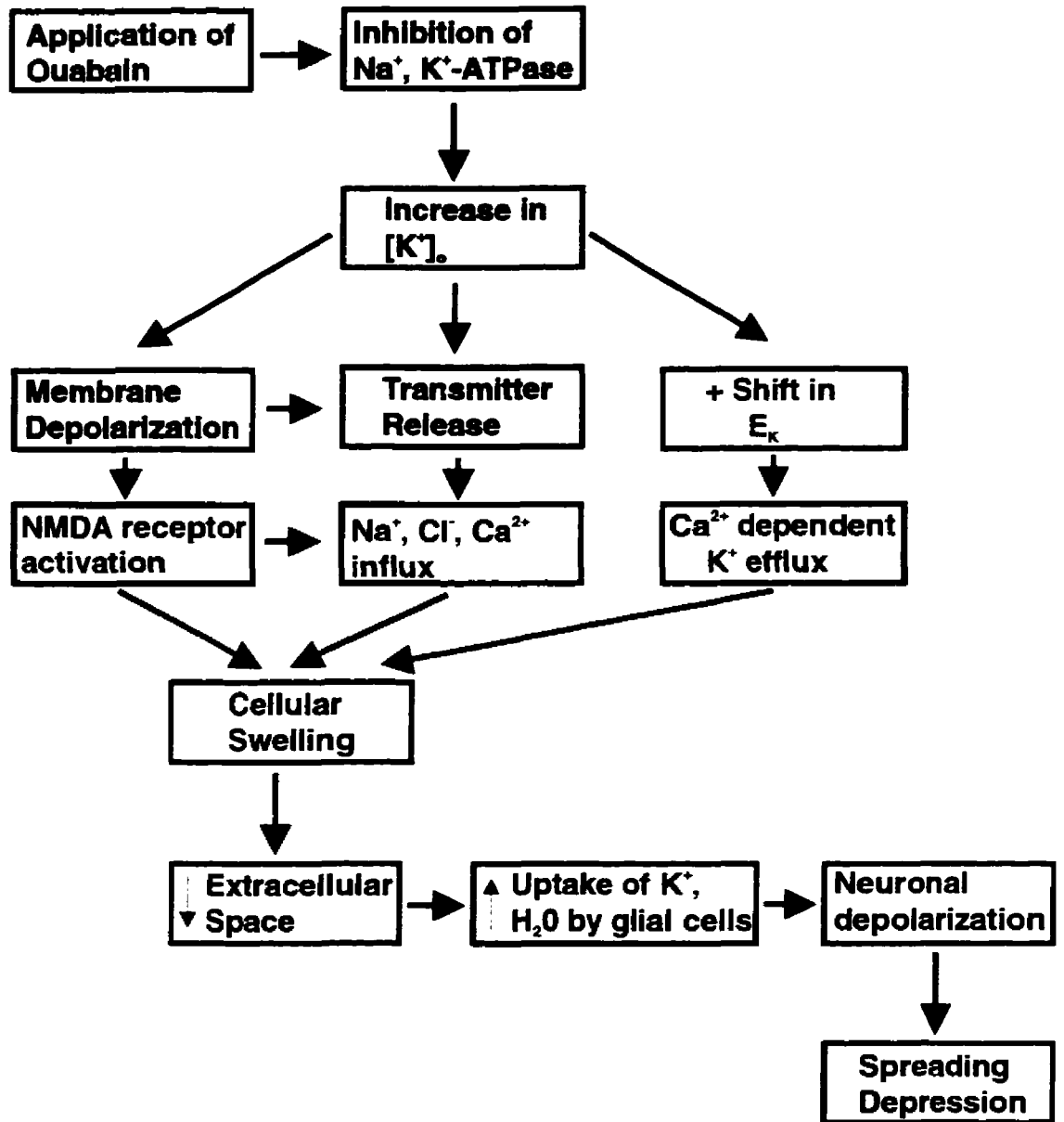
The generation of SD is highly sensitive to the level of extracellular potassium which is regulated by the  $\text{Na}^+/\text{K}^+$ -ATPase (Haglund and Schwartzkroin, 1990). A model was proposed by Haglund and Schwartzkroin (1990), essentially expanding on that presented earlier by Traynelis and Dingledine (1988), in which the elevated  $[\text{K}^+]_o$ , results in a series of events which lead to SD. The major underlying assumption is that similar mechanisms are involved in triggering seizures and SD (Haglund and Schwartzkroin, 1990), and that SD represents a “poorly controlled” seizure in which  $[\text{K}^+]_o$  regulation is completely disrupted (Kraig and Nicholson, 1978).

Any defect or low activity of the  $\text{Na}^+/\text{K}^+$ -ATPase, for example its inhibition by ouabain, results in a rise of  $[\text{K}^+]_o$ , which may then trigger SD (Haglund and Schwartzkroin, 1990). In addition to a rise in  $[\text{K}^+]_o$ , once ouabain is bound there is also an increase in intracellular sodium,  $[\text{Na}^+]_i$  (Archibald and White, 1974; Goddard and Robinson, 1976), which can act to induce additional neurotransmitter release.

A model of ouabain-induced SD is presented in Fig. 4, adapted from Haglund and Schwartzkroin (1990) and Lauritzen (1994), and can be summarized as follows. The application of ouabain results initially in a slow blockade of the  $\text{Na}^+/\text{K}^+$ -ATPase. As the enzyme is further inhibited, there is an increasing build-up of extracellular potassium. As external  $[\text{K}^+]_o$  rises, there is a positive shift in the reversal potential for potassium and a reduced potassium efflux at a given cell membrane potential (Haglund and Schwartzkroin, 1990). The reduced potassium efflux reduces the potassium afterhyperpolarizing potentials (both Ca-dependent and independent) and hence the preceding depolarizing events (eg. calcium spikes) increase in magnitude and duration (Haglund and Schwartzkroin, 1990).

The increase in  $[\text{K}^+]_o$  may then lead to the opening of voltage-dependent presynaptic channels, and an increase in the release of neurotransmitters (Haglund and Schwartzkroin, 1990). The release of excitatory neurotransmitters would trigger an influx of sodium and calcium, whereas the release of inhibitory neurotransmitters would result in

**Figure 4.** A model of the regenerative processes assumed to occur during ouabain-induced spreading depression, adapted from Haglund and Schwartzkroin (1990) and Lauritzen (1994). The application of ouabain results in a slow inhibition of the  $\text{Na}^+, \text{K}^+$  - ATPase, and an increase in  $[\text{K}^+]_o$ . The resulting  $\text{Na}^+$ ,  $\text{Cl}^-$ ,  $\text{Ca}^{2+}$  influx leads to cellular swelling, a reduction in the extracellular space, and further neuronal depolarization until there is initiation of SD.



an influx of chloride and efflux of potassium (Haglund and Schwartzkroin, 1990), as shown in Fig. 4. This massive influx of sodium, calcium and chloride will result in the influx of water, leading to cellular swelling (Van Harreveld, 1978). The size of the extracellular space would be decreased due to these ion fluxes and the entry of potassium and water into glial cells (Hablitz and Heinemann, 1989; Snow *et al.*, 1983).

Glutamate may also play a role in the cellular swelling, as increases in extracellular glutamate will stimulate NMDA receptors and open non-selective cation channels (Hoffmann and Dunham, 1995). This would potentiate the cellular depolarization, resulting in  $\text{Na}^+$  and  $\text{Cl}^-$  uptake, and cellular swelling (Andrew *et al.*, 1996) followed by a massive  $\text{Ca}^{2+}$  influx (Choi, 1988; Choi and Rothman, 1990).

The above changes not only increase neuronal firing activity, but in addition lead to an increase in the base-line  $[\text{K}^+]_o$ . Essentially, a positive feedback cycle is setup, leading to further rises in base-line  $[\text{K}^+]_o$ , loss of  $\text{K}^+$ -dependent mechanisms, a reduction in the activity normally regulated by  $[\text{K}^+]$  efflux, and finally further neuronal depolarization (Haglund and Schwartzkroin, 1990). The loss of  $\text{K}^+$  by neurons would lead to massive depolarization of astrocytes (Sweeney *et al.*, 1995). In a study of ouabain-induced spreading depression in immature hippocampal slices, it was determined that ouabain resulted in an increase in the baseline  $[\text{K}^+]_o$  in the CA1 of the immature hippocampal slice from  $6.2 \pm 0.4$  mM to  $10.8 \pm 0.5$  mM, and a decrease in the peak  $[\text{K}^+]_o$  during SD from  $69.8 \pm 4.0$  mM to  $60.3 \pm 4.2$  mM (Haglund and Schwartzkroin, 1990). This depolarization of astrocytes would open voltage-sensitive anion channels, leading to passive electroneutral  $\text{K}^+$ ,  $\text{Cl}^-$ , and  $\text{HCO}_3^-$  flux into astrocytes mediated by Donnan forces. The gain of these electrolytes would lead to astrocytic swelling and a reduction of extracellular space (Sweeney *et al.*, 1995). This process will continue under the influence of ouabain, when there is sufficient depolarization to initiate an explosive SD episode.

Potassium plays a central role for SD and it is reasonable to assume that any disturbance of  $K^+$  homeostasis would make the region of brain susceptible to SD (Haglund and Schwartzkroin, 1990). For this reason, although SD can be initiated by a number of mechanical, electrical, and chemical stimuli (Somjen *et al.*, 1992), the method of choice has been the focal application of high  $K^+$  solution (Somjen *et al.*, 1992). In fact, the level of  $[K^+]_o$  greatly exceeds normal physiological levels during SD, even exceeding the 12-20 mM "ceiling level" observed during seizure activity in the immature CNS (Swann *et al.*, 1986).

Previous work in our laboratory has confirmed that spreading depression can be initiated in the *in vitro* hippocampal slice with a bath-application of high  $[K^+]_o$  solution (Duffy and MacVicar, unpublished results), consistent with the findings of several studies (Somjen *et al.*, 1992). However, there are several limitations to initiating SD in this way. First, the application of high  $[K^+]_o$  fails to initiate SD reproducibly. In addition, it has been demonstrated that a prolonged exposure to high potassium results in an irreversible loss of synaptic transmission in hippocampal slices, and severe cell loss occurs in regions directly in contact with the solution *in vivo* (Kawasaki *et al.*, 1988).

A more consistent method of initiating spreading depression has been developed using the application of ouabain (Duffy and MacVicar, 1995 unpublished results). Ouabain (50-500  $\mu$ M) was used to initiate spreading depression in the chicken retina (Van Harrevelde, 1978), and a wave of spreading depression occurred spontaneously within 1.5-2.5 minutes. This finding is consistent with the suggestion of Snow *et al.* (1983) that inhibiting the  $Na^+, K^+$ -ATPase would result in SD being more easily initiated. As ouabain-induced initiation of spreading depression is reproducible and consistent, the experiments in this thesis will employ bath-applications of ouabain to initiate SD.

### 1.13 Purinergic Receptors

Adenosine 5'-triphosphate (ATP) has been shown to be released from multiple cell types including neurons in general (Gordon, 1986; O'Conner and Kimelberg, 1993) and hippocampal neurons in particular (Wieraszko *et al.*, 1989). The release of ATP has been proposed to be involved in intercellular signaling in various systems of the CNS (Evans *et al.*, 1992; Salter and Hicks, 1994; Zimmermann, 1994; Lyons *et al.*, 1995). Extracellular ATP interacts with specific receptors on cells and regulates many biological processes (Dubyak and el-Moatassim, 1993).

The receptors known to be stimulated by ATP or one of its by-products are called purinergic receptors (purinoceptors), and were originally classified as P<sub>1</sub> or P<sub>2</sub> (Burnstock and Kennedy, 1985). The P<sub>1</sub>-purinoceptors are activated by adenosine and were further sub-classified into A<sub>1</sub>, A<sub>2</sub> and A<sub>3</sub> subtypes (van Calker *et al.*, 1979; Williams, 1987; Zhou *et al.*, 1992). The P<sub>2</sub>-purinoceptors are activated by ATP and/or its metabolic by-product ADP. These receptors were originally sub-divided into the P<sub>2x</sub> and P<sub>2y</sub> purinoceptors (Burnstock and Kennedy, 1985), however, additional receptor subtypes exist, namely the P<sub>2u</sub>, P<sub>2z</sub> and P<sub>2T</sub> receptors (Gordon, 1986; Dubyak and el-Moatassim, 1993; O'Connor and Kimelberg, 1993).

The different subtypes of P<sub>2</sub>-purinergic receptors are further classified into two groups: the ionotropic and metabotropic receptors. The ionotropic receptors, P<sub>2x</sub>, P<sub>2T</sub> (platelet) and P<sub>2z</sub> (mast cell), are receptors coupled directly to non-selective cation channels permeable to Ca<sup>2+</sup> (Benham and Tsien, 1987; Burnstock, 1990; Bean, 1992). The metabotropic receptors, P<sub>2y</sub> and P<sub>2u</sub> are linked to G-protein-mediated second messenger mechanisms for release of Ca<sup>2+</sup> from intracellular stores (Burnstock, 1990; O'Conner and Kimelberg, 1993; Barnard *et al.*, 1994).

Two relatively recent reviews by Barnard *et al.* (1994) and Fredholm *et al.* (1994) have recommended reclassifying cloned P<sub>2</sub> receptors into the two major families: the G-protein coupled P<sub>2y</sub> receptor and the intrinsic ion channel type P<sub>2x</sub> receptor. They proposed

termining newly discovered G-protein-coupled  $P_2$  receptors as  $P_{2y1}$ ,  $P_{2y2}$  etc. by consecutive numbering.

Studies characterizing  $P_{2y}$  and  $P_{2x}$  receptors at the molecular level have found that three different cloned genes for  $P_{2y}$  receptors demonstrated a strong homology to G-protein-coupled receptors (Barnard *et al.*, 1994), and two cloned  $P_{2x}$  receptors showed homologies with the transmitter-gated ion channel superfamily (Barnard, 1992). In fact,  $P_{2x1}$  isolated from vas deferens smooth muscle (Valera *et al.*, 1994),  $P_{2x2}$  from PC12 cells (Brake *et al.*, 1994), and  $P_{2x3}$  from rat brain (Séguéla *et al.*, 1996) are structurally closer to inward rectifier  $K^+$  channels and amiloride-sensitive  $Na^+$  channels than to receptor channels of the glutamate-gated channel family (Séguéla *et al.*, 1996).

Classification to date of the  $P_2$ -purinoceptors has relied almost exclusively on the pharmacological specificity of the agonist analogues of ATP and ADP (Gordon, 1986), although agonist potencies in some cases for the ionotropic and metabotropic receptors are similar (Khakh *et al.*, 1995). The most potent agonist at the  $P_{2x}$ -purinoceptor is  $\alpha,\beta$ -methylene ATP, shown to be even more effective than ATP (Pintor and Miras-Portugal, 1995), although it is much less effective for  $P_{2x3}$  receptors (Séguéla *et al.*, 1996) and completely ineffective at PC12  $P_{2x}$ -purinoceptors (Nakazawa *et al.*, 1990a; Brake *et al.*, 1994). The best agonists for  $P_{2y}$ -purinoceptors are 2-methylthioATP and ADP- $\beta$ -S (Pintor and Miras-Portugal, 1995; Salter and Hicks, 1994).

The presence of  $P_{2x}$ -purinoceptors in the hippocampus has been demonstrated in radioligand binding studies with [ $^3H$ ]- $\alpha,\beta$ -methylene ATP (Michel and Humphrey, 1993), with a relatively high density of binding sites in the hippocampus (Bo and Burnstock, 1994; Balcar *et al.*, 1995). Functionally, both  $P_{2x}$  (Séguéla *et al.*, 1996) and  $P_{2y}$  receptors (Kastritsis *et al.*, 1992; Salter and Hicks 1994, 1995) have been demonstrated in hippocampal neuronal cultures (Mironov, 1993), and in astrocytic cell cultures (Porter and McCarthy, 1995).

Several compounds known to interact with multiple ATP binding proteins have proved useful as antagonists to the purinergic receptors (Boyer *et al.*, 1994), although potent, specific, and competitive antagonists have not yet been identified (Gordon, 1986; O'Connor and Kimelberg, 1993; Chen *et al.*, 1994; Séguéla *et al.*, 1996). The most well characterized purinergic antagonists to date are reactive blue 2 (RB-2), suramin, and PPADs (pyridoxal phosphate 6-azophenyl-2'-4'-disulphonic acid). RB-2 has been demonstrated to antagonize ATP actions at the P<sub>2y</sub>-purinoceptor subtype in various tissues (Choo, 1981; Manzini *et al.*, 1986; Reilly *et al.*, 1987; Rice and Singleton, 1989) including P<sub>2x3</sub> receptors on *Xenopus* oocytes (Séguéla *et al.*, 1996), and glutamate-activated currents in the hippocampus (Motin and Bennett, 1995).

The trypanocidal drug, suramin hexasodium (8,8'-[Carbonylbis[imino-3,1,-phenylenecarbonylimino(4-methyl-3,1,-phenylene)carbonylimnio]]bis-1,3,5-naphthalenetrisulfonic acid hexasodium) known more commonly as suramin, was originally synthesized around 1916 by German workers at Farbenfabriken Bayer AG (Voogd *et al.*, 1993). Suramin has been shown to antagonize non-selectively both the P<sub>2x</sub> (Chen *et al.*, 1994) and P<sub>2y</sub> subtypes in various tissues (Dunn and Blakeley, 1988; Hoyle *et al.*, 1990) including neuronal tissues (Dunn and Blakeley, 1988; Silinsky *et al.*, 1990; Evans *et al.*, 1992) and more specifically in the hippocampus (Inoue *et al.*, 1995; Motin and Bennett, 1995). Suramin was ineffective at blocking ATP receptors in *Xenopus* oocytes (Kuptiz and Atlas, 1993), although the subtype of native receptors on these oocytes has not yet clearly been identified (Ziganshin *et al.*, 1996). Suramin has also been suggested as a selective, competitive antagonist of P<sub>2y</sub>-mediated increases in intracellular Ca<sup>2+</sup> in astrocytes (Salter and Hicks, 1994). In addition, the action of suramin is not limited to P<sub>2</sub> purinergic receptor antagonism, as suramin has a multitude of effects (reviewed in Voogd *et al.*, 1993). Red blood cells are impermeable to suramin (Fortes *et al.*, 1973), suggesting suramin cannot penetrate neuronal membranes (Wieraszko, 1995). Therefore the target of action of suramin would most likely be molecules and enzymes located on the cellular surface (Wieraszko, 1995). Suramin is a potent inhibitor of Na<sup>+</sup>,K<sup>+</sup>-ATPase (Fortes *et al.*,

1973), and therefore could also block neuronal ecto-ATPase (Nagy *et al.*, 1986; Wieraszko, 1995). Suramin may also interact with intracellular enzymes, such as protein kinase C (PKC) (Mahoney *et al.*, 1990). In addition, it has been suggested that as suramin inhibits PKC it may also inhibit ecto-protein kinases (Ehrlich *et al.*, 1986; Wieraszko, 1995). Suramin has also been shown to inhibit the activity of some hydrolytic enzymes (Wilson and Wormall, 1950), and modulates activity of enzymes using ATP as a substrate (Fortes *et al.*, 1973; Mahoney *et al.*, 1990). Furthermore, suramin is an inhibitor of human immunodeficiency virus (HIV) reverse transcriptase (Mitsuya *et al.*, 1984).

PPADs was shown to selectively antagonize responses to the P<sub>2x</sub> subtype of receptors in various tissues (Lambrecht *et al.*, 1992; Ziganshin *et al.*, 1993), although it did not inhibit P<sub>2x3</sub> receptors in *Xenopus* oocytes to the same extent as suramin and RB-2 (Séguéla *et al.*, 1996).

#### 1.14 NMDA, AMPA and Kainate Receptors: Inhibition by Selective Antagonists

There are at least four receptor subtypes for the excitatory amino acids, glutamate and aspartate. The three major subtypes of postsynaptic receptors are named according to the agonist of highest affinity: NMDA, AMPA and kainate receptors.

The NMDA receptor functionally consists of a glutamate (Glu) or NMDA recognition site, an allosteric glycine site, a zinc (Zn<sup>2+</sup>) binding site, and the ligand-gated cationic ionophore (Young and Fagg, 1990). Within the channel there is i) a binding site for Mg<sup>2+</sup>, found to non-competitively inhibit Na<sup>+</sup> and Ca<sup>2+</sup> influx ii) a phencyclidine (PCP) recognition site where PCP and the anticonvulsant MK-801 [(+)-5-methyl-10,11-dihydro-5H-dibenzo[a,d]cyclo-hepten-5,10-imine maleate] bind to inhibit ion flux through the channel (Wong *et al.*, 1988; Johnson and Jones, 1990). The distribution of NMDA receptors in the rat brain has been studied, and there is an abundance within the hippocampus, especially within both the CA1, specifically st. radiatum (Andreasen *et al.*, 1988), and the dentate gyrus regions (Jansen *et al.*, 1989; Monaghan *et al.*, 1989).

The AMPA receptor functionally consists of an AMPA/quisqualate recognition site and the ligand-gated cationic ionophore (Young and Fagg, 1990). The AMPA receptor gates cation conductances that underlie fast depolarizing responses, and is permeable primarily to  $\text{Na}^+$ . CNQX (6-cyano-7-nitroquinoxaline-2,3-dione) shows some selectivity as an antagonist (Young and Fagg, 1990), however only recently have selective antagonists been identified (Wilding and Huettner, 1997). GYKI 53655 is a selective non-competitive AMPA receptor antagonist (Paternain *et al.*, 1995; Wilding and Huettner, 1995) recently shown to inhibit the selectivity of AMPA receptors allowing for the recording of the activation of kainate receptors in cultured rat hippocampal neurons (Wilding and Huettner, 1997). The distribution of AMPA receptors in the rat brain has been studied, and within the hippocampus there is an abundance specifically within the CA1 and dentate gyrus (Hawkins *et al.*, 1995). It has also been shown that the largest AMPA distribution is on CA1 dendrites (Blackstone *et al.*, 1992; Nielsen *et al.*, 1995). The distribution of AMPA receptors corresponds closely to that of NMDA receptors (Cotman *et al.*, 1987), and AMPA and NMDA receptors probably share the same synapse in ~ 7 of 10 cases (Bekkers and Stevens, 1989).

The non-NMDA receptor family includes the kainate and AMPA receptor-coupled ionophores (Andreasen *et al.*, 1988), which, unlike the NMDA receptors, conduct in essentially a non-rectifying manner (Mayer and Westbrook, 1987). CNQX has been shown to be a relatively selective and potent non-NMDA receptor antagonist (Andreasen *et al.*, 1989). When studied in the hippocampal slice, the responses to both kainate and quisqualate were reduced with  $\text{IC}_{50}$  values of 1.2 and 4.8  $\mu\text{M}$  respectively (Andreasen *et al.*, 1989). The distribution of non-NMDA receptors in the rat brain has been studied, and within the hippocampus the highest density of kainate receptors is found in st. lucidum in the CA3 region, and the highest density of quisqualate receptors is found in st. pyramidalis of the CA1 (Andreasen *et al.*, 1988).

### 1.15 Regulation of Cell Volume

One of the most fundamental homeostatic mechanisms of cells is the regulation of their volume (Hoffmann and Dunham, 1995). Cells maintain a constant volume in physiological conditions, and most cells have mechanisms which are activated during changes in their volume. Regulatory volume decrease (RVD) is a process activated during cellular swelling and results in the activation of transport systems for  $K^+$ ,  $Cl^-$ , and organic molecules, resulting in a loss of osmolytes and water (Hoffman and Dunham, 1995). Conversely, regulatory volume increase (RVI) is a process whereby cells can increase their volume by the net uptake of  $Na^+$ ,  $Cl^-$ , and often  $K^+$ , with the concomitant uptake of water.

Following many brain insults such as ischemic strokes, hypoxia or anoxia, and including spreading depression (Van Harreveld, 1978) there is cellular swelling (Van Harreveld and Khattab, 1967). Cellular swelling results from an increased uptake of  $Na^+$  and  $Cl^-$  following a volume regulatory response in which  $K^+$  is lost from the neuron, resulting in high  $[K^+]_o$ . Recovery of high  $[K^+]_o$  has been suggested to occur in two ways: by active uptake into glial cells, or alternatively by washout of the steadily flowing aCSF (Kawasaki *et al.*, 1988).

Astrocytic RVD subsequent to swelling induced by hyposmolarity has been repeatedly demonstrated (Olson *et al.*, 1986; Pasantes-Morales and Schousboe, 1988; Bender *et al.*, 1992). Swelling of glial cells has been demonstrated in neuropathologies such as ischemia, and epilepsies (Pasantes-Morales *et al.*, 1993). Far less is known about conditions leading to changes in cell volume in neurons (Ballanyi and Grafe, 1988), however swelling of dendrites has been observed during spreading depression (Van Harreveld and Khattab, 1967).

RVD in hypo-osmotically swollen astrocytes involves the transient activation of separate  $K^+$  and  $Cl^-$  channels, both of which may be activated by  $Ca^{2+}$  (O'Connor and Kimelberg, 1993) and by the release of amino acids such as glutamate, aspartate and taurine (Kimelberg *et al.*, 1990). During hypo-osmotic stress,  $Ca^{2+}$  enters astrocytes from

both the extracellular space and intracellular stores (O'Connor and Kimelberg, 1993). Furthermore, an intracellular  $\text{Ca}^{2+}$  increase can lead to activation of  $\text{Ca}^{2+}$ -sensitive  $\text{K}^+$  channels (Miller, 1991). These channels are known to be expressed in astrocytes (Quandt and MacVicar, 1986), and during hypo-osmotic stress, or conditions such as spreading depression in which agonists are released, there could be activation of  $\text{Ca}^{2+}$ -sensitive  $\text{K}^+$  and  $\text{Cl}^-$  channels, which would be accompanied by additional loss of cellular  $\text{K}^+$ ,  $\text{Cl}^-$ , and water, thus enhancing RVD.

### **1.16 Clinical Significance: Spreading Depression as a Pathological Model for Migraines**

The migraine aura is defined as any neurological disturbance that appears shortly before or during the development of a migraine headache (Lauritzen, 1994). The headache associated with a migraine is most often throbbing and unilateral, on the side of the head relative to the focal symptoms. The focal symptoms develop in a characteristic 'creeping' fashion, commonly used to differentiate migraine from epilepsy. It has been suggested that the orderly development of a migraine aura makes a vascular origin a remote possibility (Lauritzen, 1994), while CSD is a more attractive explanation (Leão and Morison, 1945; Moskowitz, 1984; Lauritzen, 1994; Obrenovitch and Zilkha, 1996).

Propagation of a SD wave may account for the traveling scotoma in the visual cortex during a migraine (Milner, 1958; Lauritzen, 1987), although it is far less probable that SD triggers the later headache phase of the migraine attack. Similarly, CSD in animals gives rise to changes in behaviour which mimic important features of the migraine aura (Bures *et al.*, 1974). For example, in the rat, unilateral waves of CSD induce contralateral sensory neglect, and motor impairment of the forepaw lasting a much shorter time than the blood flow reduction (Lauritzen, 1987). Rats do not experience hippocampal or cortical SD as aversive (Koroleva and Bures, 1993), suggesting that SD may not necessarily be involved in the pain-triggering mechanism during a migraine attack.

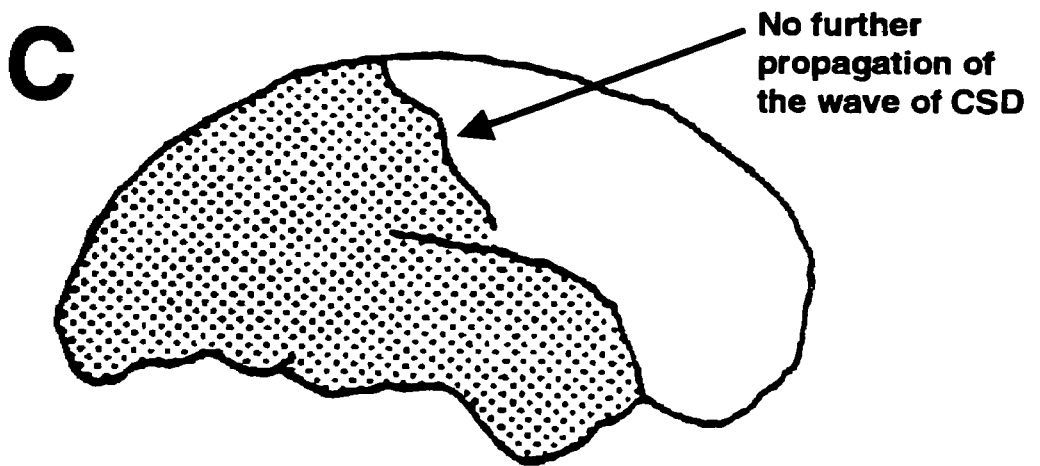
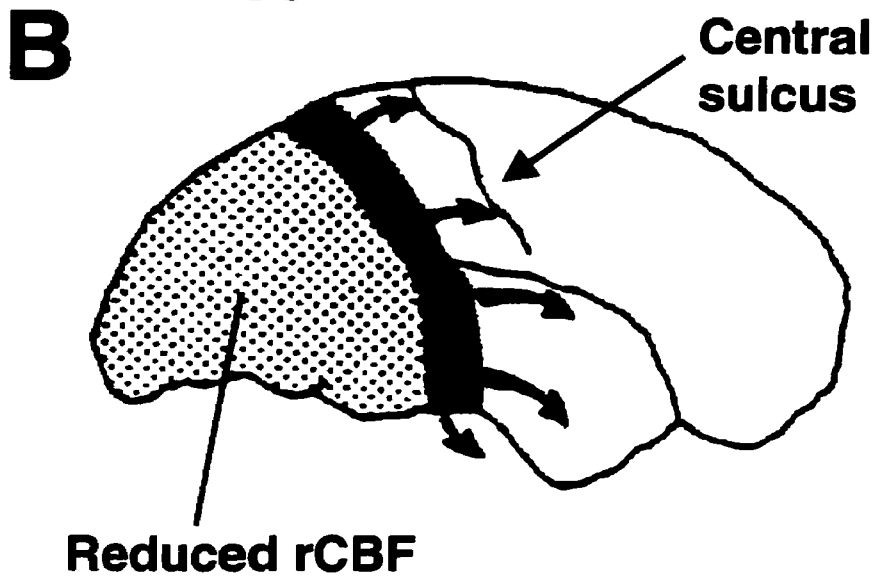
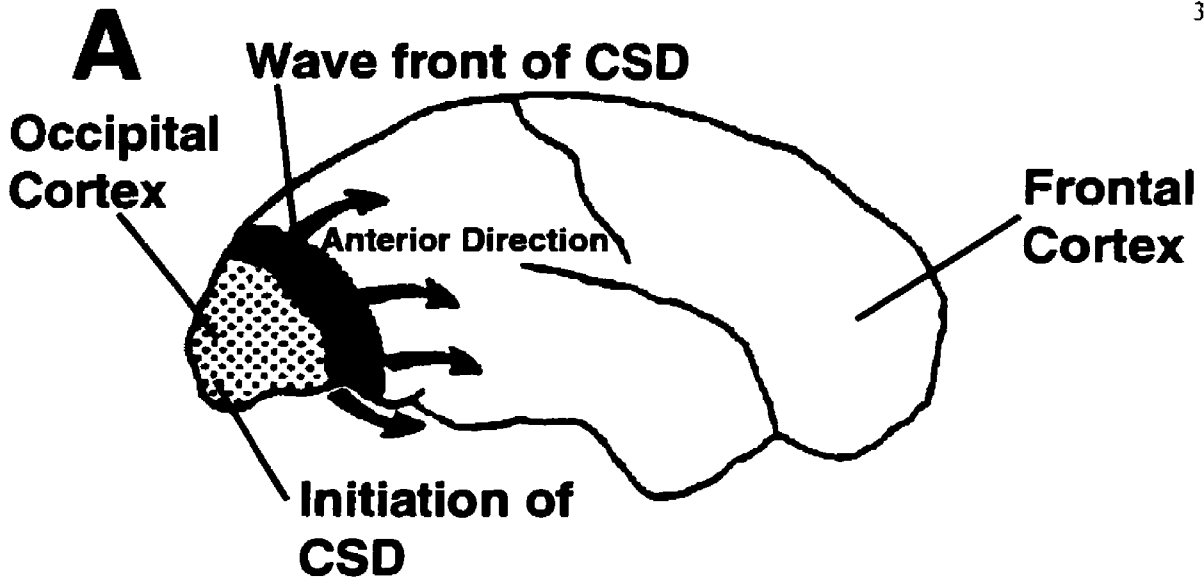
Consistent with the idea that SD can occur independently of pain, several studies have demonstrated that SD can serve as a stimulant to a wide range of biological behaviours. It was shown that SD in the frontal cortex of an unanesthetized rat resulted in increased eating and drinking (Huston and Bures, 1970; Huston *et al.*, 1974), yawning, and penile erection (Huston, 1971), behaviours which pain would inhibit. Intriguingly, these same symptoms may occur during classical migraines in humans, but during these migraines, the painful headache is usually absent.

The wave of spreading depression propagates in all directions without relation to blood supply or neuronal pathways (Leão, 1944). It has been observed that the propagation rate of SD is similar to calculations of the “visual march” in humans, (Lauritzen, 1994) and the spread of oligemia associated with the aura of induced migraine headaches (Olesen *et al.*, 1981). A possible link between SD and the painful phases of migraine headaches has been proposed. Extracellular potassium concentrations frequently reach 60 mM during SD (Hansen and Olsen, 1980; Hansen *et al.*, 1980; Hansen and Zeuthen, 1981; Moskowitz, 1984). These increases may be sufficient to depolarize trigeminal nerve fibers surrounding pial arteries, activating the pain-promoting fibers of the trigeminovascular system. This would result in the initiation of a vascular headache (Moskowitz, 1984).

Low brain magnesium, a condition which increases the probability of CSD initiation in turtle, rat, and human brain tissue *in vitro* (Mody *et al.*, 1987; Lauritzen *et al.*, 1988; Avoli *et al.*, 1991), occurs in migraine patients (Ramadan *et al.*, 1989). In addition, it has been reported that plasma levels of glutamate and aspartate are elevated in migraine patients, suggesting the impairment of amino acid re-uptake mechanisms (Ferrari *et al.*, 1990).

Fig. 5 is a schematic based on a theory (reviewed in Lauritzen, 1994) that migraine attacks are initiated by a CSD originating in the posterior region of the brain. From this region the SD moves anteriorly at a speed of 2-3 mm/min. The migraine aura is thought to occur at the wavefront where the neuronal cell depolarization is occurring (Fig. 5A).

**Figure 5.** A schematic (adapted from Lauritzen, 1994) based on a theory that migraine attacks are initiated by a wave of cortical spreading depression. **A)** CSD initiates at the occipital pole, spreading anteriorly across the brain. At the CSD wave front, regional cerebral blood flow (rCBF) is reduced. **B)** The region of reduced rCBF expands as the wave continues propagating anteriorly. CSD usually stops upon reaching the central sulcus. **C)** The wave of CSD is now stopped, and the migraine is in full-scale attack, as the ventral spread of CSD causes activation of pain-sensitive fibers and the ensuing headache.



In the region immediately posterior to the spreading wavefront there is a reduced regional cerebral blood flow (rCBF), as shown in Figs. 5A-C. The wave typically stops upon reaching the central sulcus, although in many patients it does not propagate this distance (Lauritzen, 1994). The ventral spread induces the activation of pain-sensitive fibers and the ensuing headache. In Fig. 5C the wave of CSD has stopped and the migraine is in a full-scale attack.

For the generation of the headache to occur during the migraine, pain-sensitive fibres must be activated at the ventral surface of the brain. The latency period between a headache and the onset of the migraine aura may in fact reflect the time it takes for the SD to propagate from the occipital cortex to this pain-triggering zone (Moskowitz, 1984). However, the mechanism by which SD is able to inflict pain is still far from understood (Lauritzen, 1994).

Many drugs used for migraine treatment are ineffective as blockers of CSD, and this has been attributed to the possibility that they influence the sequence of events which cause pain (Moskowitz, 1992) rather than the CSD itself. Certainly CSD displays enough similarities to the migraine that it can be considered as a disease model (Lauritzen, 1994). For this reason, although the purpose of this thesis is to investigate the basic physiological mechanisms of SD, there are most certainly clinical implications to an understanding of the mechanism of initiation and propagation of SD.

## **2. MATERIALS AND METHODS**

### **2.1 Tissue Preparation**

Six to eight (6-8) transverse hippocampal slices (400  $\mu\text{M}$ ) were obtained from each Sprague-Dawley rat (P<sub>18</sub>-P<sub>26</sub>, *Rattus sp.*). Slices were sectioned using a vibratome (DSK-100), and incubated in artificial cerebrospinal fluid (aCSF) containing (mM) 124 NaCl, 5 KCl, 26 NaHCO<sub>3</sub>, 1.3 MgCl<sub>2</sub>, 2 CaCl<sub>2</sub>, 10 D-glucose (pH 7.35-7.4) at room temperature (21-23 °C) within an aerated (95% O<sub>2</sub>, 5% CO<sub>2</sub>) storage vial.

Individual slices were removed from the storage chamber and transferred via a transfer pipette to a recording and imaging chamber (MacVicar, 1984). The imaging chamber was mounted on the stage of an inverted microscope (Zeiss). Slices were held in position, completely submerged in flowing aCSF, using two flattened platinum wires. Slices were viewed from below through a 2.5x objective (Zeiss). The bath was superfused with aCSF (33.5 - 34.5 °C) by a peltier controller (Cambion, PCVER2), and monitored visually by a microprocessor-driven thermometer (Omega, HH21). The aCSF was superfused at a constant rate of approximately 0.5-0.7 ml/min using a peristaltic pump (Gilson Medical, Villiers Le Bel, France, Minipulus-2).

### **2.2 Drug Application**

Most solutions containing drugs were made up fresh before each series of experiments. In the case of glibenclamide, ATP, and other agonists, the drugs were made up as a stock solution and divided into single-use aliquots and stored at -30 °C. Aliquots were thawed immediately prior to use, and the solutions were prepared by diluting the stock solution to obtain the necessary concentration. Aqueous stock solutions were used except in the case of glibenclamide which was dissolved in dimethyl sulfoxide (DMSO). In this case, the use of DMSO was required to dissolve the drug to facilitate its entry into aqueous solution. In the case of glibenclamide, control experiments consisted of aCSF with the same percentage of DMSO, typically < 0.05 %. The Ca<sup>2+</sup>-free solution contained no added CaCl<sub>2</sub> and 100  $\mu\text{M}$  EGTA.

To maintain the osmolarity and concentration of divalent cations, the concentration of  $Mg^{2+}$  was increased from 1.3 - 3.3 mM to compensate for the decrease of  $Ca^{2+}$  from 2 mM to ~ 0 mM.

Suramin, RB-2, PPADs, benzamil hydrochloride, MK-801, CNQX, bicuculline, DIDS, H-7, AMP-PNP, and glibenclamide were obtained from RBI (Research Biochemicals Incorporated, Natick, MA, USA). Ouabain, amiloride, and tolbutamide were obtained from Sigma (Sigma Chemicals Inc.).

### **2.3 Experimental Protocol**

Following a 2 minute control period to ensure the stability of the intrinsic optical signals (IOS), spreading depression was elicited in the hippocampal slices by a bath-application of aCSF containing 100  $\mu$ M ouabain. The ouabain solution was applied until the wave had passed through the hippocampal slice, at which point the perfusate was switched to control aCSF. In the case of drug applications, the slices were typically pre-treated with the drug while in the submersion imaging chamber for a period of 15-25 minutes.

All experiments were conducted on separate slices, as ouabain-induced spreading depression can only be initiated once. Controls were alternated with drug applications on separate slices to ensure the stability of the slice preparation and the acquisition of intrinsic optical images. In addition, between experiments, control aCSF was perfused through the imaging chamber for 5-10 minutes to ensure a thorough washing of the submersion chamber before the subsequent experiment.

The purinergic agonists were applied during a modified experimental protocol. In this modified protocol, hypo-osmotic aCSF was superfused onto the tissue without the presence of ouabain. The goal of applying the hypo-osmotic aCSF was to swell the tissue to approximately the same level as would otherwise occur during ouabain-induced SD. Once a stable level of tissue transmittance was obtained, typically 4-5 minutes following the application of hypo-osmotic aCSF, the agonists were applied to determine their effect. Following this, the hypo-osmotic aCSF was washed off with normosmotic aCSF.

## 2.4 Imaging Techniques

During experiments, the hippocampal slices were transilluminated using a tungsten lamp that was powered by a voltage-regulated power supply (NAG 100W). Video images were obtained using a charge-coupled device (CCD) camera (COHU, 4915-2001), mounted to the secondary port on the microscope. Images were averaged and digitized for storage on an IBM-PC compatible computer using Axon Imaging Workbench (Ver 1.0-2.0). Imaging signals were transferred to either a 486 DX2/50 (Comtex, 486/50) or a Pentium-90 (Comtex, P90) IBM-PC compatible computer, imaged on the imaging board DT2867 (486/50) or DT3155 (P90) and stored digitally on a Seagate (1.05 GB) or Fujitsu (1.08 GB) harddrive. The images were then transferred for permanent storage on a read-writable optical disk cartridge (Plasmon, 1.5 GB). All images were saved in the MS-DOS extension .aif format by Axon Imaging Workbench.

As the goal of the experiments was to examine changes in the intrinsic optical properties of hippocampal slices, each experiment required the acquisition of a series of averaged images. Each image was an average of 8 frames. The average images were acquired using video-frame rates (30 Hz), and hence required approximately 0.27 seconds to acquire and average 8 frames. The first image was used as a control ( $T_{\text{cont}}$ ), and was subtracted from all subsequent images ( $T_{\text{exp}}$ ; total of 450-600 typically, and as many as 2000-2300). For this reason, the differences in the subtracted images allowed us to examine areas of the hippocampus in which light transmission through the slice had changed, over a relatively long (<25 minutes) period of time. The change in light transmittance (LT) was quantified using the following equation (Andrew *et al.*, 1997):

$$LT = \frac{(T_{\text{exp}} - T_{\text{cont}})}{T_{\text{cont}}} \times 100\% = \Delta T/T (\%)$$

where the digital intensity of the subtracted image ( $T_{\text{exp}} - T_{\text{cont}}$ ) divided by the gain of the intrinsic signal set in the imaging program was then divided by  $T_{\text{cont}}$  to be expressed as a percentage (Andrew *et al.*, 1997). The activity-dependent changes in light tissue transmittance, quantified as  $\Delta T/T$ , during ouabain-induced spreading depression are strikingly large ( $> 50\%$ ). The noise, analyzed by subtracting control images averaged 2-5%. This gave a respectable signal-to-noise ratio of 20:1. Due to the large nature of the signal, and comparatively small noise level, no additional image enhancement was necessary during image acquisition.

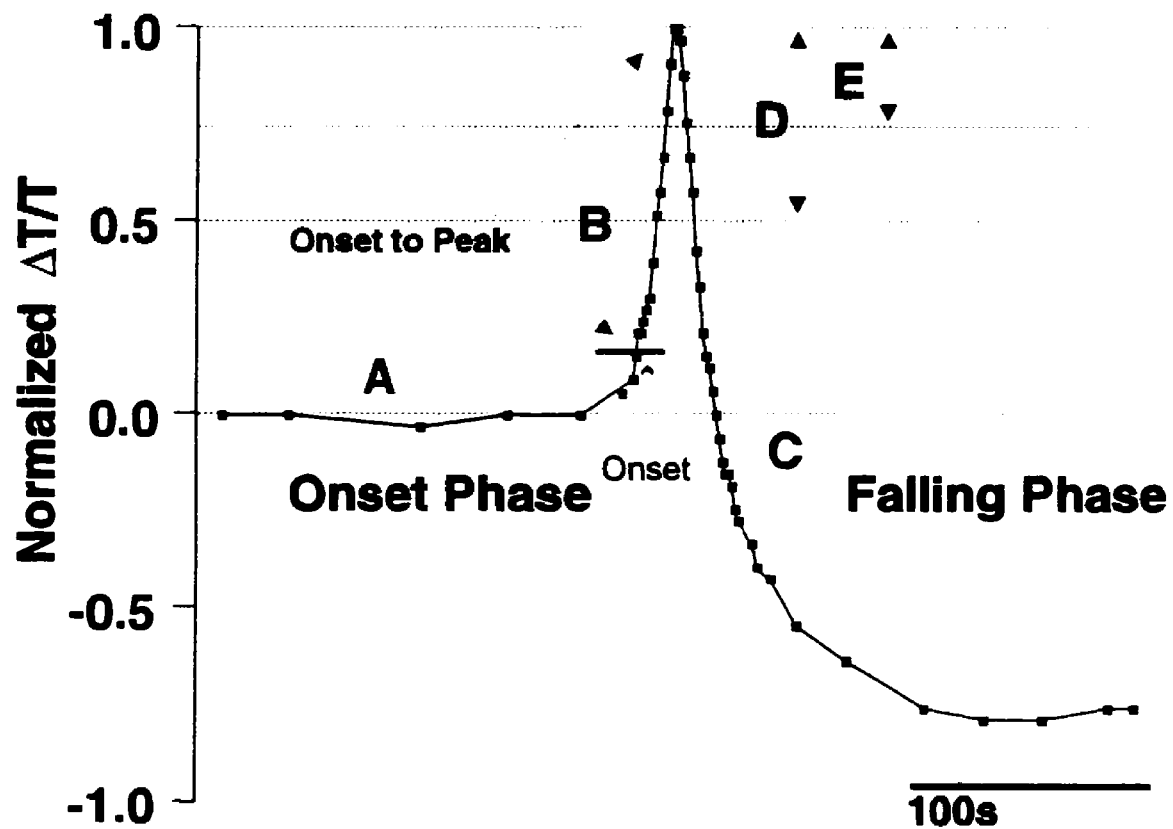
## **2.5 Statistical Analysis and Parameters of Ouabain-Induced Spreading Depression**

Fig. 6 illustrates a typical control response to ouabain-induced SD as measured in *st. radiatum* of the CA1. There are essentially three phases in the figure which merit a brief explanation as they will be referred to throughout this thesis

The first phase, Fig. 6A, is the baseline phase. This phase consists of the time from application of ouabain to the initiation or onset of the tissue transmittance changes. Baselines calculated in all data analyses were an average of the data points after the application of ouabain and before the onset of the transmittance changes.

The second phase, Fig. 6B, is the onset phase. This phase is quantified by the time from the onset of the transmittance changes to peak transmittance. The parameters extracted from this phase include the onset to peak time, slope, and maximum slope. The onset to peak time (a) is quantified as the time required for the tissue transmittance to change from 20% of peak to peak. The slope (b) is measured at fixed time points between 20% and 40% of peak transmittance and is the normalized change in tissue transmittance divided by the time and expressed in the units  $\Delta T/T/s$ , and the maximum slope (c) is calculated from a two-point data comparison in the onset phase and also expressed in the units  $\Delta T/T/s$ .

**Figure 6.** A tissue transmittance profile for a control response during ouabain-induced spreading depression as measured in *st. radiatum* of the CA1. There are two general phases of ouabain-induced SD, the onset phase and falling phase. **A)** Baseline phase, consisting of the time from application of ouabain to the initiation of the transmittance changes. **B)** Onset phase, quantified from the onset of the transmittance changes to peak transmittance. **C)** Falling phase, time from the peak onwards. Typically, in control slices there is a complete decay or return to baseline of the tissue transmittance. **D)** Decay to 75% of peak transmittance. **E)** Decay to 50% of peak transmittance.



The third phase, Fig. 6C, is the falling phase. This phase is quantified by the time from peak onwards. Typically in control slices in *st. radiatum* there is a complete decay or return to baseline of the IOS. The parameters extracted from this phase are indicated: decay to 75% of peak transmittance (Fig. 6D), decay to 50% of peak transmittance (Fig. 6E). The decays to 75 and 50 percent of peak respectively is simply the time required for the signal to decay to the percentage of the peak value.

The propagation rate or velocity was calculated in *st. oriens* and *st. radiatum* of the CA1. The rate was calculated by dividing the distance ( $\mu\text{m}$ ) between two zones by the time difference (s) for the change in the tissue transmittance at 20% of peak. The propagation rate or velocity was therefore expressed with the units  $\mu\text{m/s}$ .

Both the Mann-Whitney U non-parametric test and the unpaired Student's t-test were used for statistical analysis in this thesis. Both tests were used for n values greater than 6, as the latter makes the assumption that the data it is analyzing follows a Gaussian distribution. For n values under 6, the Student's t-test was utilized to establish significance. Differences were considered statistically significant at the 95% confidence level ( $p < 0.05$ ). Values reported in this thesis are mean  $\pm$  s.e.m. In all data figures, the following key is used in labeling statistically significant data sets: \* is  $p < 0.05$ , \*\*  $p < 0.01$ , \*\*\*  $p < 0.001$ .

### 3 RESULTS

#### 3.1 Characteristics of ouabain-induced spreading depression in the hippocampal slice

Spreading depression can be initiated in the rat hippocampal slice by a variety of chemical, electrical, or mechanical methods (Bures *et al.*, 1974; Somjen *et al.*, 1992). Previous work in our laboratory demonstrated that although SD can be initiated with a high-potassium solution (Duffy and MacVicar, personal communication), a much more consistent method of eliciting SD is with the application of 100  $\mu\text{M}$  ouabain.

The first series of experiments was conducted to determine the tissue transmittance changes, or changes in the intrinsic optical signals (IOS), during ouabain-induced SD in the absence of any other treatment. Fig. 7 demonstrates the effect of ouabain on the change in tissue transmittance in the hippocampal slice.

Fig. 7A is a bright-field image, showing the CA1 (stratum pyramidale, stratum radiatum, oriens), CA2, and dentate gyrus (stratum moleculare, stratum granulosum) regions of the hippocampus. Figs. 7B-F are a series of pseudo-colored digital images of the changes in light tissue transmittance following the onset of ouabain-induced spreading depression. The numbers in the upper right-hand corner of the panels indicate the time in seconds, following the onset, and correspond to B-F as labeled in Fig. 7G. Fig. 7G is the transmittance profile of normalized change in transmittance ( $\Delta T/T$ ) of two regions: st. radiatum and st. pyramidale of the CA1. The regions analyzed are demarcated by the circles in Fig. 7B. The curves have been normalized relative to the peak transmittance levels in st. radiatum.

Ouabain was superfused for the period of time indicated in Fig. 7G. The tissue transmittance profile during ouabain-induced SD in control conditions demonstrates several important characteristics. During the first two to three minutes from the application of ouabain, the levels of the intrinsic optical signals are relatively stable, hovering around the baseline. Subsequently there is a sudden initiation of spreading depression (onset phase), indicated by the rapid rise in the intrinsic optical signals (Fig. 7G) in st. radiatum and during the latter phase, st. pyramidale.

**Figure 7.** Ouabain-induced spreading depression in the hippocampal slice in control conditions. **A.** Bright-field image showing the CA1 (st. oriens, st. pyramidale, st. radiatum), CA2, and dentate gyrus (st. moleculare, st. granulosum) regions. **B-F.** Pseudo-colored digital images of the changes in light tissue transmittance following the onset of ouabain-induced spreading depression. The small white circles indicates the regions analyzed and presented in Fig. 7G. **G.** Normalized change in transmittance relative to maximum transmittance in st. radiatum of the CA1. The arrows (B-F) correspond to the panels above. The peak response of st. pyramidale (cell body layer) is as large as 50% greater than that of st. radiatum. Scale bar = 400  $\mu\text{m}$ .

# Spreading Depression (Control)

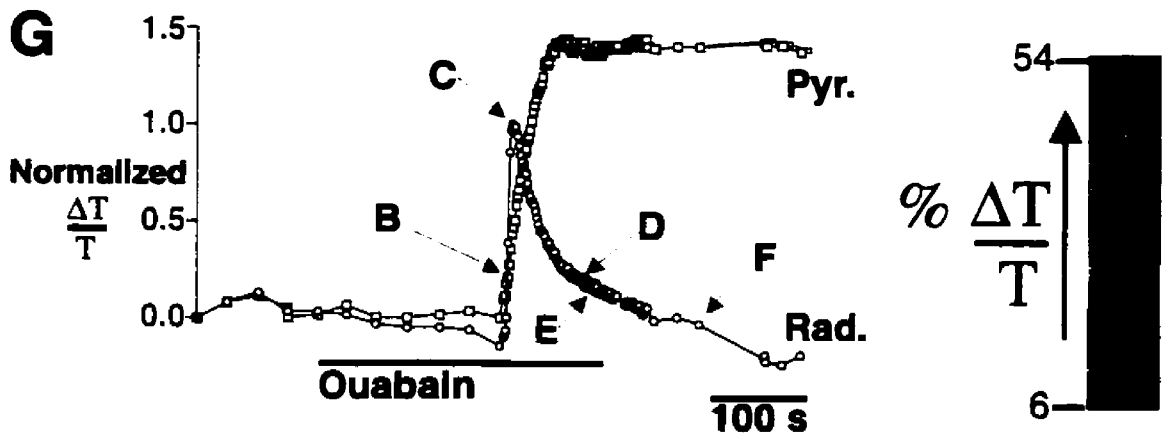
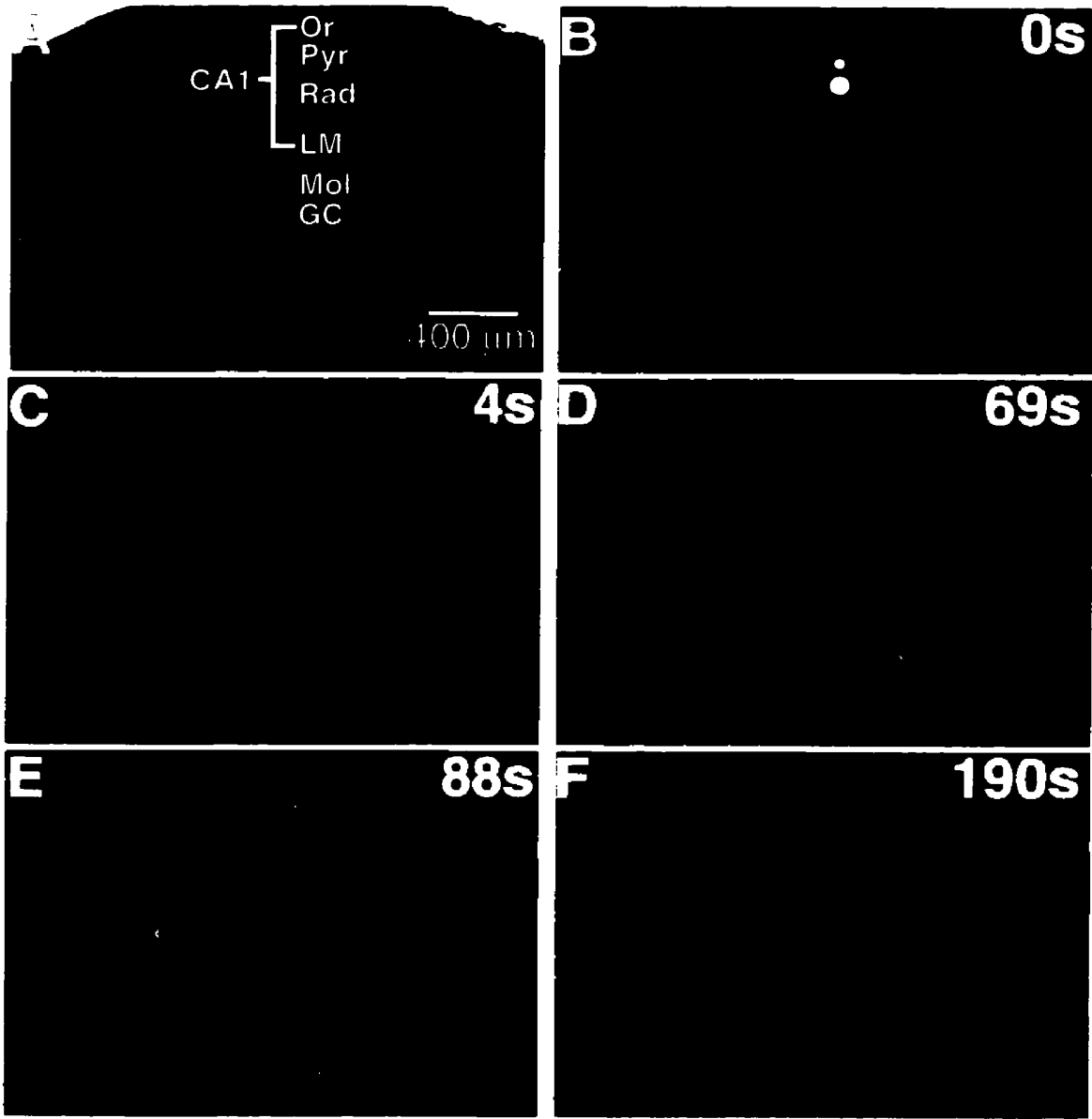


Fig. 7B demonstrates the large and rapid increase in IOS during the onset of spreading depression. From the initiation point in the CA1, the wave propagated in both directions: rostrally towards the CA3 and caudo-ventrally towards the subicular region of the hippocampus.

As the wave began propagating towards the subicular region, it jumped across the hippocampal fissure and began propagating in the dentate gyrus (Fig. 7D). Typically, the propagation in the dentate gyrus initiated in the upper leaf and traversed towards the distal region of the lower leaf.

One of the most striking characteristics of ouabain-induced SD is that the kinetics of the change in tissue transmittance are remarkably different in the two layers of the CA1 (Fig. 7F, in the latter part of the falling phase). In *st. radiatum*, there is a rapid time to peak in the onset phase, followed by a relatively rapid decay of the tissue transmittance to baseline during the falling phase. In *st. pyramidale*, there is an increase to peak which occurs during the late onset phase/early falling phase and plateaus. This maximum transmittance is as much as 50% greater than in *st. radiatum*, and unlike *st. radiatum*, there is no decay of the tissue transmittance in *st. pyramidale* of the CA1.

### **3.2 Ouabain-induced spreading depression occurs in low calcium conditions**

Previous work in our laboratory demonstrated that ouabain-induced SD occurs in conditions of low extracellular calcium (Duffy and MacVicar, unpublished results). Our next series of experiments was to investigate the effect of low extracellular calcium on ouabain-induced SD. 0  $[Ca^{2+}]_o$  aCSF solution was composed of no added calcium ( $\sim 0 [Ca^{2+}]_o$ ), and 100  $\mu M$  EGTA. In these conditions synaptic transmission would be severely depressed, and cellular processes dependent on an influx of extracellular calcium would be inhibited.

Fig. 8A is a comparison of the onset to peak time during ouabain-induced SD both in the presence and absence of extracellular calcium as measured in *st. radiatum* of the CA1. In control conditions the average onset to peak time was  $4.5 \pm 0.5$  s ( $n=15$ ), and in low calcium conditions this was significantly increased to  $11.2 \pm 1.5$  s ( $p<0.001$ ;  $n=14$ ). In control, the average rate of propagation in *st. radiatum* was  $100 \pm 11$   $\mu\text{m/s}$  (Table 1;  $n=15$ ) and in *st. oriens*  $99 \pm 13$   $\mu\text{m/s}$  (Table 1;  $n=15$ ), indicating that the rates in the two regions were comparable. In low calcium conditions the propagation rates were significantly decreased to  $63 \pm 10$   $\mu\text{m/s}$  (Table 1;  $p < 0.05$ ,  $n=14$ ) in *st. radiatum* and  $36 \pm 6$   $\mu\text{m/s}$  (Table 1;  $p < 0.001$ ,  $n=14$ ) in *st. oriens*. These results indicate that the propagation and the time required for onset to peak of ouabain-induced SD is partially dependent on the presence of extracellular calcium.

The lack of extracellular calcium does not effect the falling phase of ouabain-induced SD as measured in *st. radiatum* of the CA1. Fig. 8B indicates the time for the peak transmittance to decay to 75% and 50% of peak. It required  $7.2 \pm 0.8$  s and  $13.6 \pm 1.3$  s for control slices in the presence of calcium to fall to 75% and 50% of peak and in low calcium conditions it required  $6.9 \pm 0.6$  s and  $12.1 \pm 1.5$  s respectively. These changes are not statistically significant ( $p > 0.05$ ;  $n=14$ ), indicating that the falling phase of SD is a process not dependent on the presence of extracellular calcium or synaptic transmission.

### 3.3 Suramin effects both the onset and falling phases of spreading depression

A preliminary study in our laboratory indicated that suramin may have an effect on the propagation of SD, although the analysis was incomplete (Duffy and MacVicar, personal communication). In order to test the hypothesis that purinergic receptors play a role in SD, the next series of experiments was conducted in the presence of the P<sub>2</sub>-purinergic antagonist suramin (1 mM).

**Table 1** The propagation velocities of ouabain-induced spreading depression in the hippocampus in st. radiatum and st. oriens of the CA1. Control is the propagation velocity in control slices, and +Drug is the propagation velocity in the presence of the treatment listed in the first column. All velocities are expressed as a rate ( $\mu\text{m/s}$ ) and statistically significant data is denoted as \*\*\*  $p < 0.001$ , \*\*  $p < 0.01$ , \*  $p < 0.05$ .

**Table 1: The propagation velocities of ouabain-induced spreading depression in the hippocampus in *st. radiatum* and *st. oriens* of the CA1.**

Treatment	Propagation Rates ( $\mu\text{m/s}$ )			
	St. Radiatum		St. Oriens	
	<u>Control</u>	<u>+ Drug</u>	<u>Control</u>	<u>+ Drug</u>
Suramin (1 mM)	89 $\pm$ 12	64 $\pm$ 8	84 $\pm$ 17	127 $\pm$ 17
RB-2 (200 $\mu\text{M}$ )	108 $\pm$ 18	120 $\pm$ 11	91 $\pm$ 2	108 $\pm$ 6
PPADs (200 $\mu\text{M}$ )	61 $\pm$ 15	53 $\pm$ 12	58 $\pm$ 12	38 $\pm$ 10
AMP-PNP (40 $\mu\text{M}$ )	123 $\pm$ 27	68 $\pm$ 11	82 $\pm$ 11	52 $\pm$ 6
Amiloride (100 $\mu\text{M}$ )	138 $\pm$ 14	34 $\pm$ 7**	89 $\pm$ 38	75 $\pm$ 31
Benzamil (500 $\mu\text{M}$ )	75 $\pm$ 10	21 $\pm$ 7**	60 $\pm$ 14	24 $\pm$ 7
Glibenclamide (100 $\mu\text{M}$ )	112 $\pm$ 16	86 $\pm$ 10	118 $\pm$ 15	58 $\pm$ 5**
Tolbutamide (5 mM)	95 $\pm$ 17	76 $\pm$ 18	104 $\pm$ 54	79 $\pm$ 31
26mM Na <sup>-</sup>	123 $\pm$ 27	24 $\pm$ 8**	82 $\pm$ 11	43 $\pm$ 18
0 Ca <sup>2+</sup>	100 $\pm$ 11	63 $\pm$ 10*	99 $\pm$ 13	36 $\pm$ 6***
Suramin (1 mM)	47 $\pm$ 12	46 $\pm$ 7	41 $\pm$ 6	31 $\pm$ 9
Gliben. (100 $\mu\text{M}$ )	80 $\pm$ 15	36 $\pm$ 9*	39 $\pm$ 9	43 $\pm$ 7

\*\*\* p < 0.001, \*\* p < 0.01, \* p < 0.05 indicate statistically significant data sets relative to control.

**Figure 8.** Low extracellular calcium slows the onset phase but not the falling phase in stratum radiatum of the CA1 during ouabain-induced spreading depression.

- (A)** In low extracellular calcium (0  $\text{Ca}^{2+}$ , 100  $\mu\text{M}$  EGTA), the onset to peak time is increased relative to control (calcium-containing aCSF). \*\*\* denotes data significantly different than control ( $p < 0.001$ ;  $n = 14$ ).
- (B)** In low extracellular calcium (0  $\text{Ca}^{2+}$ , 100  $\mu\text{M}$  EGTA), the decays from peak transmittance to 75% and 50% respectively do not significantly differ from control ( $p > 0.05$ ;  $n = 14$ ).

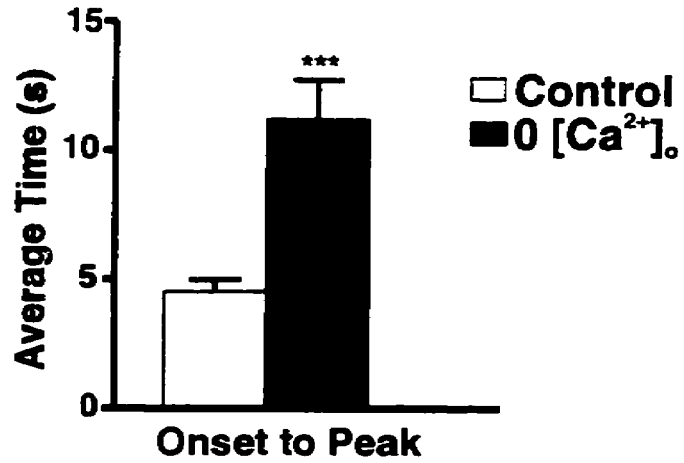
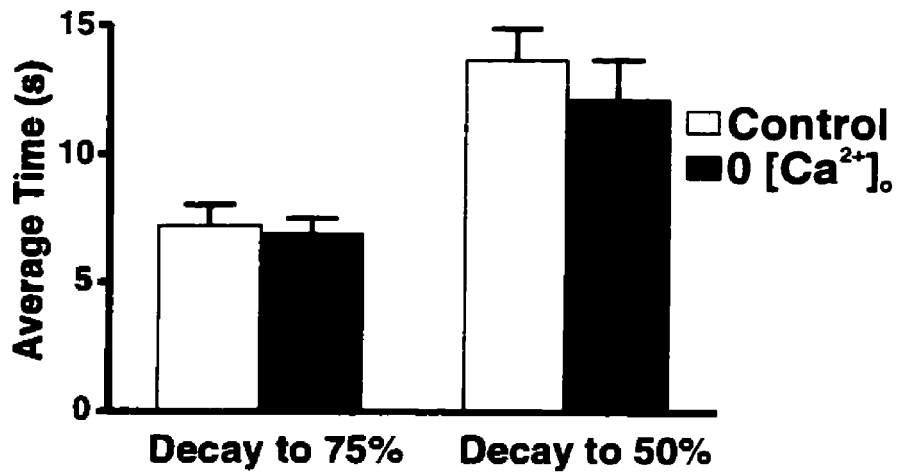
**A****B**

Fig. 9A is a tissue transmittance profile in control conditions of the pseudo-colored digital images in Fig. 9B. The transmittance profile consists of the normalized change in transmittance ( $\Delta T/T$ ) in two regions of the CA1: st. pyramidale and st. radiatum. The upper left-hand panel in Fig. 9B is a bright-field image, and regions of the CA1 (st. pyramidale, radiatum and oriens), CA2, and dentate gyrus of the hippocampus are presented. The areas of the regions analyzed are demarcated by the circles in Fig. 9B. Fig. 9B is a series of pseudo-colored digital images following the onset of ouabain-induced SD, with 0 s labeled as the onset time (20% of peak transmittance).

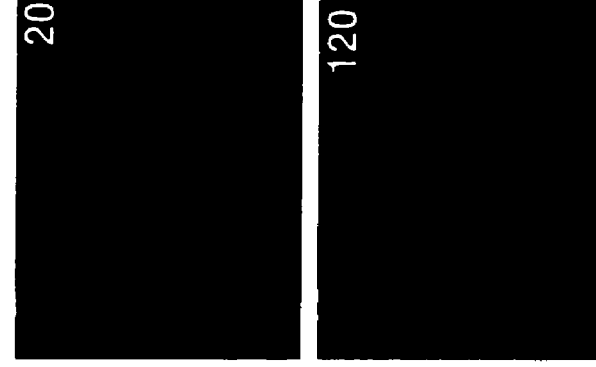
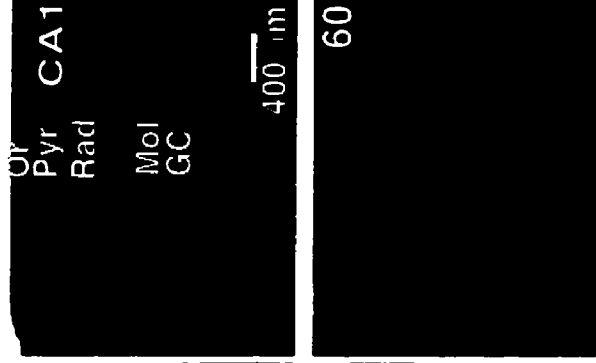
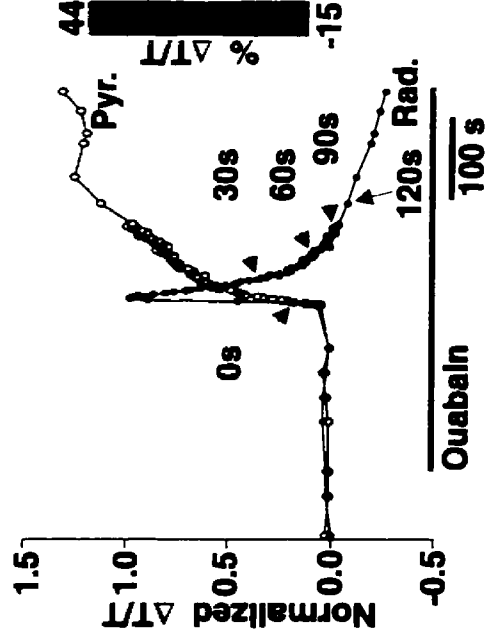
Fig. 9C is a tissue transmittance profile in the presence of suramin (1 mM) of the pseudo-colored digital images in Fig. 9D. As in Fig. 9A, the bright-field image is presented in Fig. 9D, and the areas of the regions analyzed are demarcated with circles. Similar to Fig. 9A, the onset time (20% of peak transmittance) is labeled as 0 s, and the digital images presented are chosen at similar timepoints to allow a representative comparison.

Suramin effects both the onset and falling phases of SD. The transmittance profile in Fig. 9C demonstrates that during the onset phase the time to peak relative to control (Fig. 9A) is increased. Following the initiation of SD in suramin, during the early stage of the onset phase there is a rapid increase in tissue transmittance, followed by a slowing of the rate of increase until the peak is reached (between 30-90 s in Fig. 9C). Suramin (1 mM) also has an effect on the falling phase. During the falling phase in suramin, there is a much slower return to baseline (90 s onwards), as compared to control conditions (Fig. 9A).

The results of spreading depression in 1 mM suramin were then quantified using the analysis parameters as outlined in the materials and methods. Fig. 10A indicates the three parameters analyzed in the onset phase of SD: the onset to peak, slope, and maximum slope as measured in st. radiatum of the CA1. Suramin resulted in a statistically significant effect on all three parameters: an increase in the onset to peak, and decrease in the slope and maximum slope.

**Figure 9.** Ouabain-induced spreading depression in the hippocampal slice in the presence of suramin (1 mM). **A.** Tissue transmittance profile consisting of the normalized change in transmittance ( $\Delta T/T$ ) in two regions of the CA1: st. pyramidale and st. radiatum. **B.** A series of pseudo-colored digital images following the onset of ouabain-induced spreading depression, with 0s labeled as the onset time (20% of peak transmittance). The upper left-hand image is the bright-field image showing the CA1 (st. oriens, st. pyramidale, st. radiatum), CA2, and dentate gyrus (st. moleculare, st. granulosum) regions. The areas of the regions analyzed are demarcated by the circles. **C.** Tissue transmittance profile in suramin (1 mM). **D.** Series of pseudo-colored digital images in suramin, chosen at similar timepoints to Fig. 9B. Scale bar = 400  $\mu\text{m}$ .

### A Control



### C Suramin (1 mM)

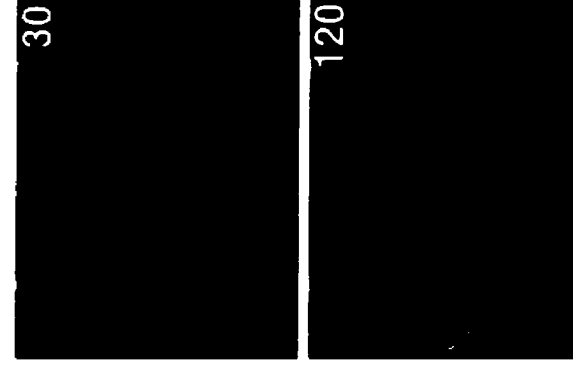
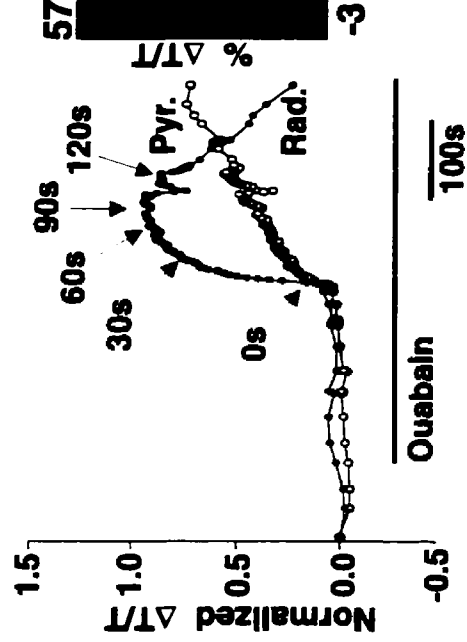
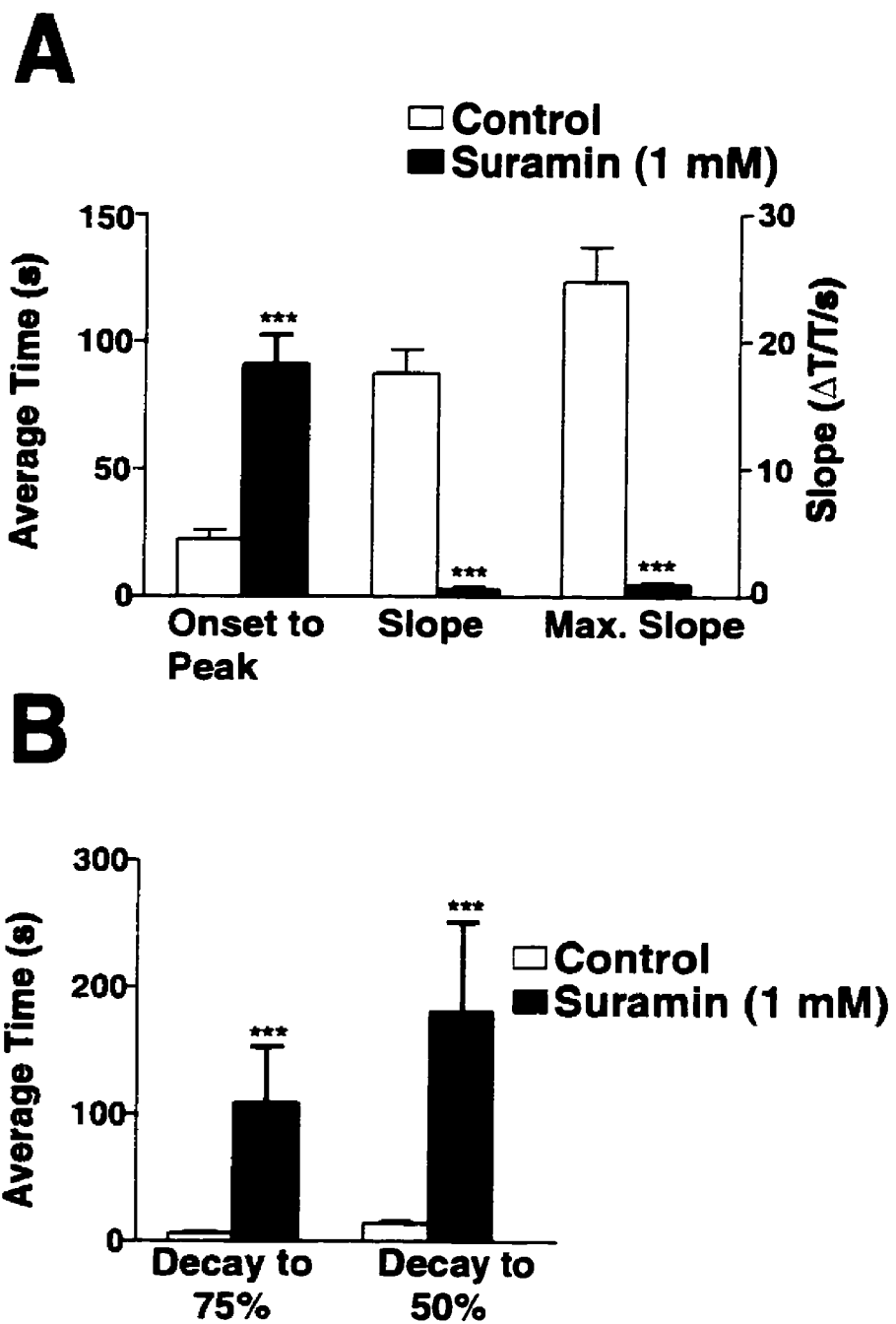


**Figure 10.** Suramin slows both the onset and falling phases in *st. radiatum* of the CA1 during ouabain-induced spreading depression.

- (A)** In suramin (1 mM), the onset to peak time is significantly increased relative to control (absence of suramin). The slope (measured from 20%-40% of peak transmittance) and maximum slope are significantly decreased. \*\*\* denotes data significantly different than control ( $p < 0.001$ ;  $n = 8$ ).
- (B)** In suramin (1 mM), the decays from peak transmittance to 75% and 50% of peak transmittance are significantly increased relative to control. \*\*\* denotes data significantly different than control ( $p < 0.001$ ;  $n = 8$ ).



In control conditions the onset to peak was  $4.5 \pm 0.8$  s ( $n=8$ ), and in suramin, as illustrated, the onset to peak significantly increased to  $91.2 \pm 11.6$  s ( $p < 0.001$ ;  $n=8$ ). The slope and maximum slope were found to be  $17.5 \pm 1.9$   $\Delta T/T/s$  and  $24.7 \pm 2.8$   $\Delta T/T/s$  in control respectively. In suramin, the slope and maximum slope were significantly lower ( $p < 0.001$ ;  $n=8$ ) at  $2.94 \pm 0.48$   $\Delta T/T/s$  and  $4.80 \pm 0.45$   $\Delta T/T/s$  respectively. The propagation rates as measured in *st. radiatum* and *st. oriens* in the presence of suramin did not significantly differ from control (Table 1;  $p > 0.05$ ;  $n=8$ ). This indicates that although suramin (1 mM) did not effect the propagation rate of the wave of ouabain-induced SD, it did maintain a significant effect on the onset to peak, slope and maximum slope of ouabain-induced SD, indicating that purinergic receptors may be involved in this phase of ouabain-induced SD.

In addition to its effects on the onset phase, suramin also had a significant effect on the falling phase, as measured in *st. radiatum* during ouabain-induced SD. Fig. 10B illustrates the time for the peak transmittance to fall to 75% and 50%. It required  $6.7 \pm 1.0$  s ( $n=8$ ) for the peak transmittance response to fall to 75%, and  $14.0 \pm 2.1$  s ( $n=8$ ) for the response to fall to 50% in control. In suramin, there was a significant increase in both of these decay times: requiring  $108.4 \pm 44.6$  s ( $p < 0.001$ ;  $n=8$ ) for the response to fall to 75% and  $180.8 \pm 70.0$  s ( $p < 0.001$ ;  $n=8$ ) for the response to fall to 50% of peak transmittance.

### **3.4 Suramin affects both the onset and falling phases of SD in low calcium conditions**

SD in calcium-containing aCSF in the presence of suramin resulted in a slowing of both the onset and falling phases, suggesting the involvement of purinergic receptors. Involvement of purinergic receptors indicates a presumed release of ATP (or related compound) during ouabain-induced SD. This raises the possibility that ATP may be released in a calcium-dependent manner similar to that shown during Schaffer collateral

stimulation (Wieraszko *et al.*, 1989). To determine if the inhibition of the falling phase by suramin is dependent on the presence of extracellular calcium, the next series of experiments tested the effect of suramin in  $0 \text{ Ca}^{2+}$  conditions.

A comparison of the tissue transmittance during ouabain-induced SD in  $0 \text{ Ca}^{2+}$  conditions and in the presence of suramin is presented in Fig. 11. Fig 11A is a transmittance profile of the changes as measured in st. radiatum and st. pyramidale of the CA1 during ouabain-induced SD. The series of pseudo-colored digital images are presented in Fig. 11B. These digital images are the changes in light tissue transmittance following the onset (20% of peak transmittance) of ouabain-induced SD. The panel in the upper left-hand corner is a bright-field image showing the CA1 (st. pyramidale, radiatum and oriens), CA2, and dentate gyrus (st. moleculare and granulosum) regions of the hippocampus, with the regions analyzed demarcated by circles.

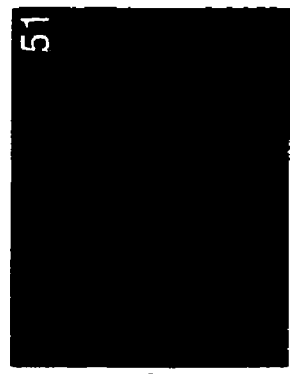
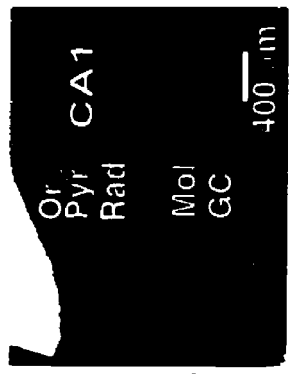
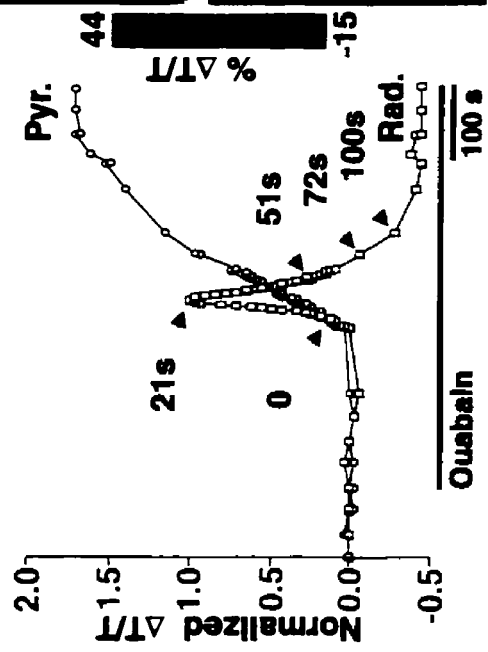
The remaining panels are pseudo-colored digital images with the time indicated following the onset of ouabain-induced SD as labeled in Fig. 11A. In  $0 \text{ Ca}^{2+}$  control conditions, there is a rapid increase to peak following onset, followed by a relatively rapid return to transmittance levels below baseline (Fig. 11A).

Fig. 11C is a light tissue transmittance profile for the changes in tissue transmittance in st. radiatum and st. pyramidale of the CA1 during ouabain-induced SD in  $0 \text{ Ca}^{2+}$  conditions and in the presence of suramin (1 mM). As in Fig. 11B, Fig. 11D is pseudo-colored digital images of the changes in light tissue transmittance following the onset of ouabain-induced SD as labeled in Fig. 11C. The bright field image is indicated showing the CA1 and dentate gyrus regions. In the presence of suramin, there is a much slower increase to peak following onset, and during the falling phase, the decay to baseline is inhibited, decaying to nearly 50% of peak transmittance at a time when the control slice had decayed to nearly 50% below baseline (Fig. 11A).

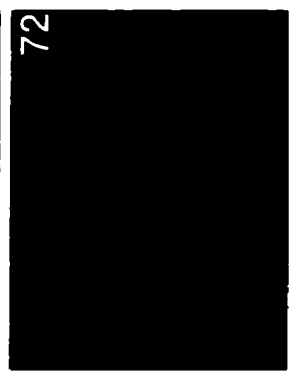
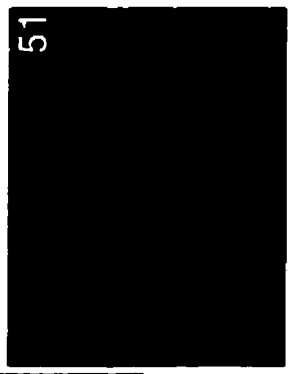
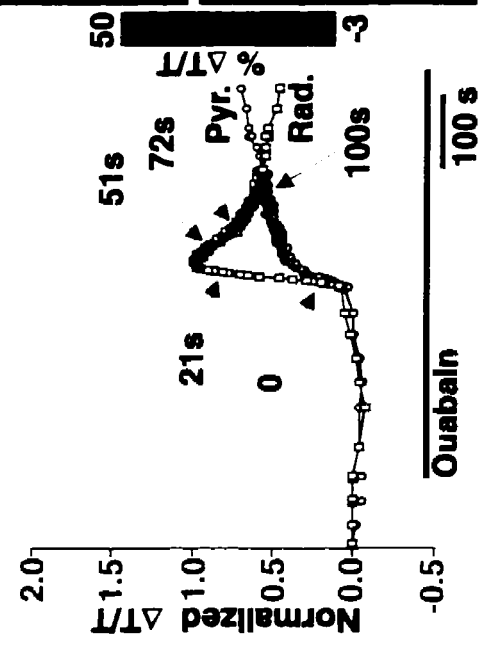
The application of suramin in low-calcium conditions resulted in an effect on the parameters analyzed in both the onset and falling phases of ouabain-induced SD, and no effect on the propagation rates, similar to its effect in calcium-containing aCSF. In control,

**Figure 11.** A comparison of the changes in tissue transmittance during ouabain-induced spreading depression in 0  $\text{Ca}^{2+}$  conditions (100  $\mu\text{M}$  EGTA) and in the presence of suramin (1 mM). **A.** Tissue transmittance profile consisting of the normalized change in transmittance ( $\Delta T/T$ ) in two regions of the CA1: st. pyramidale and st. radiatum. **B.** A series of pseudo-colored digital images following the onset of ouabain-induced spreading depression, with 0s labeled as the onset time (20% of peak transmittance). The upper left-hand image is the bright-field image showing the CA1 (st. oriens, st. pyramidale, st. radiatum), CA2, and dentate gyrus (st. moleculare, st. granulosum) regions. The areas of the regions analyzed are demarcated by the circles. **C.** Tissue transmittance profile in 0  $\text{Ca}^{2+}$  and suramin (1 mM). **D.** Series of pseudo-colored digital images in suramin, chosen at similar timepoints to Fig. 11B. Scale bar = 400  $\mu\text{m}$ .

### A Control (0 [Ca<sup>2+</sup>]<sub>o</sub>)



### C Suramin (1 mM)



the propagation rate in *st. radiatum* was  $47 \pm 12 \mu\text{m/s}$  (Table 1;  $n=7$ ) and in *st. oriens*  $41 \pm 6 \mu\text{m/s}$  (Table 1;  $n=7$ ). Suramin in low-calcium conditions did not have a significant effect on these rates, as the propagation rate in *st. radiatum* was  $46 \pm 7 \mu\text{m/s}$  (Table 1;  $p > 0.05$ ,  $n=7$ ) and in *st. oriens*  $31 \pm 9 \mu\text{m/s}$  (Table 1;  $p > 0.05$ ,  $n=7$ ).

Fig. 12A illustrates the effect of suramin on the onset to peak time. In control low-calcium conditions this was determined to be  $14.0 \pm 2.4 \text{ s}$ , and suramin resulted in a statistically significant increase in this time to  $75.2 \pm 21.5 \text{ s}$  ( $p < 0.05$ ;  $n=7$ ).

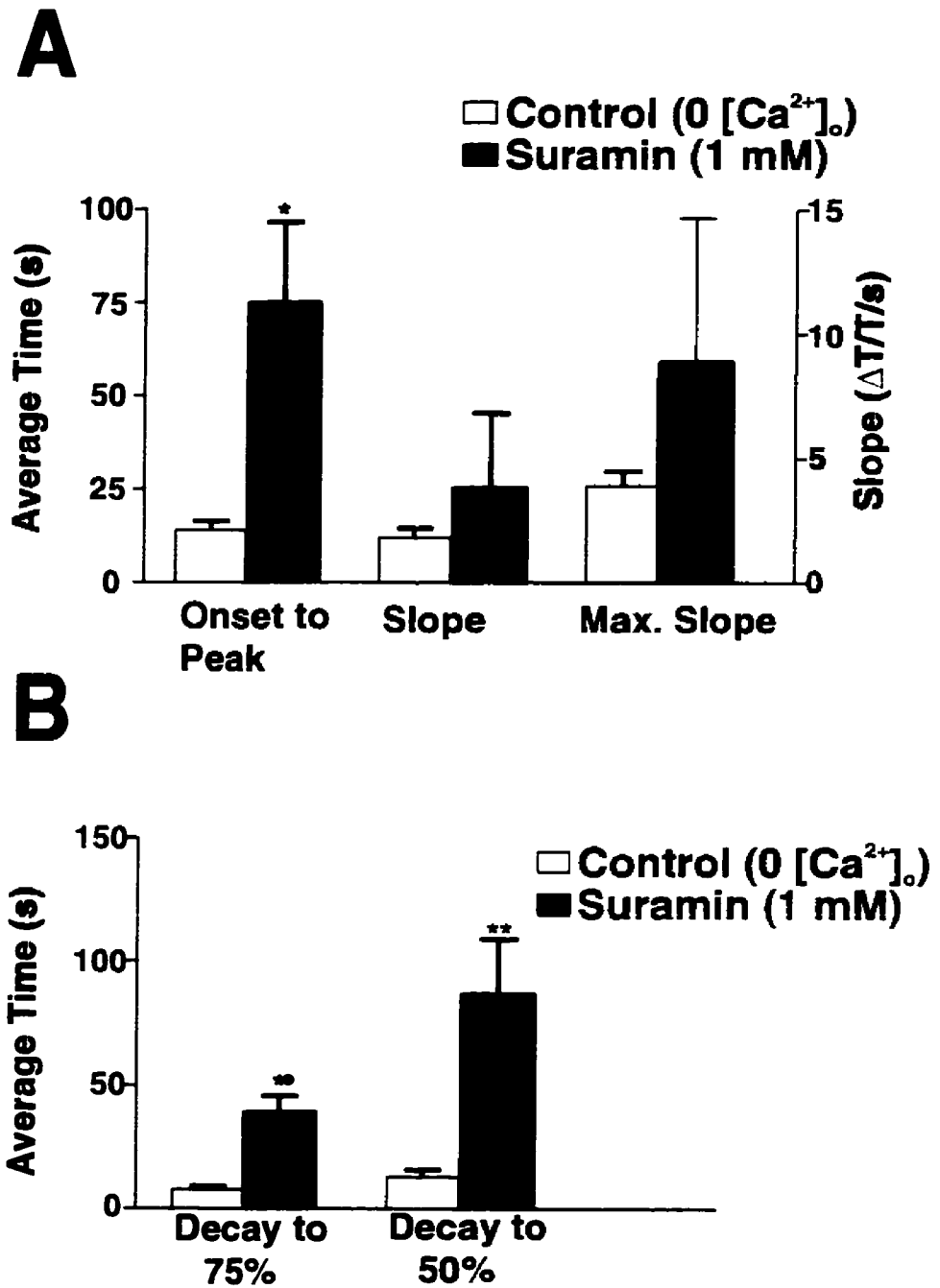
The application of suramin also resulted in a slowing of the falling phase of ouabain-induced SD. Fig. 12B illustrates the effect of suramin on the falling phase of SD as measured in *st. radiatum* of the CA1. In low-calcium control conditions the decay times to 75% and 50% were  $7.8 \pm 1.5 \text{ s}$  ( $n=7$ ), and  $13.2 \pm 2.9 \text{ s}$  ( $n=7$ ) respectively. In suramin, these times were significantly increased to  $39.4 \pm 6.3 \text{ s}$  ( $p < 0.05$ ;  $n=7$ ), and  $86.8 \pm 21.9 \text{ s}$  ( $p < 0.01$ ;  $n=7$ ) respectively.

### **3.5 Suramin in the presence of glutamatergic and GABAergic receptor antagonists effects the falling phase of SD**

Suramin (30  $\mu\text{M}$ - 300  $\mu\text{M}$ ) in whole-cell voltage clamp conditions in rat hippocampal neurons has been shown to inhibit a current activated by 10  $\mu\text{M}$  GABA in a concentration-dependent manner (Nakazawa *et al.*, 1995). In addition, suramin (100 and 300  $\mu\text{M}$ ) has also been shown to inhibit an inward current activated by kainic acid (100  $\mu\text{M}$ ), an agonist at non-NMDA receptor channels. Suramin also inhibited an inward current activated by NMDA (100  $\mu\text{M}$ ), an agonist at NMDA receptor channels in rat hippocampal neurons (Nakazawa *et al.*, 1995) and in *Xenopus* embryos (Dale and Gilday, 1996). The Nakazawa *et al.* (1995) study demonstrated for the first time that suramin, in addition to  $P_2$ -purinoceptor antagonism, can block GABA- and glutamate-gated channels.

**Figure 12.** Suramin slows both the onset and falling phases in *st. radiatum* of the CA1 during ouabain-induced spreading depression in low calcium conditions.

- (A)** In suramin (1 mM) and 0  $\text{Ca}^{2+}$  (100  $\mu\text{M}$ ), the onset to peak time is significantly increased relative to control (absence of suramin). The slope (measured from 20%-40% of peak transmittance) and maximum slope are not significantly effected relative to control ( $p > 0.05$ ;  $n=7$ ). \* denotes data significantly different than control ( $p < 0.05$ ;  $n= 7$ ).
- (B)** In suramin (1 mM) and 0  $\text{Ca}^{2+}$  (100  $\mu\text{M}$ ), the decays from peak transmittance to 75% and 50% of peak transmittance are significantly increased relative to control. \* denotes data significantly different than control ( $p < 0.05$ ;  $n=7$ , \*\*  $p < 0.01$ ;  $n=7$ ).



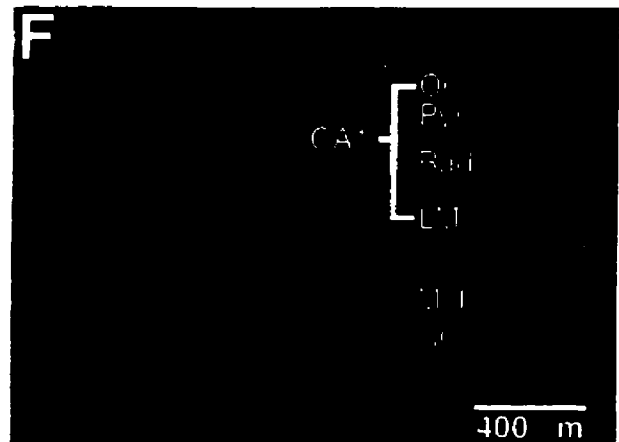
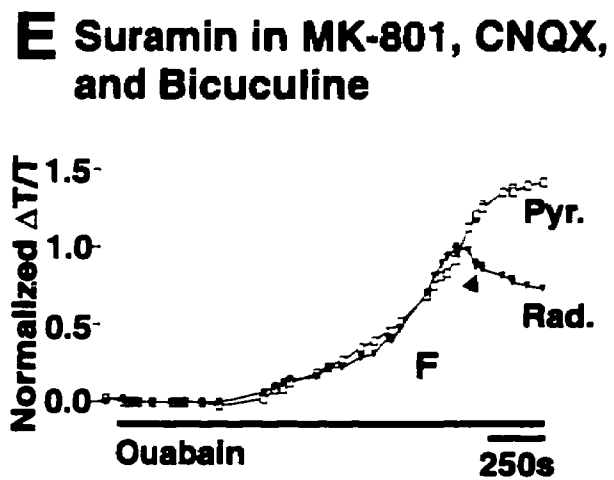
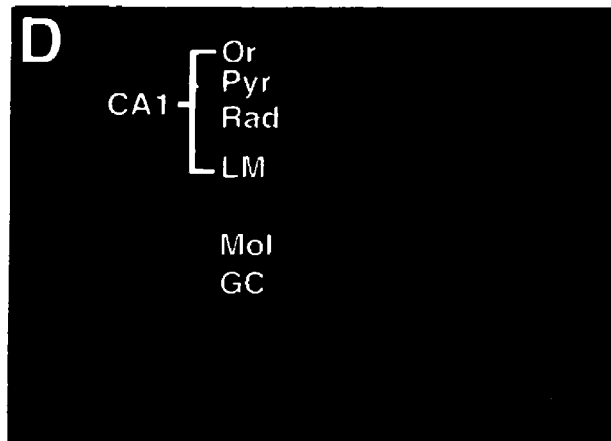
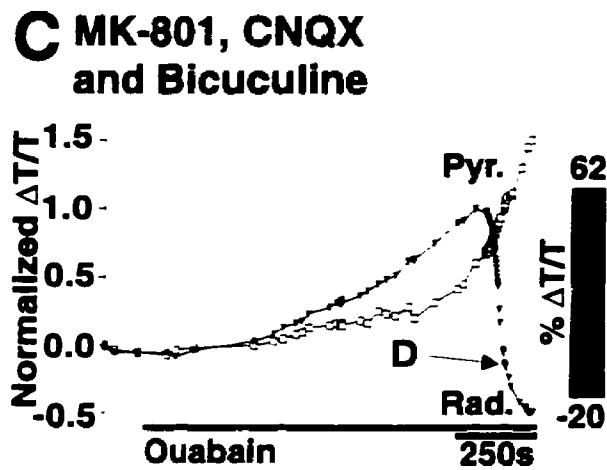
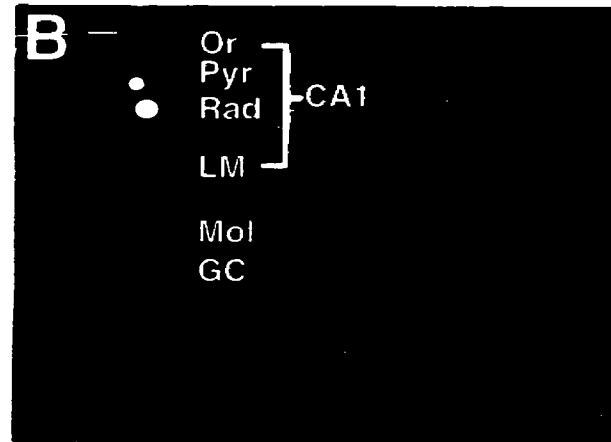
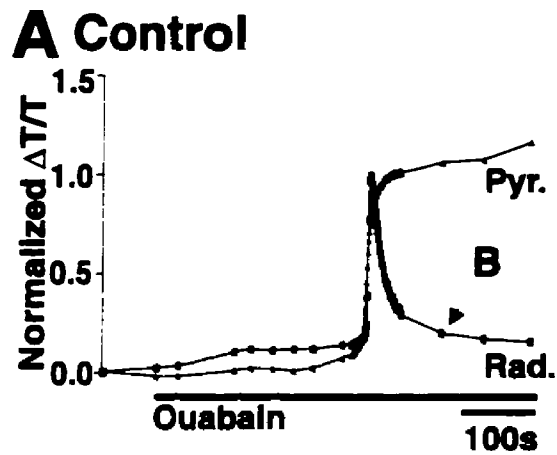
In order to control for the non-specific effect of suramin on GABA- and glutamate-gated channels, a relatively recent study was conducted in cultured rat hippocampal neurons to determine the effect of suramin in the presence of TTX (3  $\mu\text{M}$ ), hexamethonium (C6; 100  $\mu\text{M}$ ; an acetylcholine nicotinic channel antagonist), APV (100  $\mu\text{M}$ ; an NMDA receptor antagonist), CNQX (30  $\mu\text{M}$ ; a non-NMDA receptor antagonist), bicuculline (10  $\mu\text{M}$ ; a GABA<sub>A</sub> receptor antagonist) and cadmium (300  $\mu\text{M}$ ; a calcium channel antagonist), on glutamate-evoked release of ATP (Inoue *et al.*, 1995). Suramin in the presence of these drugs inhibited an increase in intracellular Ca<sup>2+</sup> evoked by ATP, and Inoue *et al.* (1995) concluded that the effect of suramin in the presence of these antagonists was due to a specific blockade of P<sub>2</sub>-purinergic receptors.

The next series of experiments was conducted to control for the non-specific effect of suramin on GABA- and glutamate-gated channels. The control solution consisted of a cocktail of NMDA, non-NMDA and GABAergic receptor antagonists: MK-801 (100  $\mu\text{M}$ ), CNQX (30  $\mu\text{M}$ ), and bicuculline (10  $\mu\text{M}$ ).

Fig. 13 is a comparison of the IOS during ouabain-induced SD in control conditions and in MK-801, CNQX, and bicuculline, with and without suramin. Fig. 13A is a tissue transmittance profile of normalized change in transmittance ( $\Delta T/T$ ) for ouabain-induced SD in control conditions (absence of any treatment), as measured in st. radiatum and st. pyramidale of the CA1. The control conditions represent a typical response of the tissue to ouabain. In st. radiatum, there is a baseline phase during which the tissue transmittance is relatively stable. The onset phase then commences with a rapid increase to peak, followed by a relatively rapid decrease of the IOS in the falling phase. Fig. 13B is a pseudo-colored digital image of the changes in transmittance 100 s after peak.

Fig. 13C is a tissue transmittance profile of the normalized change in transmittance ( $\Delta T/T$ ) for ouabain-induced SD in MK-801 (100  $\mu\text{M}$ ), CNQX (30  $\mu\text{M}$ ), and bicuculline (10  $\mu\text{M}$ ). This profile differs remarkably from the profile in control conditions (Fig. 13A), demonstrating the effect of GABA- and glutamatergic blockade on SD. The onset to peak

**Figure 13.** A comparison of the tissue transmittance during ouabain-induced spreading depression in control conditions and in MK-801 (100  $\mu\text{M}$ ), CNQX (30  $\mu\text{M}$ ), and bicuculline (10  $\mu\text{M}$ ), with and without suramin. **A.** Tissue transmittance profile consisting of the normalized change in transmittance ( $\Delta T/T$ ) in two regions of the CA1: st. pyramidale and st. radiatum. **B.** A pseudo-colored digital image as labeled in Fig. 13A. **C.** Tissue transmittance profile in MK-801, CNQX, and bicuculline in st. pyramidale and st. radiatum. **D.** A pseudo-colored digital image as labeled in Fig. 13C. **E.** Tissue transmittance profile in MK-801, CNQX, and bicuculline in the presence of suramin (1 mM) as measured in st pyramidale and st. radiatum. **F.** A pseudo-colored digital image as labeled in Fig. 13E. The areas of the regions analyzed are demarcated by the circles. All digital images in Figs 13. B,D,F are 100 s following peak to allow comparison. Scale bar = 400  $\mu\text{m}$ .



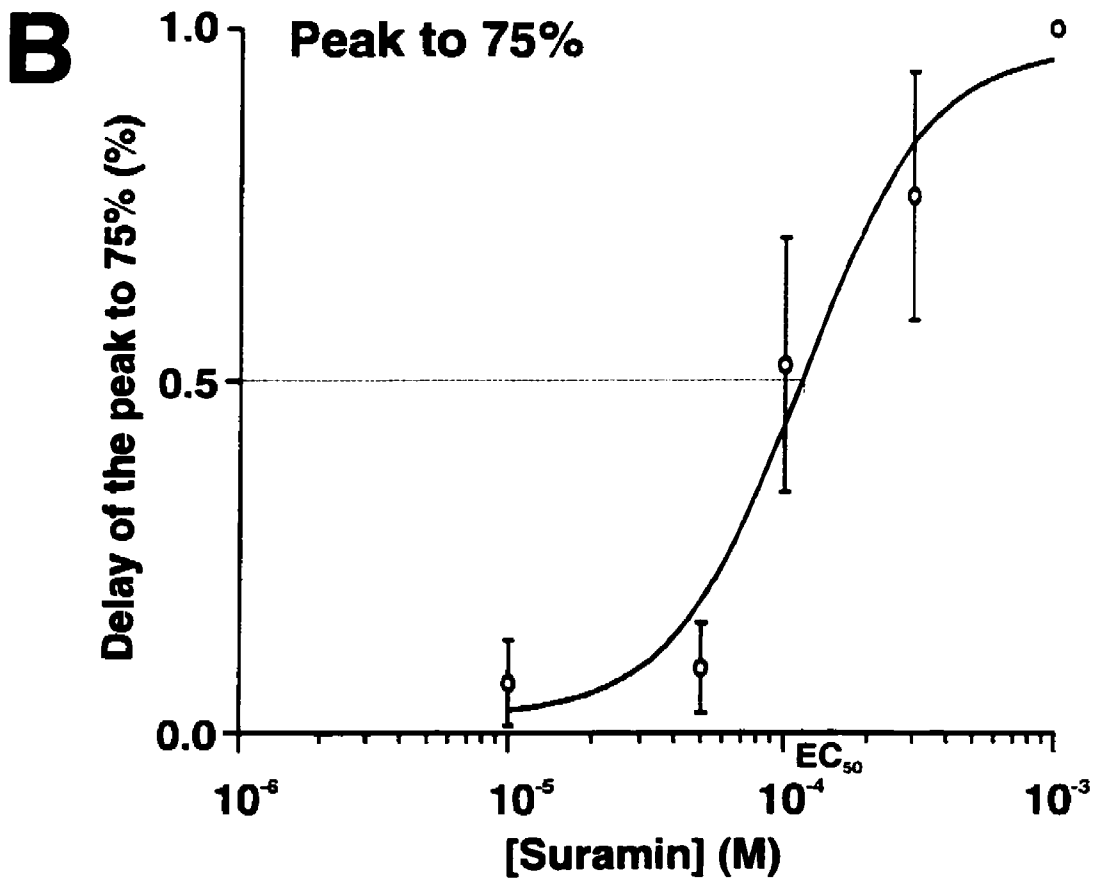
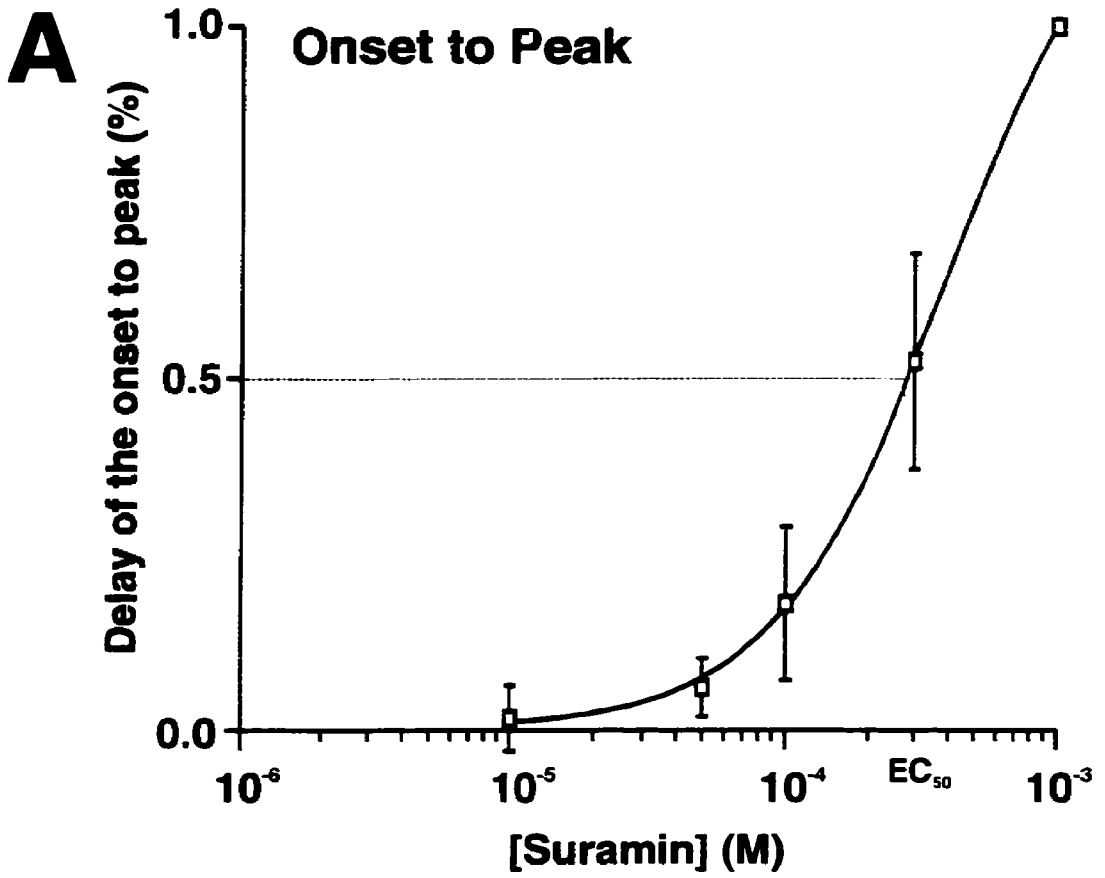
time is dramatically increased, as in both st. pyramidale and st. radiatum there is a very slow increase in the tissue transmittance to peak. In st. radiatum, following the peak tissue transmittance, there is a rapid decrease in the tissue transmittance to levels below baseline. St. pyramidale, in contrast to st. radiatum, rapidly begins an increase to maximum, reaching a level nearly 50% above that in st. radiatum. Fig. 13D is a pseudo-colored digital image of the change in transmittance 100 s after peak, to allow a comparison to the profile in Fig. 13A and digital image in Fig. 13B. In the region of the CA1 quantified, the tissue transmittance has decayed much further below baseline than in control conditions (Fig. 13A).

A tissue transmittance profile for the changes in transmittance during ouabain-induced SD in MK-801, CNQX, and bicuculline in the presence of suramin is presented in Fig. 13E. Similar to Fig. 13C (control), there is a dramatic increase in the onset to peak time in st. radiatum relative to control conditions (Fig. 13A). However, in the presence of suramin, the falling phase of ouabain-induced SD is slowed. Fig. 13F is a pseudo-colored digital image of the change in transmittance 100 s after peak. The digital image in Fig. 13F contrasts Fig. 13D, as at this point in control, the tissue transmittance has decayed to well over 100% below baseline. In the presence of suramin (Fig. 13F), the transmittance has decayed nearly 5%, indicating that suramin slows the falling phase in a manner independent of a blockade of GABA- and glutamatergic receptors.

### **3.6 Suramin demonstrates a dose-dependent inhibition of both the onset and falling phases of spreading depression**

Suramin in the presence of MK-801 (100  $\mu\text{M}$ ), CNQX (30  $\mu\text{M}$ ), and bicuculline (10  $\mu\text{M}$ ) was determined to slow both the onset and falling phases of ouabain-induced SD in st. radiatum of the CA1 in a concentration dependent manner. The dose-response curve for the effect of suramin on the onset phase is presented in Fig. 14A. The effect of suramin on the falling phase is presented in Fig. 14B.

**Figure 14.** Suramin in the presence of MK-801 (100  $\mu\text{M}$ ), CNQX (30  $\mu\text{M}$ ) and bicuculline (10  $\mu\text{M}$ ) slowed both the onset and falling phases of ouabain-induced SD in a concentration dependent manner. **A)** The dose-response curve for the effect of suramin on the onset phase. The  $\text{EC}_{50}$  and Hill coefficient were 383  $\mu\text{M}$  and 1.40. **B)** The dose-response curve for the effect of suramin on the falling phase. The  $\text{EC}_{50}$  and Hill coefficient were 115  $\mu\text{M}$  and 1.88. Each time point represents the mean  $\pm$  S.E.M. for an n=3 to 5.



The response in the onset curve was quantified using the onset to peak time, and normalized to the onset to peak obtained with 1 mM suramin, from the conventional equation:

$$\frac{t_{[x]} - t_{\text{control}}}{t_{1\text{mM}} - t_{\text{control}}}$$

where the maximal response is assumed to occur at 1 mM, and x represents the concentration of suramin either at 300, 100, 50 or 10  $\mu\text{M}$ . In Fig. 14B, the response was quantified in a similar fashion, but from peak to 75% of peak normalized to the time from peak to 75% obtained with 1 mM suramin. Each time point represents the mean  $\pm$  SEM for an n=3 to 5. The curves in Fig. 14A and B are drawn in accordance with the conventional expression:  $t/t_{\text{max}} = 1/(1 + (\text{EC}_{50}/[\text{suramin}])^n)$ , where t is the time from peak to 75% of peak,  $\text{EC}_{50}$  is the suramin concentration which evokes half-maximal inhibition, and n is the Hill coefficient. The  $\text{EC}_{50}$  and Hill coefficient values were 383  $\mu\text{M}$  and 1.40 (Fig. 14A) and 115  $\mu\text{M}$  and 1.88 (Fig. 14B) respectively.

### 3.7 PKC inhibition with H-7 does not effect the onset or falling phases of spreading depression

Suramin, in addition to its well-characterized purinergic antagonism, has also been shown to inhibit protein kinase C (PKC) in a concentration-dependent manner (Mahoney *et al.*, 1990). Conversely, it was demonstrated that at low concentrations (10–40  $\mu\text{M}$ ), suramin can activate PKC (Mahoney *et al.*, 1990). PKC activation can be ruled out as a possible non-specific effect of suramin as in the present study suramin was applied at much higher concentrations (ranging from 10  $\mu\text{M}$ - 1 mM).

The involvement of PKC has been demonstrated during SD initiated by a high KCl solution in rat cerebral cortex *in vivo* (Krivanek and Koroleva, 1996). The next series of experiments was conducted to control for the inhibition of PKC as a possible non-specific

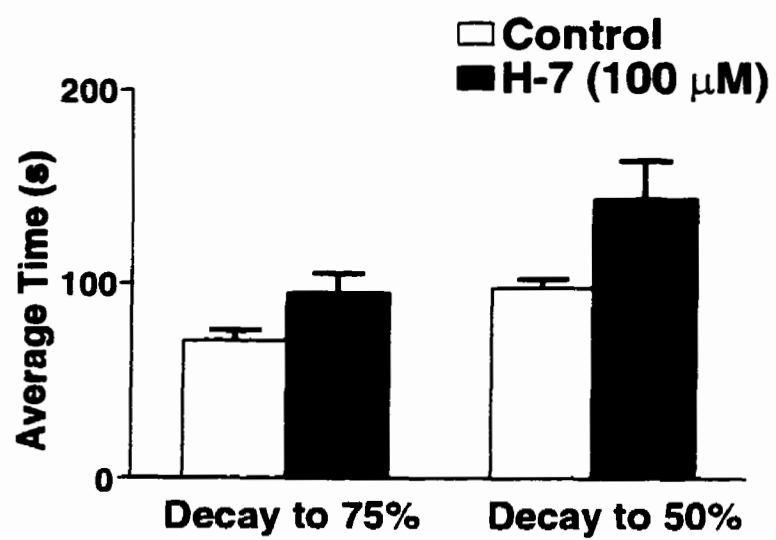
effect of suramin on the falling phase of SD. The goal was to determine if H-7, a potent inhibitor of PKC at a concentration of 100  $\mu\text{M}$ , has an effect on the falling phase of ouabain-induced SD, in the presence of the GABA- and glutamatergic antagonists: MK-801 (100  $\mu\text{M}$ ), CNQX (30  $\mu\text{M}$ ), and bicuculline (10  $\mu\text{M}$ ).

Fig. 15 illustrates the parameters analyzed during the falling phase of ouabain-induced SD as measured in *st. radiatum* of the CA1. The decays to 75% and 50% of peak were  $70.9 \pm 4.9$  s and  $97.9 \pm 4.8$  s in control respectively. In the presence of H-7, these times were  $95.3 \pm 10.0$  s and  $144.5 \pm 20.0$  s respectively, indicating no statistically significant change ( $p > 0.05$ ;  $n=5$ ). PKC inhibition by H-7 in the presence of GABA- and glutamatergic antagonists does not effect the falling phase of ouabain-induced SD. This rules out PKC inhibition as a possible explanation for a non-specific effect of suramin on the falling phase of ouabain-induced SD.

### **3.8 Reactive Blue 2 effects the falling phase of spreading depression, but not in the presence of NMDA, non-NMDA, and GABAergic receptor antagonists**

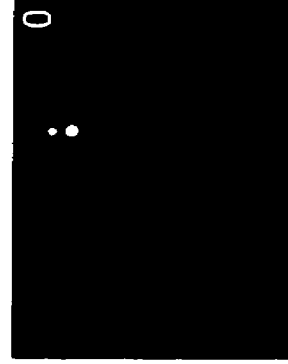
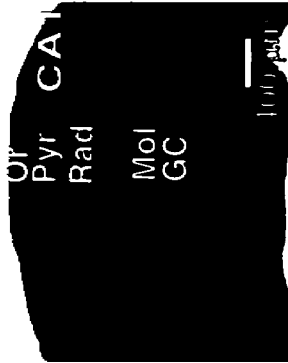
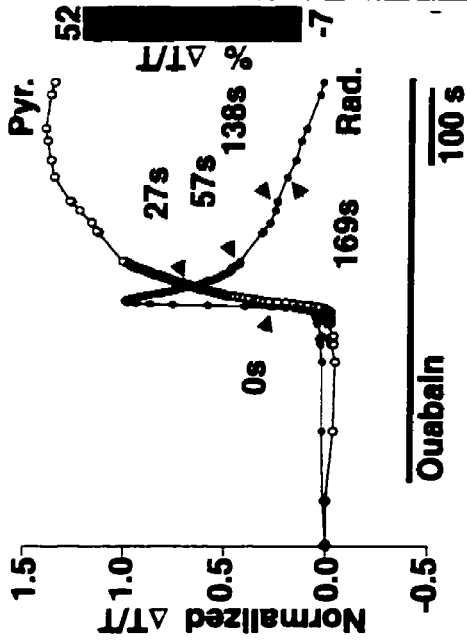
The next series of experiments was conducted to determine the effect of the purinergic receptor antagonist RB-2 (200  $\mu\text{M}$ ) on the propagation of ouabain-induced SD. RB-2 slowed the falling phase similar to suramin, but unlike suramin was without effect on the onset phase. Fig. 16A is a tissue transmittance profile in control conditions of the pseudo-colored digital images in Fig. 16B. The transmittance profile consists of the normalized change in transmittance ( $\Delta T/T$ ) in two regions of the CA1: *st. radiatum* and *st. pyramidale*. The upper left-hand panel in Fig. 16B is a bright-field image, and regions of the CA1, CA2 and dentate gyrus are presented. The areas of the regions analyzed in Fig. 16A are demarcated by the circles in Fig. 16B. The digital images are labeled at times following the onset (0 s, 20% of peak transmittance). Fig. 16C is a tissue transmittance profile in the presence of RB-2 (200  $\mu\text{M}$ ) of the digital images in Fig. 16D. As in Fig. 16A, the bright-field image is presented in Fig. 16D, and the areas of the regions analyzed

**Figure 15.** H-7 does not affect the falling phase in *st. radiatum* of the CA1 during ouabain-induced spreading depression in the presence of GABA- and glutamatergic antagonists. In H-7 (100  $\mu$ M), MK-801 (100  $\mu$ M), CNQX (30  $\mu$ M), and bicuculline (10  $\mu$ M), the decays from peak transmittance to 75% and 50% of peak transmittance are not significantly different than control (MK-801, CNQX, and bicuculline).

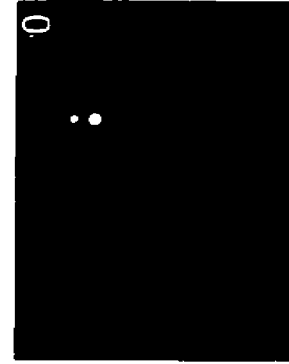
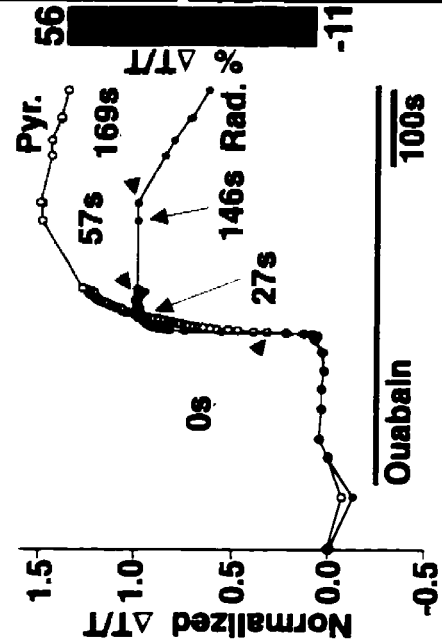


**Figure 16.** Ouabain-induced spreading depression in the hippocampal slice in the presence of RB-2 (200  $\mu\text{M}$ ). **A.** Tissue transmittance profile consisting of the normalized change in transmittance ( $\Delta T/T$ ) in two regions of the CA1: st. pyramidale and st. radiatum. **B.** A series of pseudo-colored digital images following the onset of ouabain-induced spreading depression, with 0 s labeled as the onset time (20% of peak transmittance). The upper left-hand image is the bright-field image showing the CA1 (st. oriens, st. pyramidale, st. radiatum), CA2, and dentate gyrus (st. moleculare, st. granulosum) regions. The areas of the regions analyzed are demarcated by the circles. **C.** Tissue transmittance profile in RB-2 (200  $\mu\text{M}$ ). **D.** Series of pseudo-colored digital images in RB-2, chosen at similar timepoints to Fig. 16B to allow a comparison. Scale bar = 400  $\mu\text{m}$ .

# A Control



# C RB-2 (200 $\mu$ M)



are demarcated with circles. The digital images presented in Figs. 16B and D are chosen at similar timepoints to allow a representative comparison.

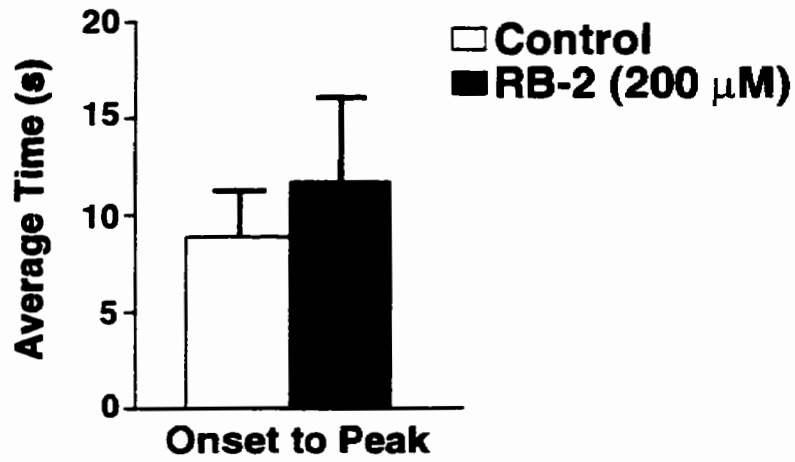
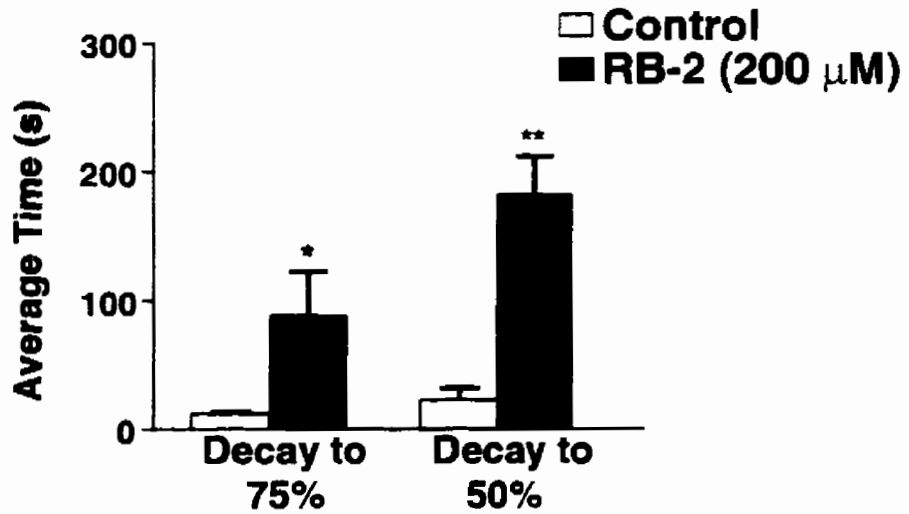
RB-2 (200  $\mu\text{M}$ ) effects the falling but not the onset phase of ouabain-induced SD. In *st. radiatum* in Fig. 16C, there is a rapid increase to peak similar to control (Fig. 16A), and subsequently the falling phase is slowed. 169 s after onset, RB-2 has decayed from peak less than 5%, as compared to controls which have nearly returned to baseline. The results were quantified according to the analysis parameters, and presented in Fig. 17. Fig. 17A indicates the onset to peak time during the onset phase of SD. In control conditions it required  $8.9 \pm 2.4$  s ( $n=7$ ) and in RB-2 it required  $11.7 \pm 4.4$  s ( $p > 0.05$ ;  $n=6$ ), indicating no statistical significance. In addition, in control conditions the propagation rate was  $108 \pm 18$   $\mu\text{m/s}$  (Table 1;  $n=7$ ) in *st. radiatum* and  $91 \pm 2$   $\mu\text{m/s}$  (Table 1;  $n=7$ ) in *st. oriens*. In the presence of RB-2 these propagation rates were not significantly effected, measured at  $120 \pm 11$   $\mu\text{m/s}$  (Table 1;  $p > 0.05$ ;  $n=7$ ) in *st. radiatum* and  $108 \pm 6$   $\mu\text{m/s}$  (Table 1;  $p > 0.05$ ;  $n=7$ ) in *st. oriens*.

Fig. 17B indicates the parameters analyzed during the falling phase of ouabain-induced SD. The decays to 75% and 50% of peak were  $12.2 \pm 1.5$  s and  $22.5 \pm 9.6$  s in control respectively. In the presence of RB-2, these times were significantly increased ( $p < 0.001$ ) to  $88.2 \pm 34.5$  s and  $181.6 \pm 29.8$  s respectively, indicating that in RB-2 the falling phase was significantly slowed.

RB-2 (10-100  $\mu\text{M}$ ), similar to suramin, has been shown to inhibit a current activated by 10  $\mu\text{M}$  GABA in a concentration-dependent manner (Nakazawa *et al.*, 1995). RB-2 (10-30  $\mu\text{M}$ ) also inhibited a current activated by kainic acid (100  $\mu\text{M}$ ) and NMDA (100  $\mu\text{M}$ ) (Nakazawa *et al.*, 1995). In order to control for the effects of RB-2 on GABA- and glutamate-gated channels, our next series of experiments was conducted employing a cocktail of NMDA, non-NMDA and GABAergic receptor antagonists.

**Figure 17.** RB-2 slows the falling phase but not the onset phase of ouabain-induced spreading depression in *st. radiatum* of the CA1.

- (A)** In RB-2 (200  $\mu\text{M}$ ), the onset to peak time is not significantly affected ( $p > 0.05$ ;  $n=6$ ), relative to control (absence of RB-2).
- (B)** In RB-2 (200  $\mu\text{M}$ ), the decays from peak transmittance to 75% and 50% of peak transmittance are significantly increased relative to control. \* denotes data significantly different than control ( $p < 0.05$ ;  $n=6$ , \*\*  $p < 0.01$ ;  $n=6$ ).

**A****B**

The control solution consisted of MK-801 (100  $\mu\text{M}$ ), CNQX (30  $\mu\text{M}$ ), and bicuculline (10  $\mu\text{M}$ ). The goal was to determine if RB-2 (200  $\mu\text{M}$ ) has an effect on the falling phase in the presence of these antagonists. Fig. 18 indicates the parameters analyzed during the falling phase of ouabain-induced SD. In MK-801, CNQX, and bicuculline, the decays to 75% and 50% of peak were  $33.8 \pm 13.6$  s and  $52.7 \pm 16.1$  s respectively. In the presence of RB-2, the decays to 75% and 50% of peak were  $32.8 \pm 7.6$  s ( $p > 0.05$ ;  $n=5$ ) and  $56.5 \pm 12.6$  s ( $p > 0.05$ ;  $n=5$ ) respectively. This indicates that the falling phase of ouabain-induced SD in the presence of the antagonists was not significantly effected by RB-2.

### **3.9 PPADs effects the onset phase of spreading depression, but not in the presence of NMDA, non-NMDA, and GABAergic receptor antagonists**

The next series of experiments was conducted to determine the effect of the purinergic receptor antagonist PPADs (200  $\mu\text{M}$ ) on the propagation of ouabain-induced SD. PPADs inhibited the onset phase but not the falling phase of ouabain-induced SD. Fig. 19A is a tissue transmittance profile in control conditions of the pseudo-colored digital images in Fig. 19B. The bright-field image is presented in the upper left-hand panel of Fig. 19B showing regions of the CA1 and dentate gyrus, and the areas of the regions analyzed are demarcated with circles. The digital images in Fig. 19B follow the onset of ouabain-induced SD, with 0 s labeled as the onset time (20% of peak transmittance).

Fig. 19C is a tissue transmittance profile in the presence of PPADs (200  $\mu\text{M}$ ) of the pseudo-colored digital images in Fig. 19D. As in Fig. 19B, the bright-field image is presented in Fig. 19D, and the areas of the regions analyzed are demarcated with circles. Similar to Fig. 19A, the onset time (20% of peak transmittance) is labeled as 0 s, and the digital images presented in Figs. 19B and 19D are chosen at similar timepoints to allow a comparison.

**Figure 18.** RB-2, in the presence of GABA- and glutamatergic antagonists, does not effect the falling phase of ouabain-induced spreading depression in st. radiatum of the CA1. In RB-2 (200  $\mu\text{M}$ ), MK-801 (100  $\mu\text{M}$ ), CNQX (30  $\mu\text{M}$ ), and bicuculine (10  $\mu\text{M}$ ), the decays from peak transmittance to 75% and 50% of peak transmittance do not significantly differ from control ( $p > 0.05$ ;  $n=5$ ).

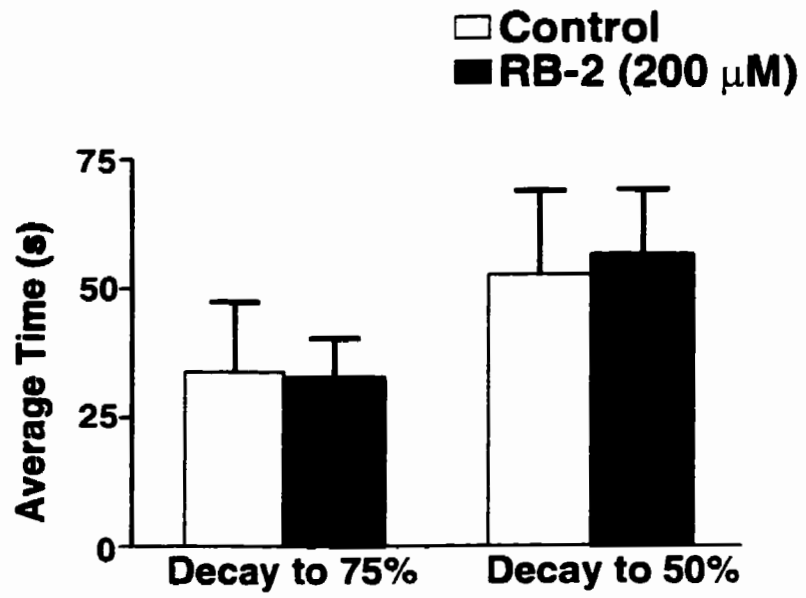
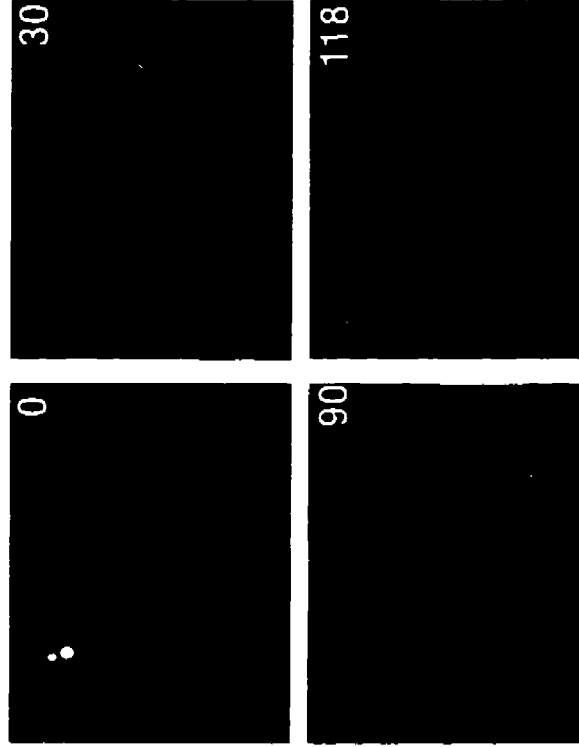
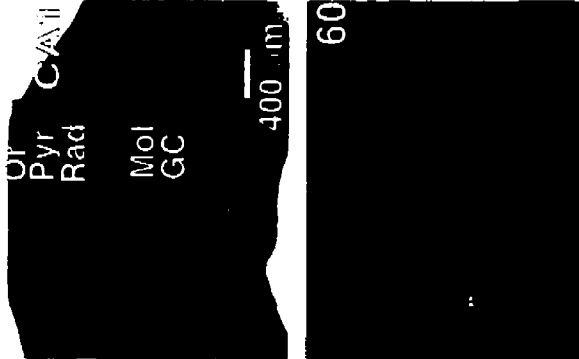
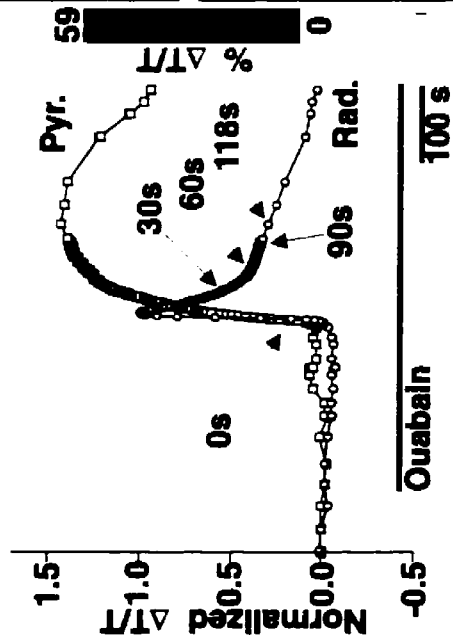
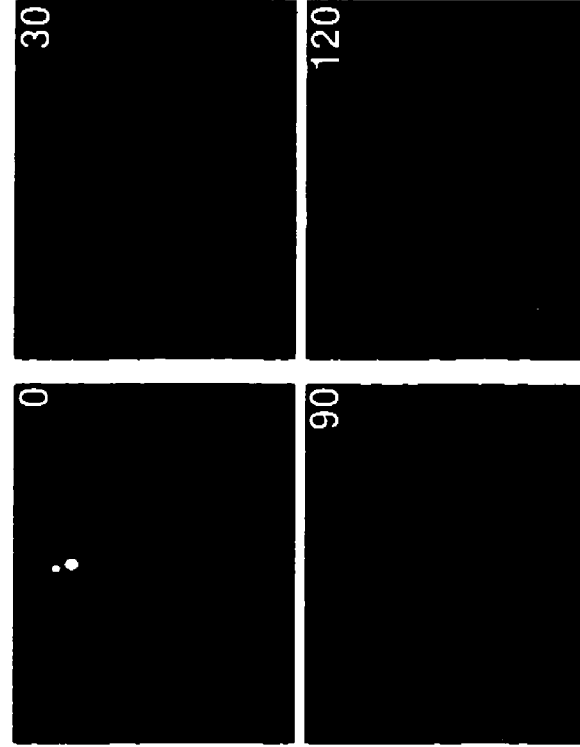
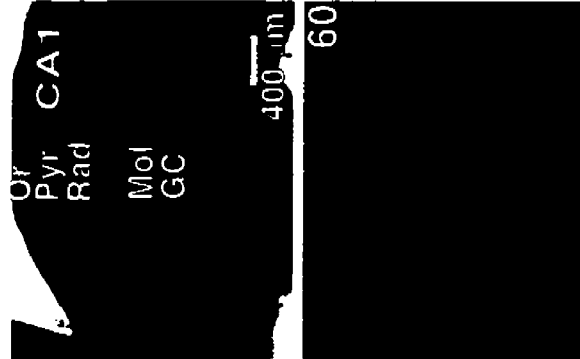
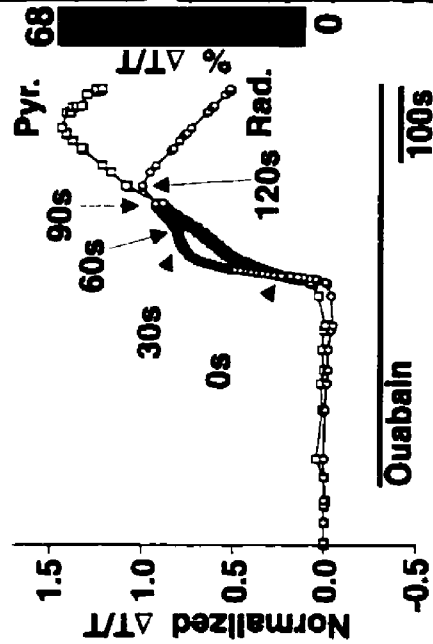


**Figure 19.** Ouabain-induced spreading depression in the hippocampal slice in the presence of PPADs (200  $\mu\text{M}$ ). **A.** Tissue transmittance profile consisting of the normalized change in transmittance ( $\Delta T/T$ ) in two regions of the CA1: st. pyramidale and st. radiatum. **B.** A series of pseudo-colored digital images following the onset of ouabain-induced spreading depression, with 0 s labeled as the onset time (20% of peak transmittance). The upper left-hand image is the bright-field image showing the CA1 (st. oriens, st. pyramidale, st. radiatum), CA2, and dentate gyrus (st. moleculare, st. granulosum) regions. The areas of the regions analyzed are demarcated by the circles. **C.** Tissue transmittance profile in PPADs (200  $\mu\text{M}$ ). **D.** Series of pseudo-colored digital images in PPADs, chosen at similar timepoints to Fig. 19B to allow a comparison. Scale bar = 400  $\mu\text{m}$ .

# A Control



# C PPADS (200 $\mu\text{M}$ )



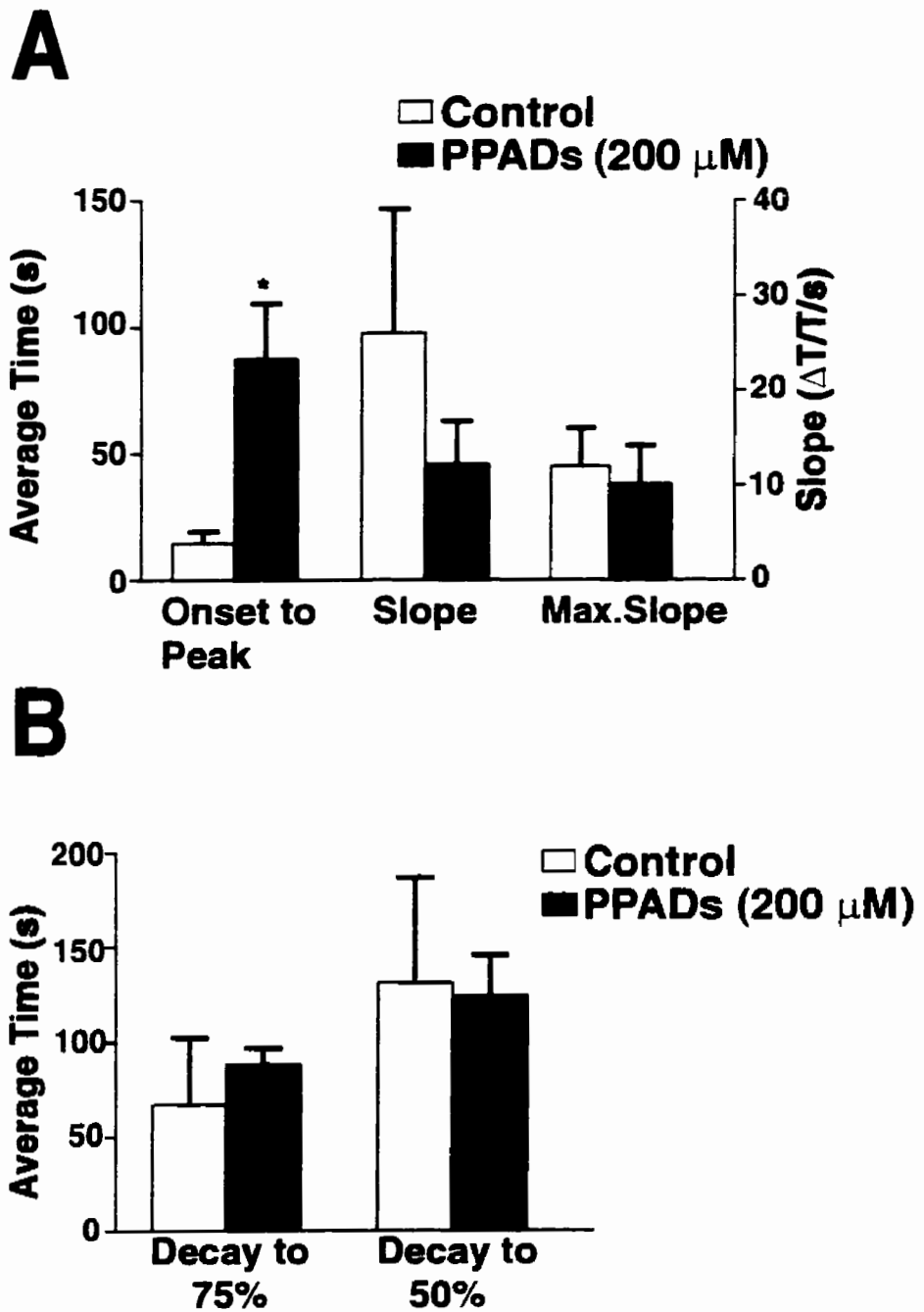
It is apparent from Fig. 19C, that in *st. radiatum*, the onset to peak time is increased from control conditions (Fig. 19A), but the falling phase occurs normally. Following the initiation of SD in PPADs, there is a rapid increase in transmittance during the early stage of the onset phase, followed by a slowing of the rate of increase until the peak is reached (around 120 s in Fig. 19C).

Fig 20A indicates the effects of PPADs (200  $\mu\text{M}$ ) on the onset phase of ouabain-induced SD. In control conditions the time to peak was  $14.7 \pm 4.5$  s ( $n=4$ ) and in PPADs this was significantly increased to  $87.7 \pm 21.9$  s ( $p < 0.05$ ,  $n=4$ ). The slope as measured from 20% to 40% of peak transmittance was not significantly affected ( $p > 0.05$ ;  $n=4$ ) by the presence of PPADs, consistent with the rapid increase in tissue transmittance during the early stage of the onset phase (Fig. 19C). In control conditions the slope was determined to be  $12.0 \pm 4.0$   $\Delta T/T/s$  and in PPADs  $10.1 \pm 4.1$   $\Delta T/T/s$ . The maximum slope was also not significantly affected ( $p > 0.05$ ;  $n=4$ ) by PPADs. In control conditions the maximum slope was  $26.1 \pm 13.0$   $\Delta T/T/s$  and in PPADs  $12.2 \pm 4.5$   $\Delta T/T/s$ . This indicates that PPADs slowed preferentially the latter part of the onset phase (shown in Fig. 19C). PPADs did not affect the propagation rates in either *st. radiatum* or *st. oriens* relative to control. In control the propagation velocity was  $61 \pm 15$   $\mu\text{m/s}$  (Table 1;  $n=4$ ) in *st. radiatum* and  $58 \pm 12$   $\mu\text{m/s}$  (Table 1;  $n=4$ ) in *st. oriens*. In PPADs the propagation velocity was  $53 \pm 12$   $\mu\text{m/s}$  (Table 1;  $p > 0.05$ ;  $n=4$ ) in *st. radiatum* and  $38 \pm 10$   $\mu\text{m/s}$  (Table 1;  $p > 0.05$ ;  $n=4$ ) in *st. oriens*.

Fig. 20B indicates the parameters analyzed during the falling phase of spreading depression. In control conditions, the decays to 75% and 50% of peak were  $67.0 \pm 35.0$  s and  $131.1 \pm 55.6$  s respectively. In the presence of PPADs, there was no significant effect ( $p > 0.05$ ) on the falling phase. In PPADs, the decays to 75% and 50% of peak were  $88.1 \pm 8.8$  s and  $124.0 \pm 21.5$  s respectively.

**Figure 20.** PPADs slows the onset phase but not the falling phase of ouabain-induced spreading depression in *st. radiatum* of the CA1.

- (A)** In PPADs (200  $\mu\text{M}$ ), the onset to peak time is significantly increased relative to control (absence of PPADs). The slope (measured from 20%-40% of peak transmittance) and maximum slope are not significantly affected relative to control ( $p > 0.05$ ;  $n=4$ ). \* denotes data significantly different than control ( $p < 0.05$ ;  $n= 4$ ).
- (B)** In PPADs (200  $\mu\text{M}$ ), the decay from peak transmittance to 75% and 50% of peak transmittance do not significantly differ relative to control ( $p > 0.05$ ;  $n=4$ ).



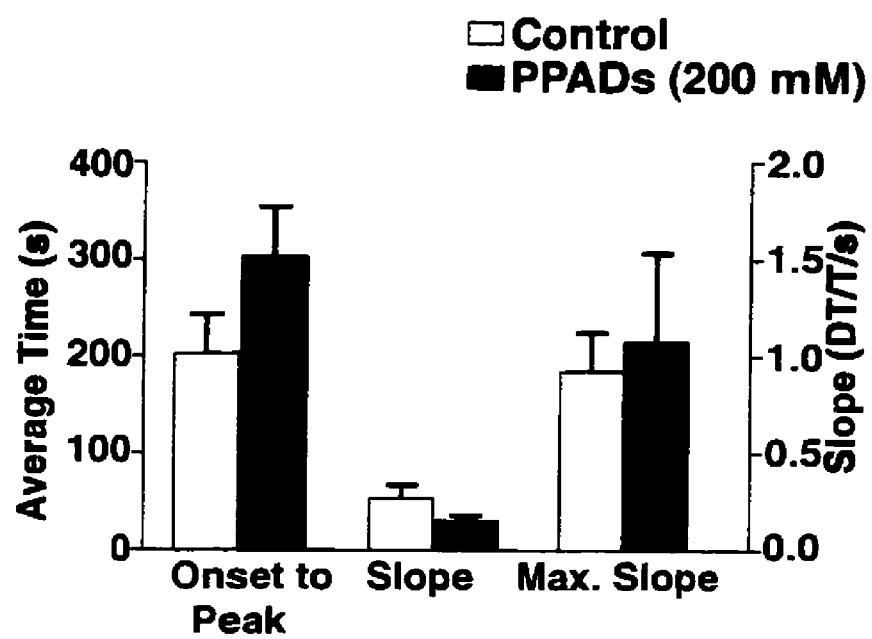
The next series of experiments tested PPADs in the presence of a cocktail of NMDA, non-NMDA, and GABAergic receptor antagonists, although PPADs has been shown to have no effect on these receptors (Dale and Gilday, 1996), or on glutamate-induced currents in CA1 pyramidal cells (Motin and Bennett, 1995). The control solution consisted of MK-801 (100  $\mu$ M), CNQX (30  $\mu$ M), and bicuculline (10  $\mu$ M).

PPADs (200  $\mu$ M) in the presence of the antagonists does not effect the onset phase of ouabain-induced SD. Fig. 21 indicates the parameters analyzed during the onset phase of ouabain-induced SD. In control conditions the onset to peak time was  $202.8 \pm 40.7$  s ( $n=3$ ) and in PPADs it was not significantly effected at  $303.9 \pm 49.9$  s ( $p > 0.05$ ;  $n=4$ ). The slope as measured from 20% to 40% of peak transmittance was also not significantly effected ( $p > 0.05$ ;  $n=4$ ) by the presence of PPADs, consistent with the extremely slow increase in tissue transmittance during the onset phase. In MK-801, CNQX and bicuculline, the slope was determined to be  $0.3 \pm 0.1$  and in PPADs it was  $0.1 \pm 0.03$   $\Delta T/T/s$ . The maximum slope (based on a two-point comparison) was also not significantly affected by PPADs in the presence of MK-801, CNQX, and bicuculline. In control conditions the maximum slope was  $0.9 \pm 0.2$  and in PPADs it was  $1.1 \pm 0.5$   $\Delta T/T/s$ . This indicates that PPADs does not maintain an effect on the onset phase of ouabain-induced SD in the presence of MK-801, CNQX, and bicuculline.

### **3.10 Ectonucleotidase inhibition with AMP-PNP does not effect the onset or falling phases of spreading depression**

A recent study determined that all currently available  $P_{2x}$  and  $P_{2y}$  purinergic antagonists, including suramin, PPADs, and RB-2, inhibit the breakdown of ATP by acting as ecto-nucleotidase inhibitors (Ziganshin *et al.*, 1996). The next series of experiments was conducted to control for ectonucleotidase inhibition as a possible non-specific effect for the results obtained with PPADs, suramin and RB-2. AMP-PNP (40  $\mu$ M), a potent ecto-

**Figure 21.** PPADs, in the presence of GABA- and glutamatergic antagonists, does not effect the onset phase of ouabain-induced spreading depression in *st. radiatum* of the CA1. In PPADs (200  $\mu\text{M}$ ), MK-801 (100  $\mu\text{M}$ ), CNQX (30  $\mu\text{M}$ ), and bicuculline (10  $\mu\text{M}$ ), the onset to peak time, slope, and maximum slope do not significantly differ from control ( $p > 0.05$ ).



nucleotidase inhibitor, was determined to have no effect on either the onset or falling phases of ouabain-induced SD. Fig. 22A indicates the onset to peak time during ouabain-induced SD. It required  $7.8 \pm 0.6$  s ( $n=5$ ) in control conditions and not significantly different at  $5.7 \pm 0.7$  s ( $p > 0.05$ ;  $n=5$ ) in AMP-PNP. The propagation rates were also not effected by the presence of AMP-PNP. In control the propagation velocity was  $123 \pm 27$   $\mu\text{m/s}$  (Table 1;  $n=5$ ) in *st. radiatum* and  $82 \pm 11$   $\mu\text{m/s}$  (Table 1;  $n=5$ ) in *st. oriens*. These rates were not significantly different at  $68 \pm 11$   $\mu\text{m/s}$  (Table 1;  $p > 0.05$ ;  $n=5$ ) in *st. radiatum* and  $52 \pm 6$   $\mu\text{m/s}$  (Table 1;  $p > 0.05$ ;  $n=5$ ) in *st. oriens* in the presence of AMP-PNP. Fig. 22B indicates the parameters analyzed during the falling phase of ouabain-induced SD. The decays to 75% and 50% of peak were  $18.4 \pm 2.4$  s ( $n=5$ ) and  $52.0 \pm 15.7$  s ( $n=5$ ) in control conditions and not significantly different at  $15.4 \pm 1.6$  s ( $p > 0.05$ ;  $n=5$ ) and  $34.5 \pm 4.5$  s ( $p > 0.05$ ;  $n=5$ ) in AMP-PNP. This rules out ectonucleotidase inhibition as a possible explanation for the effects of the purinergic antagonists suramin, PPADs, and RB-2 during ouabain-induced SD.

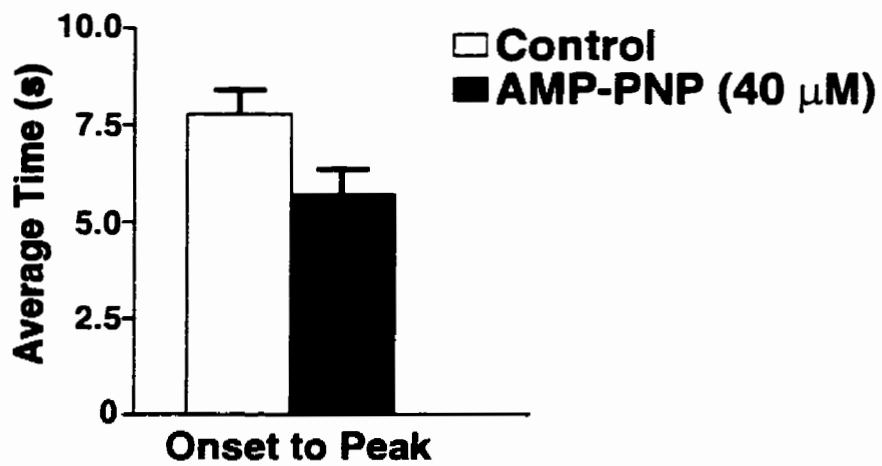
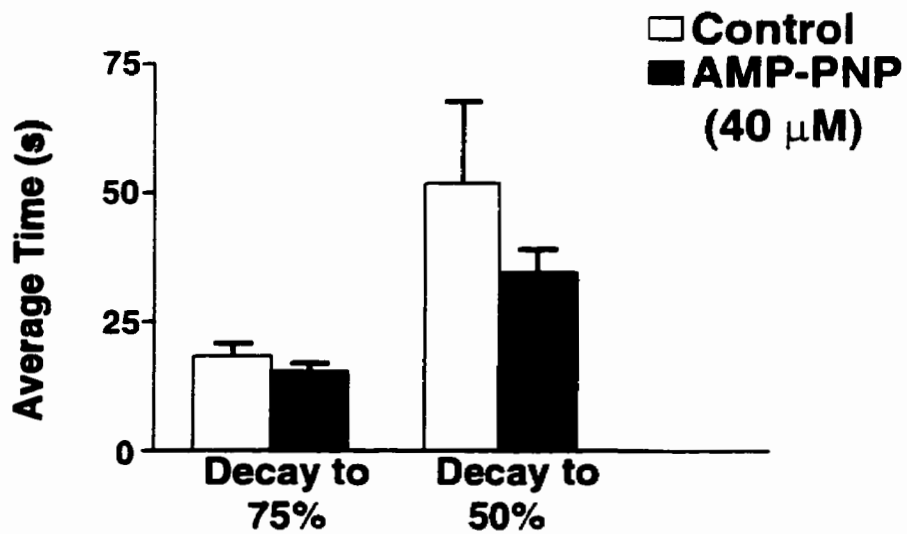
### **3.11 Glibenclamide has an effect on the onset and falling phases of spreading depression**

Glibenclamide, an antidiabetic sulfonylurea is an antagonist of intracellular ATP-sensitive  $\text{K}^+$  channels (Cook, 1988; Quast and Cook, 1989). It has been suggested that sulfonylurea receptors, which are members of ATP binding cassette proteins, may also be permeable to ATP (Al-Awqati, 1995). Shear stress in blood vessels releases ATP, and this release is blocked by glibenclamide (Hasséssian *et al.*, 1993). Diazoxide opened ATP-sensitive  $\text{K}^+$  channels when ATP or ADP were present in the cell (Larsson *et al.*, 1993), an effect that may be explained by diazoxide opening the sulfonylurea receptor and allowing the secretion of ATP (Al-Awqati, 1995).

**Figure 22.** AMP-PNP does not effect either the onset or falling phase of ouabain-induced spreading depression in *st. radiatum* of the CA1.

**(A)** In AMP-PNP (40  $\mu\text{M}$ ), the onset to peak time is not significantly effected ( $p > 0.05$ ;  $n=5$ ), relative to control (absence of RB-2).

**(B)** In AMP-PNP (40  $\mu\text{M}$ ), the decays from peak transmittance to 75% and 50% of peak transmittance are not significantly effected relative to control ( $p > 0.05$ ;  $n=5$ ).

**A****B**

Using [ $^3\text{H}$ ]-glibenclamide as a radioligand, a comparative *in vitro* autoradiographic study of glibenclamide binding sites in the rat brain, as well as other mammalian species, was conducted (Zini *et al.*, 1993). Glibenclamide binding sites were found in the hippocampus with the highest densities in the fascia dentata of the CA3 and CA4 fields of Ammon's horn, and in a lower density in the CA1 region (Zini *et al.*, 1993). It has been suggested that the presynaptic location of glibenclamide binding sites may represent the presence of ATP-sensitive  $\text{K}^+$  channels, during which activation of metabolic stress, such as anoxia, could prevent the excessive release of glutamate (Ben-Ari, 1990; Tremblay *et al.*, 1991; Zini *et al.*, 1993).

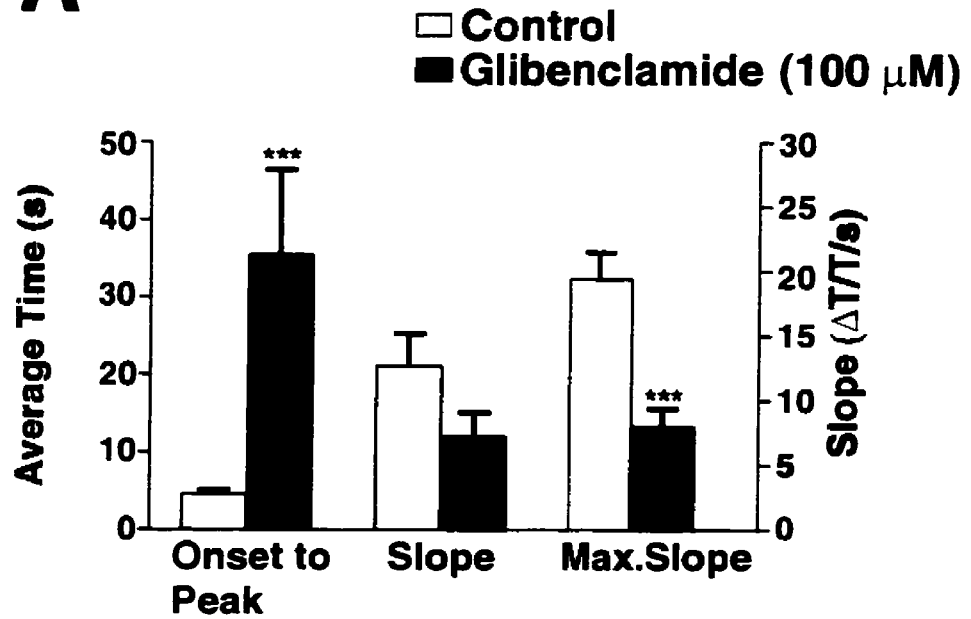
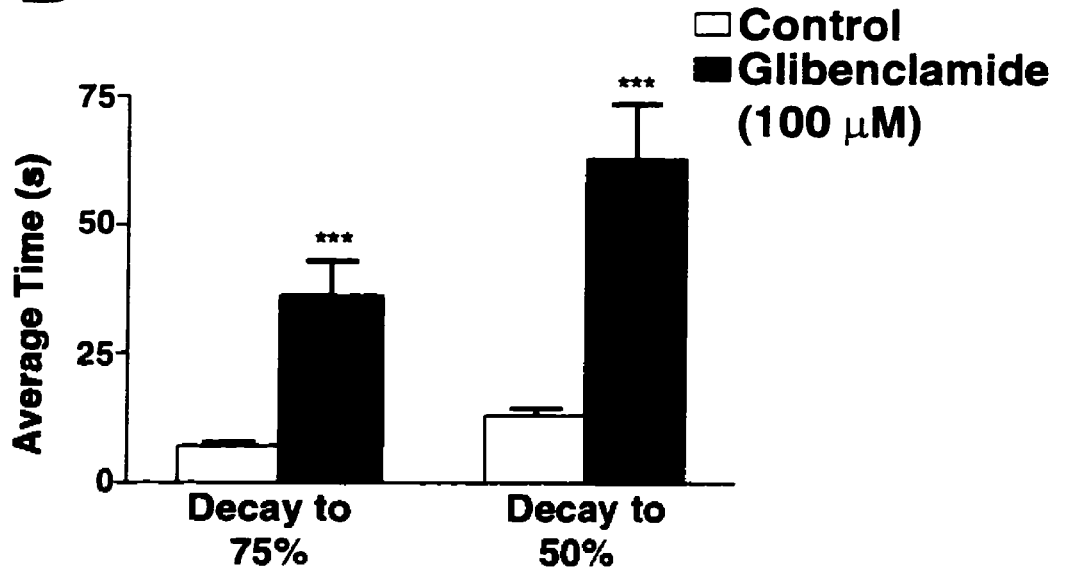
The objective of this series of experiments was to determine if glibenclamide has an effect on the propagation of spreading depression. Fig. 23A indicates the parameters analyzed during the onset phase. In control conditions the onset to peak was determined to be  $4.6 \pm 0.5$  s, and in glibenclamide the onset to peak was significantly increased to  $35.4 \pm 10.9$  s ( $p < 0.001$ ;  $n=9$ ). The slope in control conditions was  $12.6 \pm 2.5$  and in glibenclamide was  $7.2 \pm 1.9$  ( $p > 0.05$ ;  $n=9$ ). The maximum slope in control conditions was  $19.4 \pm 2.1$   $\Delta\text{T}/\text{T}/\text{s}$  and in glibenclamide was significantly lowered ( $p < 0.001$ ;  $n=9$ ) to  $8.0 \pm 1.4$   $\Delta\text{T}/\text{T}/\text{s}$ . In control, the propagation rate was  $112 \pm 16$   $\mu\text{m}/\text{s}$  (Table 1;  $n=9$ ) in st. radiatum in control. The propagation rate in st. radiatum was not significantly different at  $86 \pm 10$   $\mu\text{m}/\text{s}$  (Table 1;  $p > 0.05$ ;  $n=9$ ) in glibenclamide. However, in control, the propagation rate in st. oriens was  $86 \pm 10$   $\mu\text{m}/\text{s}$  (Table 1;  $n=9$ ) in control and significantly decreased in the presence of glibenclamide to  $58 \pm 5$   $\mu\text{m}/\text{s}$  (Table 1;  $p < 0.01$ ;  $n=9$ ).

In addition to its effects on the onset phase, glibenclamide also has a significant effect on the falling phase of the tissue transmittance in st. radiatum of the CA1. As Fig. 23B illustrates, in control conditions it required  $7.1 \pm 0.7$  s for the peak transmittance to fall to 75% of peak, and  $13.2 \pm 1.3$  s for the tissue transmittance to fall to 50% of peak. Glibenclamide resulted in a significant increase ( $p < 0.001$ ;  $n=9$ ) in both of these times,

**Figure 23.** Glibenclamide slows both the onset and falling phases in *st. radiatum* of the CA1 during ouabain-induced spreading depression.

**(A)** In glibenclamide (100  $\mu\text{M}$ ), the onset to peak time is significantly increased relative to control (absence of suramin). The slope (measured from 20%–40% of peak transmittance) does not significantly differ from control, and the maximum slope is significantly decreased. \*\*\* denotes data significantly different than control ( $p < 0.001$ ;  $n=9$ ).

**(B)** In glibenclamide (100  $\mu\text{M}$ ), the decays from peak transmittance to 75% and 50% of peak transmittance are significantly increased relative to control. \*\*\* denotes data significantly different than control ( $p < 0.001$ ;  $n=9$ ).

**A****B**

requiring  $36.1 \pm 6.8$  s and  $62.8 \pm 10.8$  s for the transmittance to fall to 75% and 50% of peak transmittance respectively.

### 3.12 Glibenclamide effects only the falling phase of spreading depression in low calcium conditions

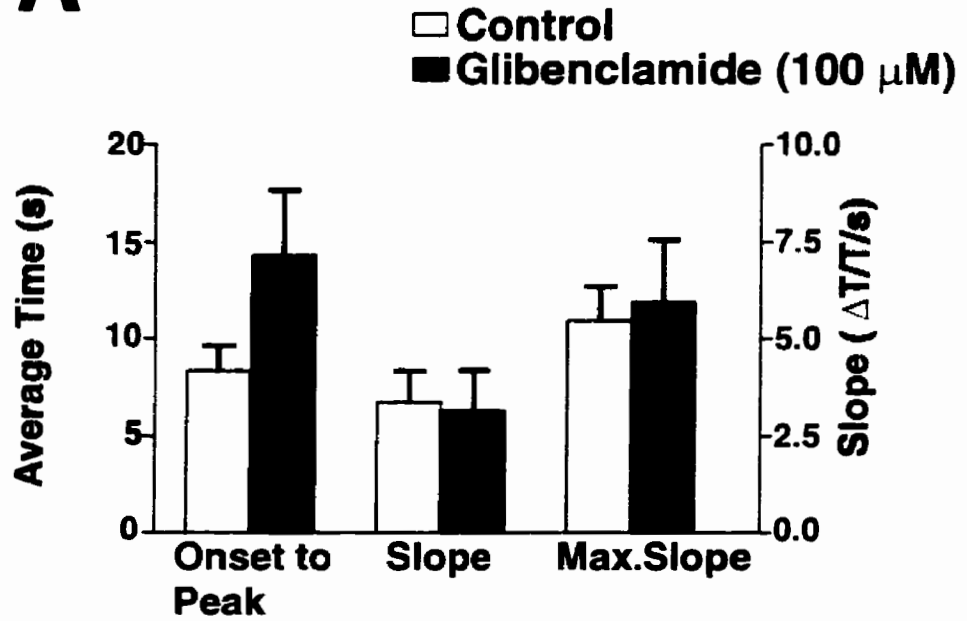
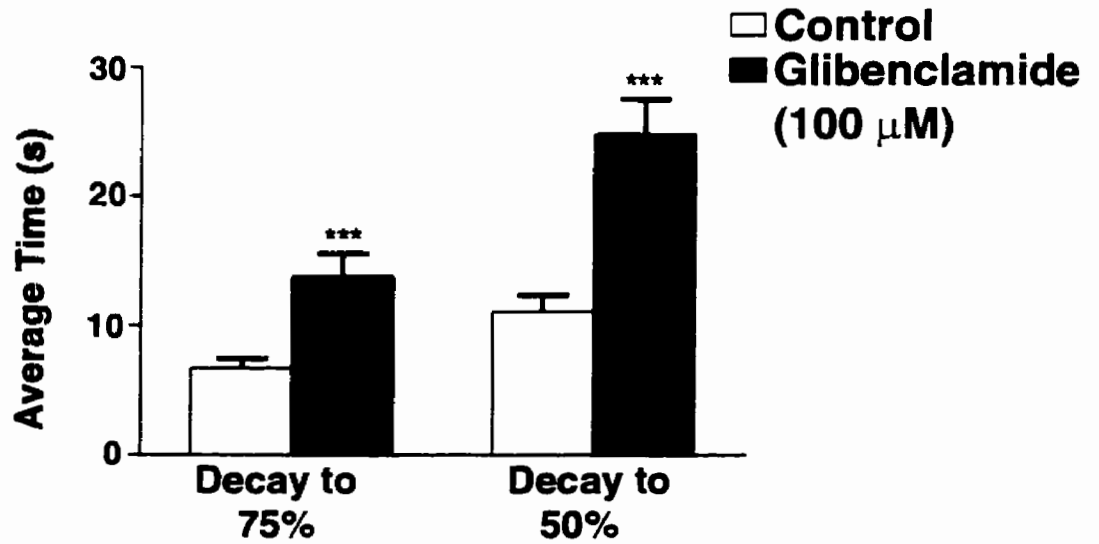
The next series of experiments was conducted to determine if glibenclamide in conditions of low calcium has an effect on the propagation of SD. It was determined that glibenclamide, unlike its effect in calcium-containing aCSF, has an effect preferentially on the falling phase of SD in conditions of low calcium. Fig. 24A indicates the parameters analyzed during the onset phase of ouabain-induced SD as measured in st. radiatum of the CA1. The onset to peak was determined to be  $8.3 \pm 1.3$  s in control, and not significantly different at  $14.3 \pm 3.3$  s ( $p > 0.05$ ;  $n=9$ ) in glibenclamide. In control, the propagation rate was  $80 \pm 15$   $\mu\text{m/s}$  (Table 1;  $n=9$ ) in st. radiatum and  $39 \pm 9$   $\mu\text{m/s}$  (Table 1;  $n=9$ ) in st. oriens. Glibenclamide significantly decreased the propagation rate in st. radiatum to  $36 \pm 9$   $\mu\text{m/s}$  (Table 1;  $p < 0.05$ ;  $n=9$ ), but did not significantly alter the propagation rate in st. oriens measured at  $43 \pm 7$   $\mu\text{m/s}$  (Table 1;  $p > 0.05$ ;  $n=9$ ). These effects are opposite to that observed in calcium-containing aCSF (see Table 1 for a comparison). In control conditions the slope and maximum slope were found to be  $3.4 \pm 0.8$   $\Delta T/T/s$  and  $5.5 \pm 0.9$   $\Delta T/T/s$  respectively. In glibenclamide the slope and maximum slope were not significantly different at  $3.1 \pm 1.0$   $\Delta T/T/s$  ( $p > 0.05$ ;  $n=9$ ) and  $6.0 \pm 1.6$   $\Delta T/T/s$  ( $p > 0.05$ ;  $n=9$ ).

Glibenclamide, in low calcium conditions, effects the falling phase of SD. As shown in Fig. 24B it required  $6.7 \pm 0.7$  s and  $11.1 \pm 1.2$  s for the peak transmittance to fall to 75% and 50% respectively in control conditions. In glibenclamide, there was a statistically significant increase to  $13.8 \pm 1.7$  s ( $p < 0.001$ ;  $n=9$ ) and  $24.8 \pm 2.8$  s ( $p < 0.001$ ;  $n=9$ ) for the peak transmittance to fall to 75% and 50% respectively. This suggests that in conditions of low calcium, unlike in calcium-containing solution, the onset phase of SD is not affected by the presence of glibenclamide.

**Figure 24.** Glibenclamide slows the falling phase in *st. radiatum* of the CA1 during ouabain-induced spreading depression in low calcium conditions.

**(A)** In 0  $\text{Ca}^{2+}$  (100  $\mu\text{M}$  EGTA) and glibenclamide (100  $\mu\text{M}$ ), the onset to peak time, slope, and maximum slope do not significantly differ from control ( $p > 0.05$ ;  $n=9$ ).

**(B)** In 0  $\text{Ca}^{2+}$  (100  $\mu\text{M}$  EGTA) and glibenclamide (100  $\mu\text{M}$ ), the decays from peak transmittance to 75% and 50% of peak transmittance are significantly increased relative to control. \*\*\* denotes data significantly different than control ( $p < 0.001$ ;  $n=9$ ).

**A****B**

However, the falling phase of ouabain-induced SD is inhibited by the application of glibenclamide with or without the presence of extracellular calcium.

### **3.13 Tolbutamide does not have an effect on the onset or falling phases of spreading depression**

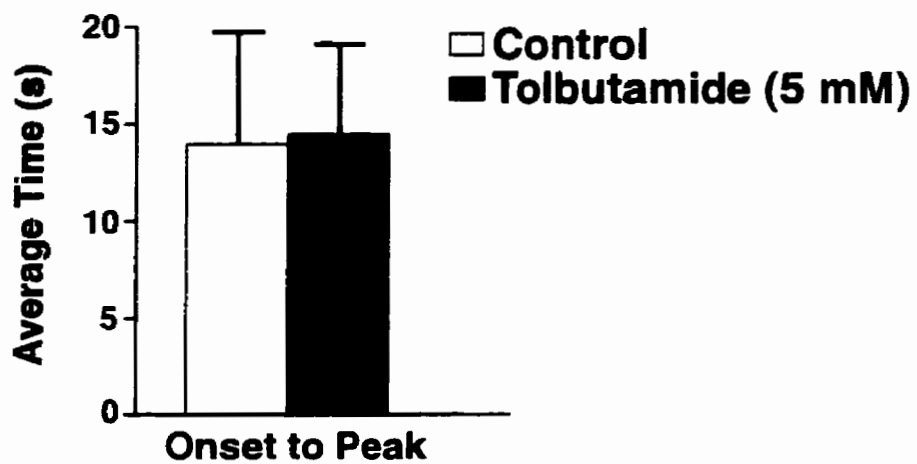
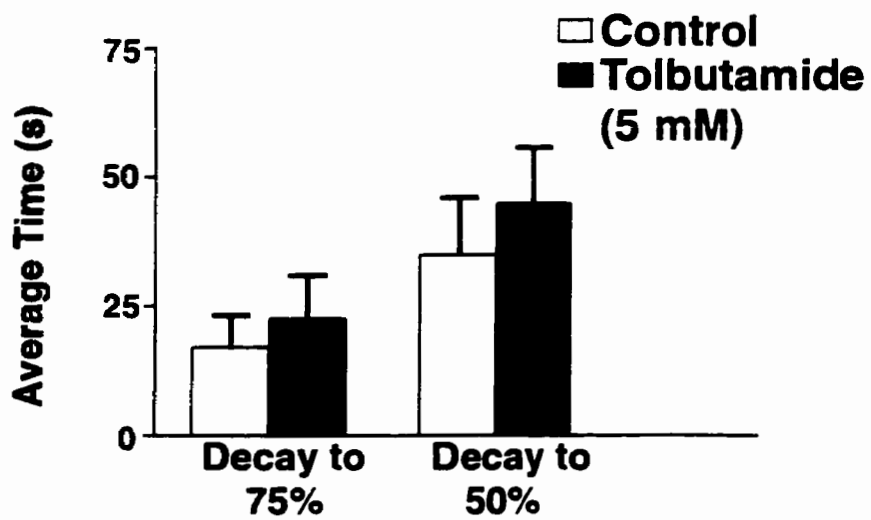
Tolbutamide, also a sulfonylurea, is an additional antagonist of ATP-sensitive  $K^+$  channels (Krnjevic, 1990). The objective of this series of experiments was to determine if tolbutamide (5 mM) has an effect on the propagation of spreading depression. Tolbutamide does not effect either the onset phase, falling phase or propagation rates of ouabain-induced SD. Fig. 25A illustrates the onset to peak parameter of the onset phase of SD. In control conditions, the onset to peak was determined to be  $14.0 \pm 5.8$  s, and in tolbutamide it was not significantly different at  $14.5 \pm 4.7$  s ( $p > 0.05$ ;  $n=4$ ). The propagation rates were also not significantly different. In control the propagation rate in *st. radiatum* was  $95 \pm 17$   $\mu\text{m/s}$  (Table 1;  $n=4$ ) and in *st. oriens* was  $104 \pm 54$   $\mu\text{m/s}$  (Table 1;  $n=4$ ). In tolbutamide the rates did not significantly differ at  $76 \pm 18$   $\mu\text{m/s}$  (Table 1;  $p > 0.05$ ;  $n=4$ ) in *st. radiatum* and  $79 \pm 31$   $\mu\text{m/s}$  (Table 1;  $p > 0.05$ ;  $n=4$ ) in *st. oriens*.

Tolbutamide did not affect the falling phase of ouabain-induced SD. As illustrated in Fig. 25B, in control conditions it required  $17.0 \pm 6.2$  s and  $34.9 \pm 11.1$  s for the peak transmittance to fall to 75% and 50% respectively. In tolbutamide, it required  $22.5 \pm 8.4$  s ( $p > 0.05$ ;  $n=4$ ) and  $44.9 \pm 10.8$  s ( $p > 0.05$ ;  $n=4$ ) for the peak transmittance to fall to 75% and 50% respectively. Neither the onset nor falling phases of ouabain-induced SD were affected by the presence of tolbutamide.

### **3.14 A slow spreading depression-like process occurs in low $\text{Na}^+$ conditions**

In order to examine the importance of extracellular sodium during ouabain-induced SD, the next series of experiments was conducted by replacing sodium chloride with NMDG chloride. The low  $\text{Na}^+$  solution contained 26 mM  $\text{Na}^+$ , from the addition of

**Figure 25.** Tolbutamide does not affect either the onset or falling phases of ouabain-induced spreading depression in *st. radiatum* of the CA1. **A)** In tolbutamide (5 mM) the onset to peak time does not significantly differ from control ( $p > 0.05$ ). **B)** In tolbutamide (5 mM) the decays from peak transmittance to 75% and 50% of peak transmittance do not significantly differ from control ( $p > 0.05$ ).

**A****B**

NaHCO<sub>3</sub> (26 mM). Fig. 26A indicates the three parameters analyzed in the onset phase of SD: the onset to peak, slope, and maximum slope as measured in st. radiatum of the CA1. Low sodium resulted in a statistically significant ( $p < 0.001$ ) effect on all three parameters: an increase in the onset to peak, and decreases in the slope and maximum slope. The onset to peak was  $10.2 \pm 2.8$  s ( $n=4$ ) in control, and significantly increased to  $201.5 \pm 41.8$  s ( $p < 0.001$ ;  $n=5$ ) in 26 mM Na<sup>-</sup>. The slope and maximum slope were found to be  $31.3 \pm 10.4$   $\Delta T/T/s$  and  $49.9 \pm 10.3$   $\Delta T/T/s$  in control respectively, and significantly decreased ( $p < 0.001$ ;  $n=5$ ) to  $0.4 \pm 0.1$   $\Delta T/T/s$  and  $1.7 \pm 0.1$   $\Delta T/T/s$  respectively in 26 mM Na<sup>-</sup>. The propagation rate in st. radiatum in control was  $123 \pm 27$   $\mu m/s$  (Table 1;  $n=5$ ) and significantly decreased in 26 mM Na<sup>-</sup> to  $24 \pm 8$   $\mu m/s$  (Table 1;  $p < 0.01$ ;  $n=5$ ). However, in st. oriens, 26 mM Na<sup>-</sup> did not have an effect on the propagation rate. In st. oriens in control the rate was  $82 \pm 11$   $\mu m/s$  (Table 1;  $n=5$ ) and in 26 mM Na<sup>-</sup>, not significantly different at  $43 \pm 18$   $\mu m/s$  (Table 1;  $p > 0.05$ ;  $n=5$ ). Low sodium conditions demonstrated a significant effect on the onset phase of ouabain-induced SD, slowing the propagation rate drastically in st. radiatum of the CA1, indicating that the presence of extracellular Na<sup>-</sup> is required for the normal propagation of ouabain-induced SD.

Low sodium conditions also had an affect on the falling phase of ouabain-induced SD as measured in st. radiatum of the CA1. Fig. 26B represents a comparison of the time for the peak transmittance to fall to 75% and 50% of peak. It required  $17.3 \pm 3.0$  s and  $43.3 \pm 6.6$  s for the peak transmittance to decay to 75% and 50% of peak in control respectively. In 26 mM Na<sup>-</sup> there was a significant increase as it required  $105.3 \pm 23.3$  s and  $168.9 \pm 35.3$  s ( $p < 0.001$ ;  $n=5$ ) for the peak transmittance to decay to 75% and 50% of peak respectively.

Fig. 27A is a series of pseudo-colored digital images of the changes in light tissue transmittance of ouabain-induced SD in 26 mM Na<sup>-</sup>. The upper left-hand panel is a bright-field image, showing the CA1 (stratum pyramidale, stratum radiatum, stratum oriens), CA2, and dentate gyrus (stratum moleculare, stratum granulosum) regions of the

**Figure 26.** Low sodium conditions (26 mM Na<sup>+</sup>) slows both the onset and falling phases in *st. radiatum* of the CA1 during ouabain-induced spreading depression.

- (A) In low sodium (26 mM), the onset to peak time is significantly increased relative to control (150 mM Na<sup>+</sup>). The slope (measured from 20%-40% of peak transmittance) and maximum slope are also significantly effected relative to control ( $p < 0.001$ ;  $n=5$ ). \*\*\* denotes data significantly different than control ( $p < 0.001$ ;  $n= 5$ ).
- (B) In low sodium (26 mM), the decays from peak transmittance to 75% and 50% of peak transmittance are significantly increased relative to control. \*\*\* denotes data significantly different than control ( $p < 0.001$ ;  $n=5$ ).

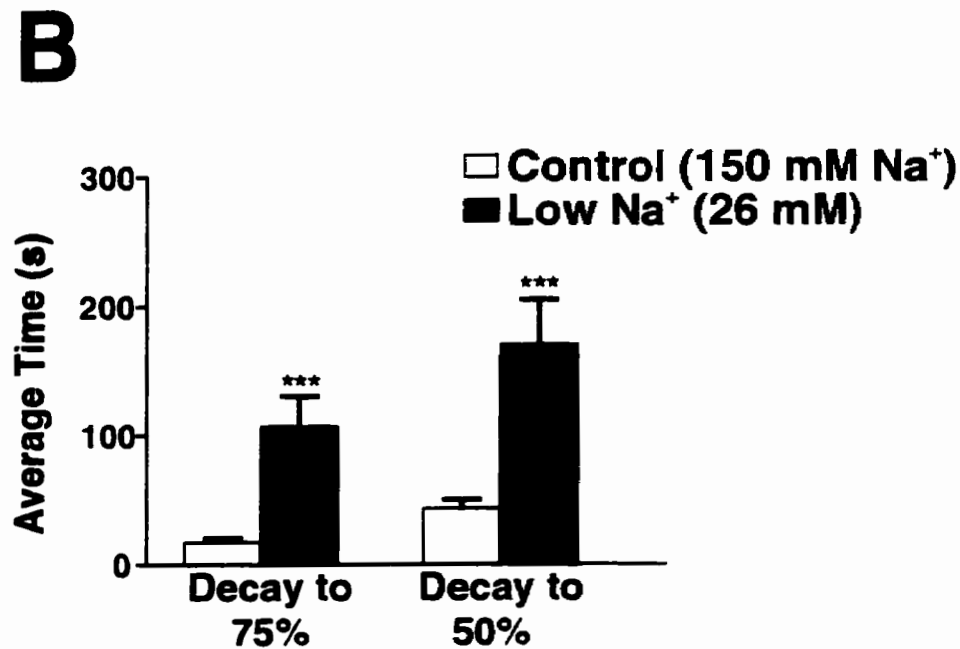
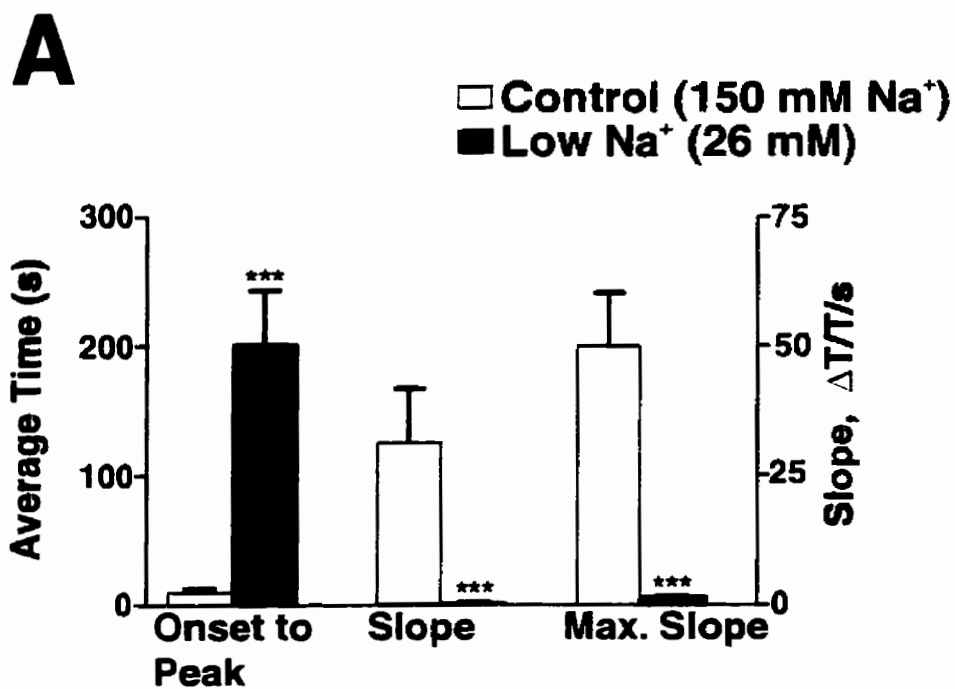
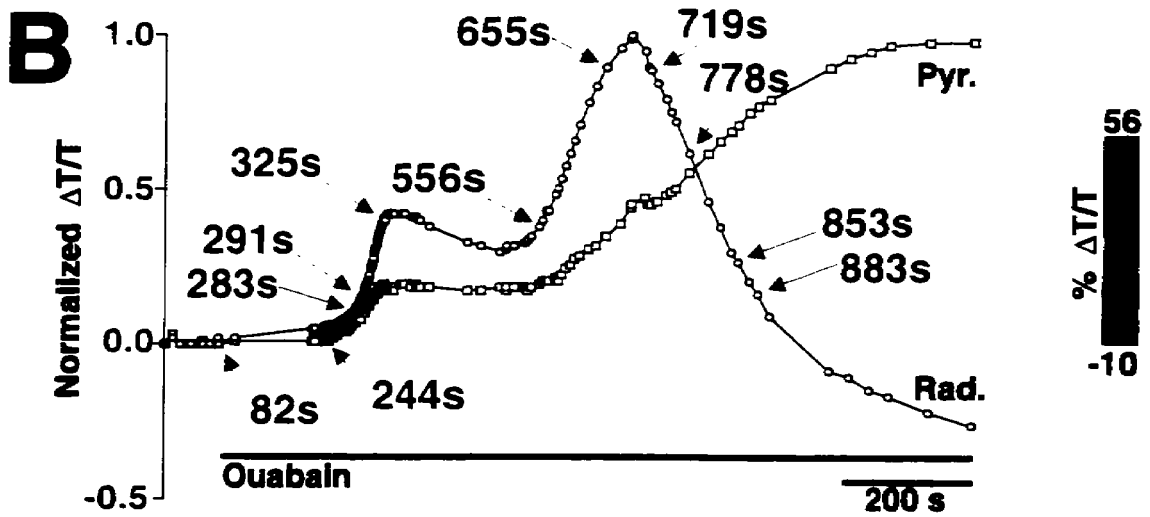
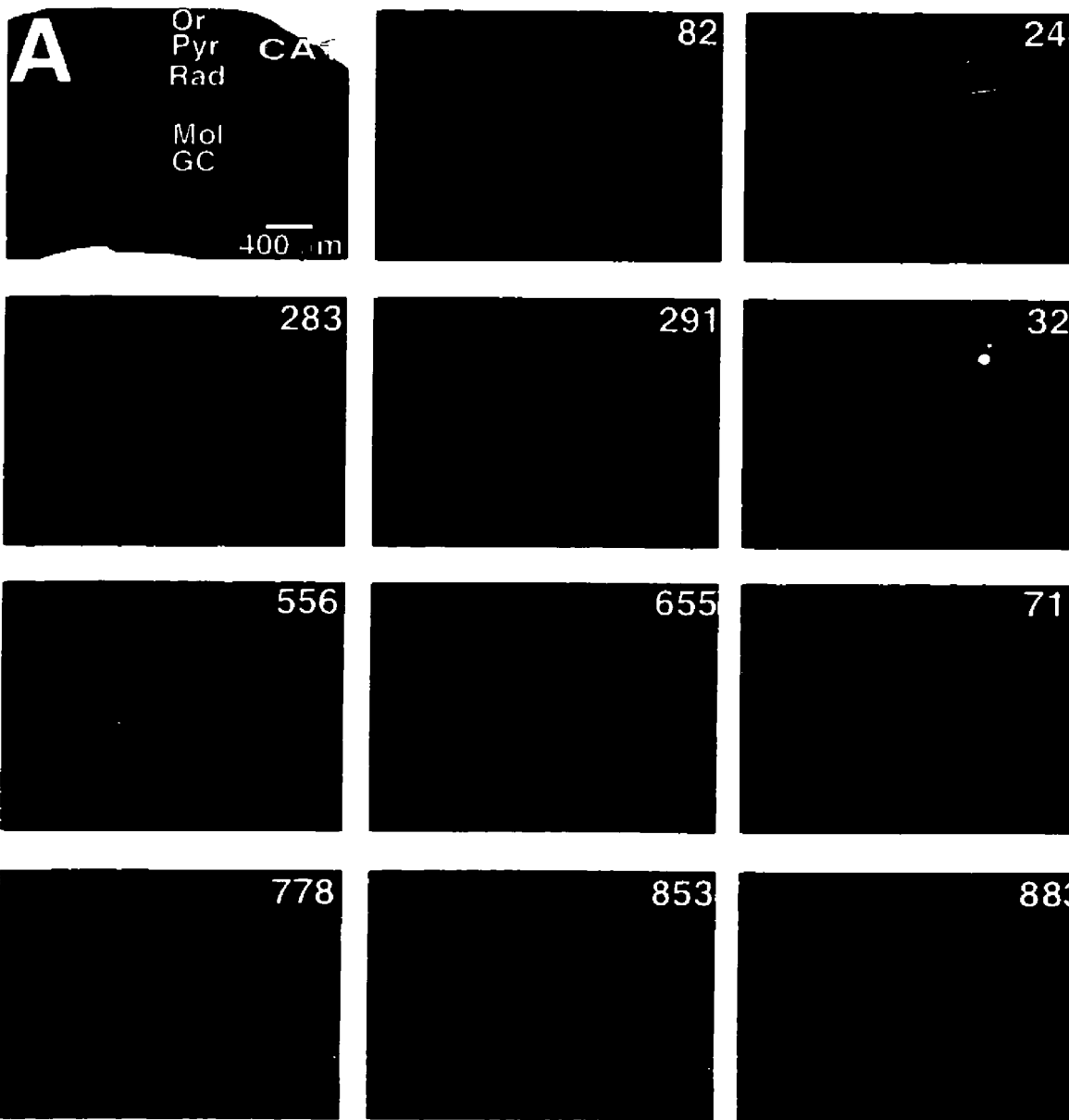


**Figure 27.** Ouabain-induced spreading depression in the hippocampal slice in low sodium (26 mM Na<sup>-</sup>) conditions. **A.** Series of pseudo-colored digital images of the changes in light tissue transmittance following the beginning of the experiment. The upper left-hand panel is a bright-field image showing the CA1 (st. oriens, st. pyramidale, st. radiatum), CA2, and dentate gyrus (st. moleculare, st. granulosum) regions. The numbers in the upper right-hand corner indicate the time in seconds. The small white circles indicate the regions analyzed and presented in Fig. 27B. **B.** Normalized change in transmittance relative to maximum transmittance in st. radiatum of the CA1. The arrows correspond to the panels above. The peak response of st. pyramidale (cell body layer) is approximately the same as that of st. radiatum. Scale bar = 400 μm.



hippocampus. The numbers in the upper right-hand corner of the remaining panels indicate the time in seconds, following the beginning of the experiment. The regions analyzed are demarcated by the circles in the upper left-hand panel. Fig. 27B is the transmittance profile of normalized change in transmittance ( $\Delta T/T$ ) of two regions: st. radiatum and st. pyramidale of the CA1. The curves have been normalized relative to the peak transmittance levels in st. radiatum.

Ouabain was superfused for the period of time indicated in Fig. 27B. The tissue transmittance profile in 26 mM Na<sup>+</sup> demonstrates several important characteristics. The first is that two peaks of tissue transmittance were observed. Following the application of ouabain, there is an increase in transmittance and subsequent decay in the first peak (between 325 and 556 s). At this point there is a slow propagation of the wave in st. radiatum (Fig. 27A) and slow increase to the second peak (> 655 s). At this point, the tissue transmittance decays to levels well below baseline in st. radiatum, with the simultaneous increase in tissue transmittance in st. pyramidale. These changes in tissue transmittance are analogous to those observed in control conditions, although at a much slower rate (Table 1). It is important to note that in control conditions two peaks are not observed, and the wave propagates at a much quicker rate. This indicates that a ouabain-induced spreading-depression like phenomenon occurs in 26 mM Na<sup>+</sup>, with an onset rate similar to that observed in MK-801, CNQX, and bicuculline (comparison not shown), but with a much slower falling phase.

### 3.15 Amiloride effects the onset phase of spreading depression

In order to further examine the importance of extracellular sodium, and whether its influx plays a role during ouabain-induced SD, the next series of experiments was conducted to determine if amiloride (100  $\mu$ M) affects the propagation of ouabain-induced SD. Amiloride is known to block epithelial Na<sup>+</sup> channels, and inhibit Na<sup>+</sup>/H<sup>+</sup> and Na<sup>+</sup>/Ca<sup>2+</sup> exchange in preparations from various tissues (Luciania *et al.*, 1992).

Fig. 28A illustrates the effect of amiloride on the onset phase of ouabain-induced SD. In control conditions the onset to peak time was  $5.0 \pm 0.7$  s. In amiloride this time was significantly increased to  $13.0 \pm 2.5$  s ( $p < 0.05$ ;  $n=3$ ). In control conditions the slope and maximum slope were  $9.1 \pm 1.9$   $\Delta T/T/s$  and  $18.0 \pm 2.1$   $\Delta T/T/s$  respectively. In amiloride, the slope and maximum slope were significantly lower at  $2.1 \pm 0.2$  ( $p < 0.05$ ;  $n=3$ ) and  $5.5 \pm 0.8$  ( $p < 0.01$ ;  $n=3$ ). In addition, amiloride significantly lowered the rate of propagation in st. radiatum but not st. oriens of the CA1. In control conditions the rate was  $138 \pm 14$   $\mu m/s$  (Table 1;  $n=3$ ) and in the presence of amiloride significantly decreased to  $34 \pm 7$   $\mu m/s$  (Table 1;  $p < 0.01$ ;  $n=3$ ). In st. oriens, amiloride did not significantly effect the propagation rate as in control it was  $89 \pm 38$   $\mu m/s$  (Table 1;  $n=3$ ) and in amiloride  $75 \pm 31$   $\mu m/s$  (Table 1;  $p > 0.05$ ;  $n=3$ ).

Amiloride does not effect the falling phase of ouabain-induced SD as measured in st. radiatum of the CA1. Fig. 28B represents a comparison of the time for the peak transmittance to fall to 75% and 50% of peak. In control conditions it required  $7.5 \pm 0.2$  s and  $15.3 \pm 0.1$  s for the peak transmittance to decay to 75% and 50% of peak respectively. In amiloride it required  $12.3 \pm 3.0$  s ( $p > 0.05$ ;  $n=3$ ) and  $25.0 \pm 4.5$  s ( $p > 0.05$ ;  $n=3$ ) for the peak transmittance to decay to 75% and 50% of peak respectively.

### 3.16 Benzamil effects the onset phase of spreading depression

Benzamil, an amiloride derivative, is an inhibitor of the  $Na^+/Ca^{2+}$  exchanger (Kaczorowski *et al.*, 1985; Markram *et al.*, 1995), but unlike amiloride does not inhibit the  $Na^+/H^+$  exchanger (Ong and Kerr, 1994). The next series of experiments was conducted to determine if the effect of amiloride on the onset phase of spreading depression might be explained by inhibition of the  $Na^+/Ca^{2+}$  exchanger. It was observed that benzamil (500  $\mu M$ ) resulted in an inhibition of the onset to peak of ouabain-induced SD, but was without effect on the falling phase of SD.

**Figure 28.** Amiloride slows the onset phase but not the falling phase of ouabain-induced spreading depression in *st. radiatum* of the CA1.

**(A)** In amiloride (100  $\mu\text{M}$ ), the onset to peak time is significantly increased relative to control (absence of amiloride). The slope (measured from 20%-40% of peak transmittance) and maximum slope are significantly decreased relative to control. denotes data significantly different than control \*  $p < 0.05$ ;  $n=3$ , \*\*  $p < 0.01$ ;  $n=3$ .

**(B)** In amiloride (100  $\mu\text{M}$ ), the decays from peak transmittance to 75% and 50% of peak transmittance do not significantly differ relative to control ( $p > 0.05$ ;  $n=3$ ).

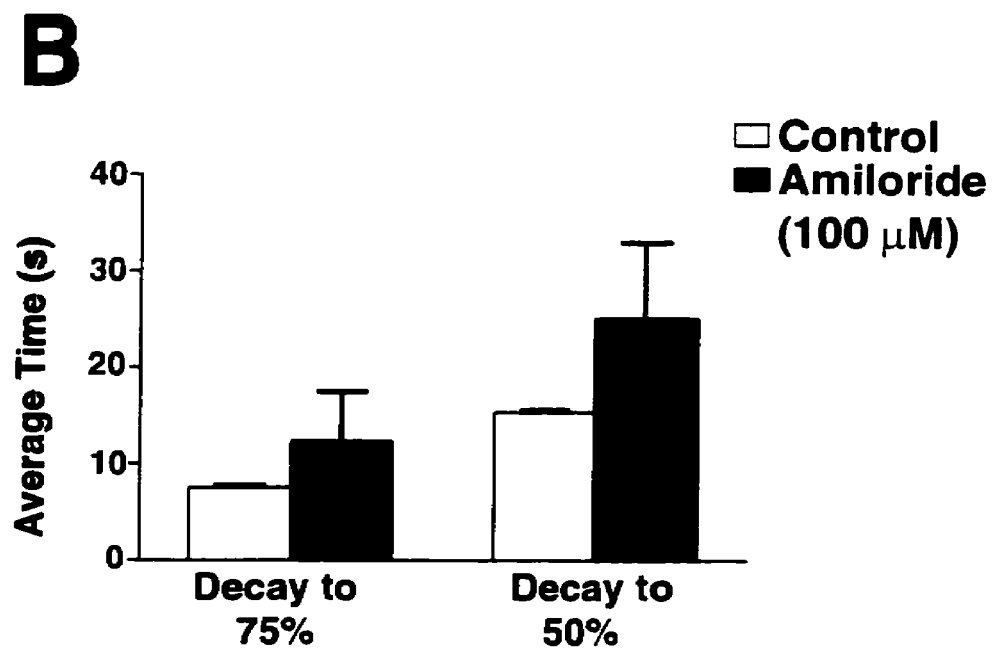
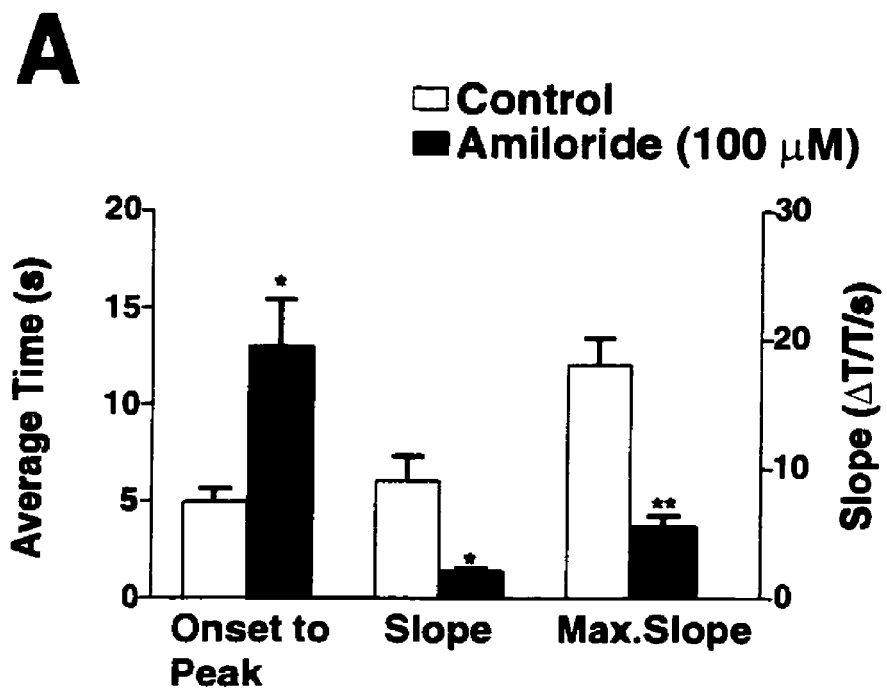


Fig. 29A is a comparison of the onset parameters in control and in the presence of benzamil. In control conditions the onset to peak time was  $12.8 \pm 3.5$  s, and in  $500\mu\text{M}$  benzamil this was significantly increased to  $67.1 \pm 13.5$  s ( $p < 0.01$ ;  $n=4$ ). Moreover, the maximum slope in benzamil was significantly decreased. The maximum slope was  $22.7 \pm 7.5$   $\Delta\text{T}/\text{T}/\text{s}$  in control and in the presence of benzamil was significantly decreased to  $3.9 \pm 0.3$   $\Delta\text{T}/\text{T}/\text{s}$  ( $p < 0.05$ ;  $n=4$ ). However, the slope (as measured from 20%-40% of peak) was not significantly effected by benzamil as it was  $14.7 \pm 5.6$   $\Delta\text{T}/\text{T}/\text{s}$  in control and  $2.5 \pm 0.6$   $\Delta\text{T}/\text{T}/\text{s}$  ( $p > 0.05$ ;  $n=4$ ) in benzamil. Similar to amiloride, the propagation rate in benzamil was significantly lower in *st. radiatum* but not *st. oriens* of the CA1. In control the rate was  $75 \pm 10$   $\mu\text{m}/\text{s}$  (Table 1;  $n=4$ ) and in benzamil significantly lowered to  $34 \pm 7$   $\mu\text{m}/\text{s}$  (Table 1;  $p < 0.01$ ;  $n=4$ ) in *st. radiatum* of the CA1.

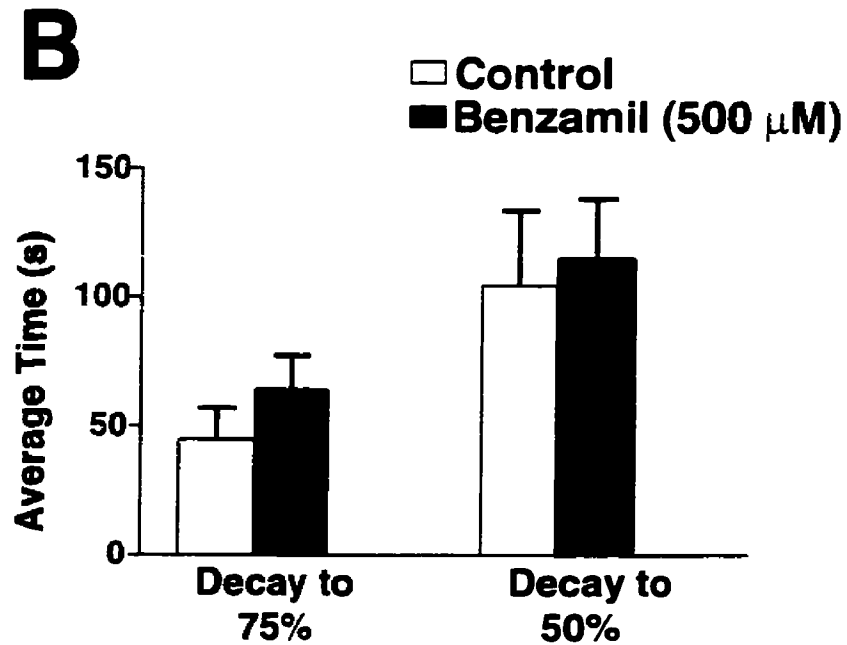
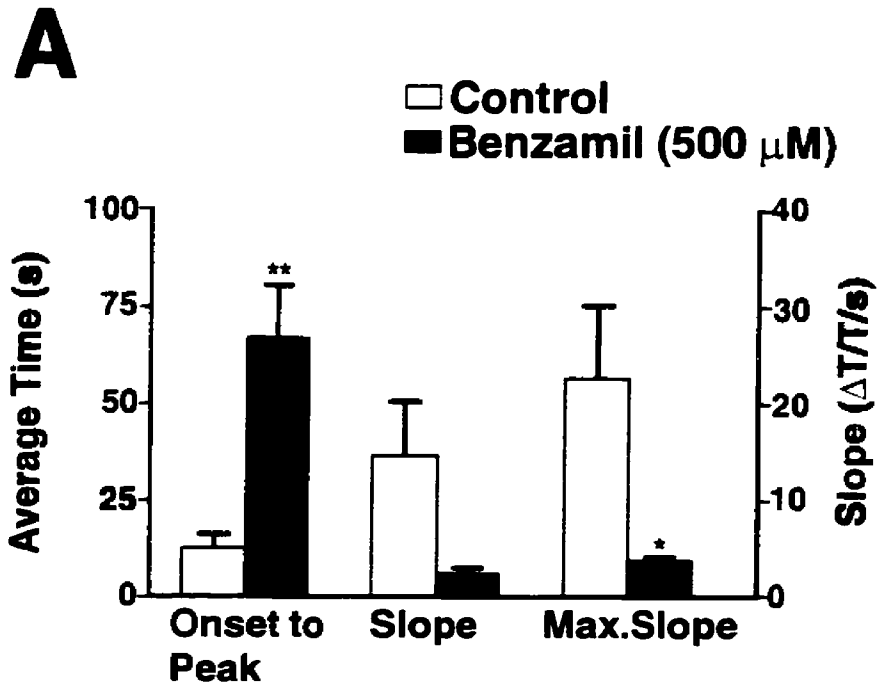
In *st. oriens*, benzamil did not significantly alter the propagation rate. In control the rate was  $60 \pm 14$   $\mu\text{m}/\text{s}$  (Table 1;  $n=4$ ) and  $24 \pm 7$   $\mu\text{m}/\text{s}$  (Table 1;  $p > 0.05$ ;  $n=4$ ) in benzamil.

Fig. 29B represents a comparison of the parameters analyzed during the falling phase of ouabain-induced SD as measured in *st. radiatum* of the CA1. Benzamil does not have an effect on the falling phase of SD. In control conditions it required  $44.6 \pm 12.2$  s for the peak to decay to 75% and  $104.6 \pm 29.0$  s to decay to 50%. In benzamil it required  $63.9 \pm 13.3$  s for the peak to decay to 75%, and  $114.9 \pm 23.3$ s for the peak to decay to 50%. This indicates that benzamil does not have an effect on the falling phase of ouabain-induced SD, suggesting a process independent of both  $\text{Na}^+/\text{Ca}^{2+}$  exchange and  $\text{Na}^+$  influx.

**Figure 29.** Benzamil slows the onset phase but not the falling phase of ouabain-induced spreading depression in *st. radiatum* of the CA1.

**(A)** In benzamil (500  $\mu\text{M}$ ), the onset to peak time is significantly increased (500  $\mu\text{M}$ ,  $p < 0.01$ ;  $n=4$ ) relative to control (absence of benzamil). The maximum slope is significantly decreased in benzamil ( $p < 0.05$ ;  $n=4$ ), but not the slope (as measured from 20% to 40% of peak;  $p > 0.05$ ;  $n=4$ ) relative to control. \* denotes data significantly different than control ( $p < 0.05$ ); \*\* ( $p < 0.01$ )

**(B)** In benzamil (500  $\mu\text{M}$ ), the decays from peak transmittance to 75% and 50% of peak transmittance do not significantly differ ( $p > 0.05$ ;  $n=4$ ) relative to control.



### 3.17 P<sub>2</sub>-purinergic receptor agonists: inconclusive results

ATP has been found to increase intracellular Ca<sup>2+</sup> concentrations in a variety of excitable and non-excitable cells (O'Conner *et al.*, 1991; el-Moatassim *et al.*, 1992). There are two principal methods by which ATP increases [Ca<sup>2+</sup>]<sub>i</sub>. The first is an influx of extracellular Ca<sup>2+</sup> through ligand-gated channels activated by ATP (Benham and Tsien, 1987) and the second is the release of Ca<sup>2+</sup> from intracellular stores.

There are two subtypes of purinergic receptors which are prevalent in the hippocampus: the P<sub>2x</sub> and P<sub>2y</sub> subtypes. The ionotropic P<sub>2x</sub> subtype has been shown to be coupled directly to channels permeable to Ca<sup>2+</sup> and the metabotropic P<sub>2y</sub> subtype stimulates a G-protein-mediated second messenger mechanism for release of Ca<sup>2+</sup> from intracellular stores.

The objective of the next series of experiments was to determine which specific subtype of purinergic receptor, P<sub>2x</sub> or P<sub>2y</sub>, is involved in the falling phase of ouabain-induced SD. There is currently a lack of specific P<sub>2</sub>-purinergic antagonists to differentiate between P<sub>2x</sub> and P<sub>2y</sub> (Chen *et al.*, 1994), and classification of specific subtypes of purinergic receptors has relied on the differing pharmacological selectivity of P<sub>2</sub>-agonists. The P<sub>2x</sub>-purinergic receptors exhibit the general potency order of α,β-methylene-ATP = β,γ-methylene ATP > ATP >> ADPβS or 2-methylthio ATP, whereas the P<sub>2y</sub> purinergic receptors have the potency order of 2-methylthio ATP > ADPβS > ATP > α,β-methylene ATP = β,γ, methylene ATP (Ralevic *et al.*, 1991; Harden *et al.*, 1995). However, this issue has recently been complicated further by the suggestion that P<sub>2x</sub> receptors have an agonist potency of 2-methylthio ATP > ATP > ADP > α,β-methylene ATP with α,β-methylene ATP being the most selective agonist (Balachandran and Bennett, 1996).

As discussed in the materials and methods, a modified experimental protocol was implemented with the application of hypo-osmotic aCSF without the presence of ouabain. The objective was to first swell the tissue to a level comparable to that which occurs

during ouabain-induced SD. The agonists could be applied and perhaps a similar change in cell volume would be observed as occurs during the falling phase of ouabain-induced SD.

Experiments applying the agonists were conducted with 101 slices (100  $\mu\text{M}$ , 40  $\mu\text{M}$  2-methyl-thio ATP, 100  $\mu\text{M}$   $\alpha,\beta$ -methylene-ATP, 100  $\mu\text{M}$   $\beta,\gamma$ -methylene ATP, 100  $\mu\text{M}$ , 50  $\mu\text{M}$ , 10  $\mu\text{M}$ , 500 nM ATP, ATP + 200  $\mu\text{M}$  suramin, 100  $\mu\text{M}$  ADP $\beta\text{S}$ ), and I did not observe a consistent effect on the IOS. The failure of the agonists to demonstrate a consistent effect may be due to the differences between the application of hypo-osmotic aCSF and ouabain. Hypo-osmotic swelling of the CA1 region has been shown, at least in the short term (minutes), to not undergo a process of volume recovery (Andrew and MacVicar, 1994). This contrasts the volume recovery we observe during ouabain-induced SD. This suggests that during SD, there are processes or mechanisms which allow conditions in which purinergic activation leads to volume recovery, processes which are not activated by simply swelling the tissue with hypo-osmotic aCSF.

Alternatively, although both 2-methylthio ATP and ADP $\beta\text{S}$  are effective  $\text{P}_{2\text{y}}$  agonists, they may be metabolized differently, possibly explaining their lack of effect in this modified protocol. ADP $\beta\text{S}$  is largely resistant to extracellular degradation by ectonucleotidases, and 2-methylthioATP is reported to be metabolized just as rapidly as ATP (Welford *et al.*, 1987). There is a possibility that in the hippocampal slice, 2-methylthioATP is unable to stimulate  $\text{P}_{2\text{y}}$  receptors due to its rapid degradation by extracellular ectonucleotidases (Porter and McCarthy, 1995), and ADP $\beta\text{S}$  may not bind with sufficient efficacy to activate  $\text{P}_{2\text{y}}$  receptors.

Although the ability to differentiate  $\text{P}_{2\text{x}}$  from the  $\text{P}_{2\text{y}}$  receptors based on ligand efficacy is generally accepted, a number of studies have produced evidence of  $\text{P}_2$ -purinergic receptors with pharmacological profiles that are not consistent with the present subclassification (Allsup and Boarder, 1990; Cowen *et al.*, 1990; Christie *et al.*, 1992; Iredale *et al.*, 1992; Chang *et al.*, 1995), including the  $\text{P}_{2\text{x3}}$  receptor found in the rat brain, and specifically hippocampus (Séguéla *et al.*, 1996). In addition, agonist potencies in some cases for both the ionotropic and metabotropic receptors are similar (Khakh *et al.*, 1995).

Another possibility is that the purinergic receptor involved in ouabain-induced SD in the hippocampus may be one which has not yet been classified, and one on which these agonists have no effect. For example,  $\alpha\beta$ -methylene ATP is ineffective at the PC12  $P_{2x}$  purinoceptor (Brake *et al.*, 1994), but is a potent agonist in the medial habenula (Edwards *et al.*, 1992). For this reason it has been suggested that other, as yet unidentified purinergic subtypes may exist in the CNS (Kidd *et al.*, 1995).

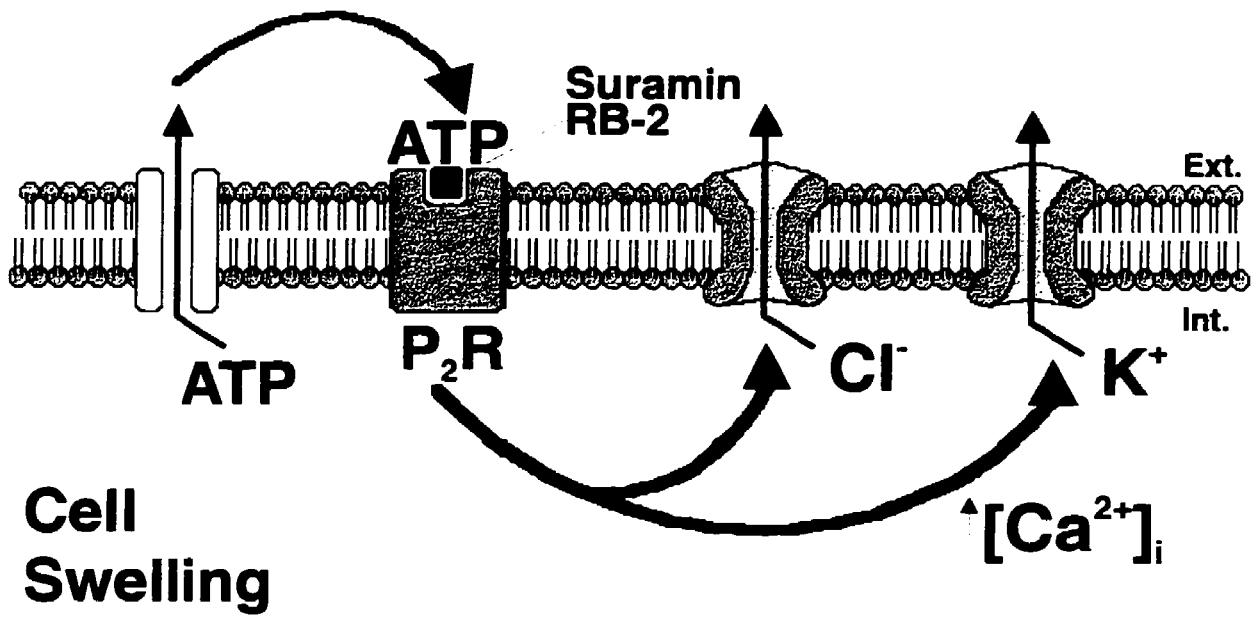
## 4 DISCUSSION

### 4.1 A novel mechanism for the recovery of cell volume during the falling phase of ouabain-induced spreading depression

The findings of this thesis suggest a novel mechanism for the recovery of cell volume during the falling phase of spreading depression. A model is proposed to describe the results of this thesis and is presented in Fig. 30 (adapted from Wang *et al.*, 1996). The first component of this model is a swelling-induced release of ATP or related compound. Following this, there is a local increase in extracellular ATP levels, and stimulation of P<sub>2</sub> purinergic receptors by ATP or ADP. This stimulation of P<sub>2</sub>-purinergic receptors results in a decrease in the tissue transmittance which is correlated with cell volume decreases. The possible mechanisms by which P<sub>2</sub>-purinergic receptor activation could lead to a decrease in cell volume are i) intracellular Ca<sup>2+</sup> release, and activation of Ca<sup>2+</sup>-activated K<sup>+</sup> channels, or ii) direct or indirect (by intracellular Ca<sup>2+</sup> release) opening of Cl<sup>-</sup> channels. Water follows the resulting efflux of Cl<sup>-</sup> or K<sup>+</sup> in an obligatory fashion and hence contributes to the recovery of cell volume during the falling phase of spreading depression.

Two principal findings from this thesis support the model presented in Fig. 30. First, the findings of this thesis indicate that the falling phase of spreading depression is delayed by the P<sub>2</sub> purinergic receptor antagonists suramin and RB-2, suggesting P<sub>2y</sub> involvement. Furthermore, it was demonstrated that the action of the purinergic receptor antagonists is not through non-specific effects such as ecto-nucleotidase inhibition, PKC inhibition, or GABA<sub>A</sub> or glutamatergic receptor blockade. The effect of suramin and RB-2 and the lack of effect of PPADs, suggests the involvement of the metabotropic P<sub>2y</sub> rather than the ionotropic P<sub>2x</sub> subtype in the falling phase.

**Figure 30.** A novel mechanism (Adapted from Wang *et al.*, 1996) proposed to describe the cell volume recovery during the falling phase in *st. radiatum* of the CA1 during ouabain-induced spreading depression. During the onset phase, there is a swelling-induced release of ATP, which activates P<sub>2</sub> purinergic receptors and the opening of either Ca<sup>2+</sup> - activated K<sup>+</sup> channels or chloride channels which contribute to the recovery of cell volume.



The second principal finding is that the presence of extracellular calcium is not required in the falling phase for cell volume recovery. Essentially, with or without extracellular calcium, the process of volume recovery occurs during the falling phase of SD. This suggests that the release of ATP i) is not dependent on an extracellular calcium influx and ii) does not occur following synaptic activation, suggesting the release of ATP through some other mechanism, possibly through the opening of a channel (Wang *et al.*, 1996).

#### **4.2 Imaging intrinsic optical signals in the hippocampal slice: changes in cell volume**

The results of this thesis indicate that activity-dependent changes in tissue transmittance can be imaged in the *in vitro* hippocampal slice preparation during ouabain-induced spreading depression. Imaging the changes in IOS in a hippocampal slice provides a non-invasive method of studying the changes in cell volume over a large area of the hippocampus simultaneously with better spatial resolution than conventional electrophysiological techniques. Imaging of IOS was utilized as a way of avoiding the problems that characterize the use of voltage-sensitive dyes, such as dye bleaching, dye toxicity, and inadequate staining.

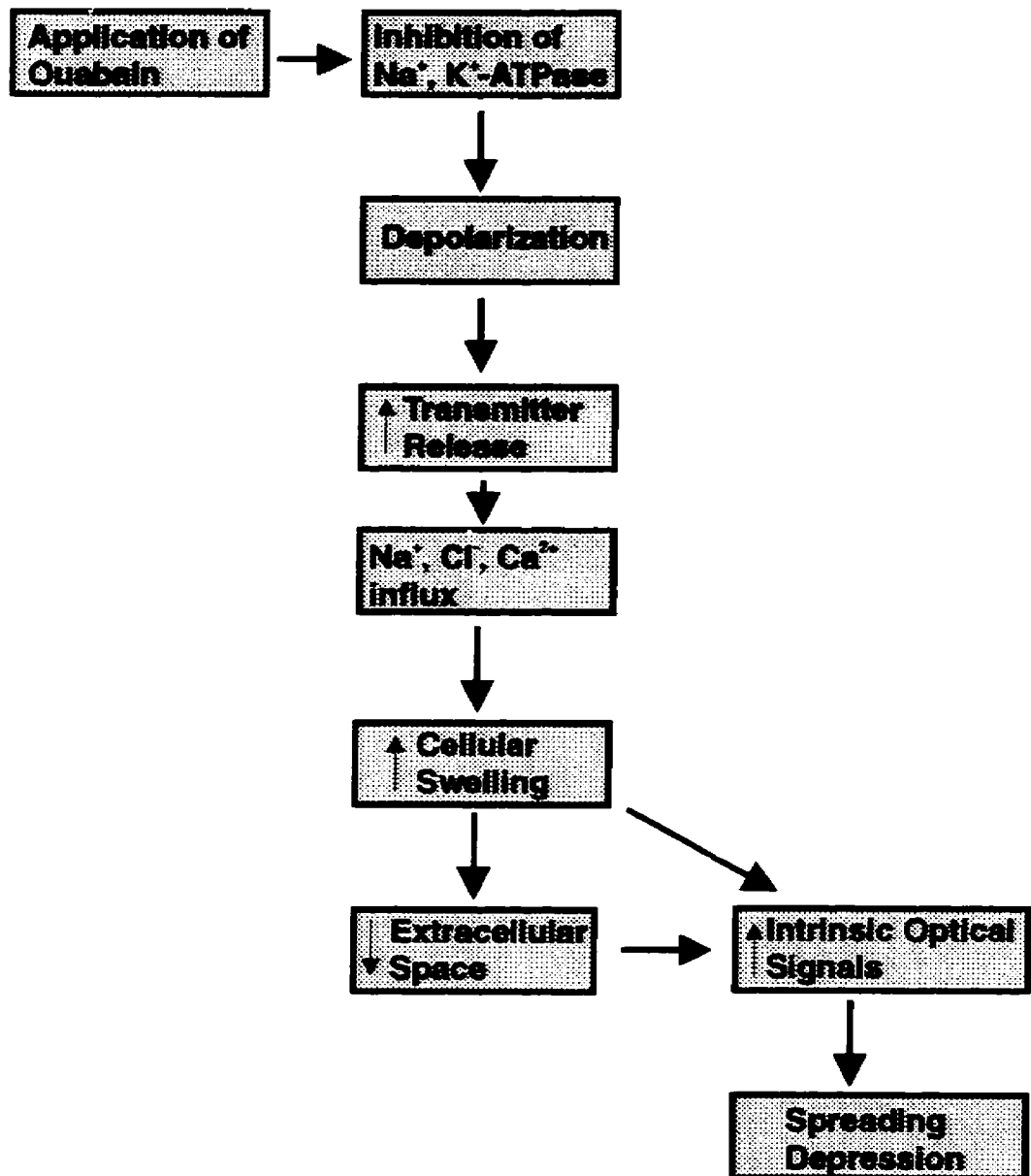
Hypo-osmotic solution has been previously shown to increase light tissue transmittance by inducing changes in cell volume (Andrew and MacVicar, 1994). These findings were confirmed by the application of hypo-osmotic aCSF. In these experiments, bath application of hypo-osmotic aCSF resulted in an increase in the tissue transmittance throughout the hippocampus, particularly in st. radiatum of the CA1. The tissue transmittance levels remained stable until washout with normosmotic aCSF, when the tissue transmittance decayed to baseline. In a recent study, activity-dependent changes in the IOS in rat neocortical slices revealed changes in extracellular space volume (Holthoff and Witte, 1996).

Consistent with the findings of several other studies, the changes in tissue transmittance can be attributed to and correlated with changes in cell volume, cellular swelling, or cellular shrinkage (MacVicar and Hochman, 1991; McManus *et al.*, 1993; Andrew and MacVicar, 1994; Kreisman *et al.*, 1995; Holthoff and Witte, 1996).

### 4.3 Ouabain-induced spreading depression in the hippocampal slice

The initiation of spreading depression by ouabain is not novel, as spreading depression had previously been initiated by the application of ouabain in the retina (Van Harreveld, 1978). In the retina, a wave of SD occurred spontaneously after 1.5-2.5 minutes (Van Harreveld, 1978). In the present study, a similar time-course was observed for the initiation of SD by ouabain in the hippocampal slice. A model is presented in Fig. 31 adapted from Lauritzen (1994) and Haglund and Schwartzkroin (1990), to describe the simplified series of events which contributes to cellular swelling during the onset phase of ouabain-induced SD. During the initial application of ouabain, the  $\text{Na}^+, \text{K}^+$ -ATPase is inhibited leading to a gradual depolarization of the tissue. As the enzyme is further inhibited, there is increased transmitter release (including glutamate), increased  $[\text{K}^+]_o$  and increased  $[\text{Na}^+]_i$ . The influx of sodium, calcium and chloride will result in water following, leading to cellular swelling (Van Harreveld, 1978). As the tissue swells, there is a reduction in the refraction of the tissue, a change in the extracellular space volume (Holthoff and Witte, 1996), an increase in the tissue transmittance, and a subsequent increase in the IOS (MacVicar and Hochman, 1991; McManus *et al.*, 1993; Andrew and MacVicar, 1994; Kreisman *et al.*, 1995; Holthoff and Witte, 1996). The increase in the IOS during the onset phase of ouabain-induced SD is indicated by swelling in the dendritic regions (st. radiatum and st. oriens). The entry of potassium and water into glial cells would decrease the size of the extracellular space (Snow *et al.*, 1983; Hablitz and Heinemann, 1989). This process will continue under the influence of ouabain during an explosive episode of SD.

**Figure 31.** A simplistic model to describe the series of events which contributes to cellular swelling during the onset phase of ouabain-induced spreading depression. (Adapted from Lauritzen, 1994 and Haglund and Schwartzkroin, 1990). The application of ouabain inhibits the  $\text{Na}^+/\text{K}^+$ -ATPase, leading to a depolarization of the tissue, increased transmitter release, and an influx of sodium, calcium and chloride with water following. This leads to cellular swelling and an increase in the tissue transmittance and consequently the intrinsic optical signals.



The changes in the IOS were analyzed in *st. radiatum* and *st. pyramidale* of the CA1. The CA1 region was the region of choice for two reasons. First, tissue transmittance changes during ouabain-induced SD in this region are pronounced, as there is an increase to peak and subsequent decay to baseline. Second, analyzing the CA1 region allows for comparison with many studies on SD which utilized electrophysiological techniques as well as imaging techniques to examine properties of cells within this region.

Ouabain-induced SD was initiated reliably (> 96%), as a wave of SD was observed in 302/312 slices. Three general patterns of initiation and propagation of SD were observed. The first, and most common, was an initiation point either within the CA1 region, or adjacent to the CA1/CA2 interface. In either region of initiation, the wave then propagated in two directions: i) towards the subicular region and ii) towards the CA3 region. The wave subsequently jumped across the hippocampal fissure and began propagation in the upper leaf of the dentate gyrus, its propagation terminating at the distal region of the lower leaf of the dentate gyrus. In the second pattern of propagation, SD initiated in the subicular region, and then propagated towards the CA2. As in the first pattern, the wave jumped across the hippocampal fissure and propagated throughout the upper leaf of the dentate gyrus, terminating in the distal region of the lower leaf of the dentate gyrus. The third pattern of initiation and propagation was exceedingly rare in control aCSF. In contrast, however, it occurred in all five slices (n=5/5; 100%) of 26 mM Na<sup>+</sup>, and in 0 Ca<sup>2+</sup> conditions 10/14 slices (n=10/14; 71%) and not at all in calcium-containing aCSF (n=0/14; 0%). In this pattern, the wave of SD initiated in the dentate gyrus region and then jumped across the hippocampal fissure and began propagating in both directions in the CA1 region: rostrally towards the CA3 and caudo-ventrally towards the subicular region of the hippocampus.

The rate of propagation of ouabain-induced SD averaged  $100 \pm 11 \mu\text{m/s}$  ( $n=14$ ) in st. radiatum and  $99 \pm 13$  ( $n=14$ ) in st. oriens of the CA1 region of the hippocampus (Table 1). In control conditions, therefore, it was observed that the velocity of propagation occurred at a comparable rate in st. oriens and st. radiatum, although the velocity of propagation varied from trial to trial (range 41-187  $\mu\text{m/s}$  in st. radiatum; range of 39-187  $\mu\text{m/s}$  in st. oriens). These observations are consistent with the findings of Somjen *et al.* (1992) in terms of the variation of the propagation rates, although in contrast to Somjen *et al.* (1992) it was determined that the rate of propagation in st. radiatum and st. oriens was comparable.

#### **4.4 P<sub>2x</sub>-purinergic receptor involvement in the onset phase of spreading depression**

The onset to peak time during the onset phase of ouabain-induced SD was inhibited by PPADs (200  $\mu\text{M}$ ) although not to the same extent as suramin (1 mM), and resistant to RB-2. This suggests the involvement of an ionotropic P<sub>2x</sub>-purinoceptor during this phase of spreading depression. P<sub>2x</sub>-purinoceptors are coupled directly to a non-selective cation channel, consistent with the depolarization, influx of Na<sup>+</sup> and Ca<sup>2+</sup> (Hansen, 1985), and cellular swelling known to occur in this phase of spreading depression.

PPADs was found to have no statistical effect on either the slope or maximum slope during the onset phase. The slope is measured from 20% to 40% of peak, suggesting that PPADs does not exert an effect in the early onset phase. As the latter onset phase progresses quickly to peak in control conditions, PPADs results in a slowing of this latter onset phase to peak. This suggests the involvement of P<sub>2x</sub> purinergic receptors in the latter onset phase, possibly activated by the implied swelling-induced release of ATP.

Suramin has been shown to inhibit glutamate receptors and GABA receptors (Nakazawa *et al.*, 1995). To control for antagonism at glutamate or GABA receptors, suramin was applied in the presence of NMDA, non-NMDA, and GABA<sub>A</sub> receptor

antagonists. PPADs was also tested to determine its effect in the presence of these antagonists, although PPADs has been shown to have no effect on these receptors (Dale and Gilday, 1996), or on glutamate-induced currents in CA1 pyramidal cells (Motin and Bennett, 1995). PPADs, unlike suramin, in the presence of these antagonists, did not slow the onset phase of ouabain-induced SD.

The reason that PPADs does not maintain its effect on the onset phase in the presence of NMDA, non-NMDA, and GABA<sub>A</sub> receptor antagonists is not currently known. One possible explanation is that the onset phase in the presence of the antagonists is slowed enormously, requiring as much as 25 minutes to reach peak. The effect of PPADs in slowing the onset phase is presumably still occurring, but as the process is already slowed so substantially, it is conceivable that the effects of PPADs are masked.

Suramin slowed the onset phase in the presence of the antagonists in a dose-dependent manner, with an EC<sub>50</sub> of 383 μM. The shape of the curve is similar to the effect of suramin on currents elicited by application of 100 μM glutamate to hippocampal neurons (Motin and Bennett, 1995), although shifted to the right into a much higher concentration range (Fig. 15). It is likely that suramin is slowing the latter part of the onset phase due to a multitude of effects: antagonism at P<sub>2y</sub> receptors, or a blockade of glutamate and/or GABA receptors.

#### **4.5 P<sub>2</sub> antagonists do not slow the falling phase of spreading depression by inhibiting ecto-nucleotidases nor by blocking GABA- and glutamate receptors**

In a recent study it was determined that all currently available P<sub>2x</sub>- and P<sub>2y</sub>-purinoceptor antagonists (including suramin, RB-2 and PPADs) inhibit significantly the breakdown of ATP by *Xenopus* oocytes (Ziganshin *et al.*, 1996). Suramin, RB-2 and PPADs inhibit the breakdown of ATP to a similar extent, suggesting that the inhibitory effect on ecto-nucleotidase activity should be taken into account when these purinergic antagonists are used in pharmacological experiments (Ziganshin *et al.*, 1996). To control

for ectonucleotidase inhibition as a possible non-specific effect of the purinergic antagonists the effect of AMP-PNP, an ectonucleotidase inhibitor was investigated. AMP-PNP failed to have an effect on either the onset or falling phases of spreading depression (Fig. 22), suggesting that the purinergic antagonists do not exert their effects by inhibiting ectonucleotidases. Furthermore, suramin, RB-2 and PPADs exhibited differential effects on ouabain-induced SD. Suramin and RB-2 affected the falling phase and suramin and PPADs the onset phase. These differential effects could not be explained if the effects of the purinergic antagonists were simply an inhibition of ecto-nucleotidases to a similar extent (Ziganshin *et al.*, 1996).

Both suramin and RB-2 have been shown to inhibit glutamate and GABA receptors in this concentration range (Nakazawa *et al.*, 1995), and glutamate-activated currents in CA1 pyramidal neurons (Motin and Bennett, 1995). The slowing of the falling phase of SD cannot be explained solely by an inhibition of glutamate and GABA receptors, as experiments in this thesis demonstrated that NMDA, non-NMDA, and GABA<sub>A</sub> receptor antagonists slow preferentially the onset phase, and are without effect on the falling phase. This rules out GABA and glutamate inhibition as a possible non-specific effect of suramin and RB-2 on the falling phase of ouabain-induced SD.

#### **4.6 Purinergic antagonists slow the falling phase of SD by P<sub>2y</sub>-purinergic receptor blockade**

One of the principal findings of this thesis is that suramin and RB-2 inhibited the falling phase of SD, in the absence of any other treatment. The model presented in Fig. 30 suggests suramin and RB-2 inhibit the binding of ATP to a P<sub>2y</sub>-purinergic receptor. This is most likely a metabotropic P<sub>2y</sub>-purinoceptor resistant to PPADs, but inhibited by RB-2 and suramin. A receptor with similar antagonist selectivity was described in the rat vas deferens (Bültmann and Starke, 1994). In C6 glioma cells, suramin and RB2 competitively antagonized the inhibitory effect of 2-methylthioATP (a potent P<sub>2y</sub> agonist) (Boyer *et al.*, 1994), whereas PPADs (concentrations up to 100µM) had no effect (Boyer *et al.*, 1994).

In addition to its well known  $P_{2x}$  antagonism, PPADs was shown to be a competitive antagonist at  $P_{2y}$ -stimulated phospholipase C (PLC) activity in turkey erythrocytes but was without effect on  $P_{2y}$ -purinoceptors on C6 glioma cells coupled to adenylyl cyclase (Boyer *et al.*, 1994). This suggests that activation of phospholipase C and inhibition of adenylyl cyclase are mediated by different  $P_{2y}$ -purinoceptor subtypes (Boyer *et al.*, 1994) with differing selectivity for PPADs. 2-methylthio ATP (a potent  $P_{2y}$  agonist) was shown in cultured rat hippocampal neurons to enhance intracellular calcium via a pathway independent of the PLC-mediated phosphatidylinositol signaling pathway (Ikeuchi *et al.*, 1996), possibly by inhibiting adenylyl cyclase. This provides an explanation for the failure of PPADs to inhibit the falling phase of SD. In the rat hippocampus, it may be that  $P_{2y}$  receptors act via a pathway independent of PLC (Ikeuchi *et al.*, 1996), receptors resistant to inhibition by PPADs.

Although both suramin and RB-2 have an effect on the falling phase of SD, indicating  $P_{2y}$  receptor involvement, there is a discrepancy in the effect of these drugs on the falling phase of SD in the presence of NMDA, non-NMDA, and GABA<sub>A</sub> receptor antagonists. Suramin, in the presence of these antagonists, results in a dose-dependent inhibition of the falling phase ( $IC_{50}$  of  $\sim 115 \mu\text{M}$ ). Conversely, RB-2 (200  $\mu\text{M}$ ) does not have an effect on the falling phase of ouabain-induced SD in the presence of these antagonists.

One explanation is that suramin, unlike RB-2, has an effect on the falling phase of SD in the presence of these antagonists as a result of an action independent of its blockade of purinergic receptors. Having ruled out ecto-nucleotidase inhibition as a possible non-specific effect of suramin, the possibility that the effect of suramin could be explained by inhibition of PKC (Mahoney *et al.*, 1990) was investigated.

The involvement of PKC has been demonstrated in SD initiated by a high KCl solution in rat cerebral cortex *in vivo* (Krivanek and Koroleva, 1996). Suramin, in addition to its well-characterized purinergic antagonism, has been shown to inhibit PKC in a

concentration-dependent manner (Mahoney *et al.*, 1990). H-7, a potent PKC inhibitor, was determined to have no effect on the falling phase of spreading depression (Fig. 16), ruling out PKC inhibition as a possible non-specific effect of suramin. Furthermore, P<sub>2y</sub> purinergic receptors in cultured rat hippocampal neurons are not regulated by PKC and enhance [Ca<sup>2+</sup>]<sub>i</sub> via a pathway independent of PLC-mediated signaling (Ikeuchi *et al.*, 1996), a finding which further re-affirms my conclusion that suramin is not affecting the falling phase through PKC inhibition.

The results of the present study suggest that the inhibition of the falling phase of SD by suramin in the presence of the GABA- and glutamate receptor antagonists is best explained by a blockade of P<sub>2</sub> purinergic receptors. The reason for the failure of RB-2 to maintain an effect on SD in the presence of the NMDA, non-NMDA, and GABA<sub>A</sub> receptor antagonists is not currently known and is difficult to explain. It may be, however, that the process underlying channel inhibition of different ligand gated channels may not be explained by a common mechanism. For example, the inhibition by RB-2 of the NMDA-activated current in rat hippocampal neurons was dependent on agonist concentration and voltage, whereas the inhibition by suramin was dependent only on voltage, in a particular concentration range (Nakazawa *et al.*, 1995). This suggests the effect of suramin may be explained by a block at channel pores (Ascher *et al.*, 1978; 1979), whereas with RB-2 it may be a combination of both a pore block and competitive antagonism. However, the blockade by both suramin and RB-2 of ATP-activated channels in PC 12 cells depended on agonist concentration but not on voltage (Nakazawa *et al.*, 1990a; 1991), suggesting competitive antagonism.

RB-2 (200 μM) results in a blockade of preferentially the P<sub>2y</sub> purinergic subtype (Motin and Bennett, 1995), whereas suramin (100-1000 μM) results in blockade of both the P<sub>2x</sub> and P<sub>2y</sub> purinergic receptor subtypes (Motin and Bennett, 1995; Nakazawa *et al.*, 1990b). P<sub>2x</sub> ionotropic receptors are coupled directly to a non-specific cation channel, and the failure of RB-2 to antagonize these receptors may result in an increased influx of Na<sup>+</sup>

and  $\text{Ca}^{2+}$  through these channels. This may lead to increased release of glutamate and consequently ATP. At these increased extracellular concentrations of ATP, RB-2 may have only a weak antagonistic effect at  $\text{P}_{2y}$  purinergic receptors. A similar dependence of antagonism by RB-2 on NMDA concentration has previously been described (Nakazawa *et al.*, 1995). RB-2 strongly inhibited an inward current induced by 100  $\mu\text{M}$  NMDA, but weakly inhibited the same current induced by a higher concentration of NMDA (500  $\mu\text{M}$ ) (Nakazawa *et al.*, 1995). Perhaps by increasing the concentration of RB-2 (greater than 200  $\mu\text{M}$ ), a greater percentage of receptors would be inhibited, and at higher concentrations RB-2 would strongly inhibit  $\text{P}_{2y}$  receptors.

An alternative explanation involves the effects of blocking NMDA receptors. It has previously been demonstrated that in cortical cell cultures hypo-osmotically swelled neurons engage in rapid RVD. However, swelling induced in these cells by a veratridine-stimulated  $\text{Na}^+$  influx does not result in a process of RVD (Churchwell *et al.*, 1996). On the other hand, if the veratridine-stimulated cells are pre-treated with NMDA antagonists (within a limited time), they engage in rapid RVD (Churchwell *et al.*, 1996). This raises the intriguing possibility that RVD in the presence of NMDA antagonists represents a different process of RVD than that activated during ouabain-induced SD; one blocked by the presence of suramin and not by PPADS and RB-2. The first line of evidence in support of this idea is that in the presence of the NMDA antagonist MK-801, the decrease in tissue transmittance during the falling phase occurs much more quickly (after the first 30 s from peak) than in control conditions in *st. radiatum* of the CA1 (Basarsky, personal communication).

It has been suggested that RVD in the presence of NMDA antagonists requires a “threshold” level of calcium to be reached (Churchwell *et al.*, 1996). It is conceivable that in the presence of NMDA antagonists and suramin, both the NMDA and  $\text{P}_{2x}$  purinergic receptors are inhibited, and for this reason, in suramin, the calcium influx is depressed such that the “threshold” of intracellular calcium is not reached. This provides an explanation as

to why, conversely, the falling phase of SD in the presence of these antagonists and RB-2 occurs: lack of P<sub>2x</sub> antagonism results in an increased influx of calcium reaching the “threshold” level, and activating a different process of volume recovery not dependent on P<sub>2y</sub> purinergic activation.

Finally, the classification of ATP receptors and the actions of purinergic antagonists are based primarily on experiments performed in non-neuronal tissue, and therefore may not explain all of the effects observed in CNS tissue (Wieraszko and Ehrlich, 1994; Illes and Nörenberg, 1993). Moreover, different P<sub>2</sub>-purinergic receptors would exist in a complex cellular preparation such as the hippocampal slice, and the final effect may be a compound effect of actions of different subpopulations of P<sub>2</sub> receptors (Wieraszko and Ehrlich, 1994). The possibility that suramin may be having an effect on the falling phase of SD in the presence of the NMDA, non-NMDA, and GABA<sub>A</sub> antagonists due to a multitude of P<sub>2</sub> purinergic effects, as well as the intriguing possibility of antagonism at an undescribed purinergic receptor subtype, cannot be ignored.

#### **4.7 Interaction of the glutamatergic and purinergic systems during spreading depression: release of ATP or related compound**

One of the earliest discoveries of spreading depression was that it could be initiated by glutamate (Van Harreveld, 1959; Hansen, 1985). Agonists of the glutamate subtype receptors, (NMDA, quisqualate, and kainate) also trigger CSD (Van Harreveld, 1959; Curtis and Watkins, 1963; Bures *et al.*, 1974; Lauritzen *et al.*, 1988). NMDA was approximated to be 100 times more potent than glutamate in initiating SD (Curtis and Watkins, 1963). Both the CA1 and dentate gyrus regions contain high levels of neuronal NMDA receptors (Monaghan and Cotman, 1985; Jansen *et al.*, 1989).

NMDA receptors do play a role in the onset phase of spreading depression, as the application of MK-801 (100 μM) prolongs the onset of SD in st. radiatum of the CA1 significantly (Basarsky and MacVicar, 1996), consistent with the findings of the effects of

other NMDA antagonists on SD (Hernández-Cáceres *et al.*, 1987; Mody *et al.*, 1987; Marrannes *et al.*, 1988; Somjen *et al.*, 1992). However, in the presence of the NMDA antagonist MK-801, the falling phase of SD in st. radiatum is not affected and occurs as rapidly as in controls, even at a slightly faster rate (Basarsky, personal communication).

Glutamate is released and involved during the onset phase of ouabain-induced spreading depression. The present study has determined that slices bathed in MK-801, CNQX (non-NMDA receptor antagonist) and bicuculline (GABA<sub>A</sub> antagonist) inhibit the onset phase of spreading depression. In the presence of these antagonists, the falling phase of SD does not occur until 15-20 minutes following the application of ouabain, a slightly longer period of time than in the presence of MK-801 alone (Basarsky, personal communication). With the addition of suramin in the presence of the same drugs, the falling phase is slowed, suggesting a role of P<sub>2</sub>-purinergic receptors in this phase of SD.

ATP has been shown to be released from hippocampal slices by the stimulation of Schaffer collaterals in rats and mice (Wieraszko *et al.*, 1989). The release of ATP is dependent on extracellular calcium concentration, and is not evoked by glutamate release itself, suggesting that perhaps both ATP and glutamate are stored and released together (Wieraszko *et al.*, 1989). ATP, a transmitter at autonomic neuromuscular junctions (Burnstock, 1990) and ganglia (Evans *et al.*, 1992; Silinsky and Gerzanich, 1993) is also a transmitter in the central nervous system (Edwards *et al.*, 1992), and acts through P<sub>2</sub>-purinoceptors.

As the falling phase of spreading depression is inhibited by the P<sub>2</sub> purinergic receptor antagonists suramin and RB-2, this implies a release of ATP or related compound during this phase of spreading depression. A recent study has demonstrated that the release of ATP in cultured rat hippocampal neurons evokes an increase in intracellular calcium through P<sub>2</sub>-purinoceptors (Inoue *et al.*, 1995). P<sub>2y</sub>-purinoceptors have been identified which in response to ATP increase intracellular calcium levels in 30% of

dissociated hippocampal neurons (Mironov, 1993). Consistent with these findings, it was determined that in cultured rat hippocampal neurons, P<sub>2y</sub> purinergic activation resulted in whole cell potassium currents and Ca<sup>2+</sup> release from intracellular calcium stores (Ikeuchi *et al.*, 1996).

The relationship between glutamate and ATP release has been studied in cultured rat hippocampal neurons (Inoue *et al.*, 1995). It was demonstrated that glutamate release from a “glutamate responder” cell resulted in the release of ATP which stimulated ATP receptors on a “non-glutamate responder” cell, resulting in an increase in intracellular calcium (Inoue *et al.*, 1995). This response was inhibited by suramin, in the presence of TTX, APV, CNQX, bicuculline, and Cd<sup>2+</sup>, indicating the involvement of P<sub>2</sub> purinergic receptors (Inoue *et al.*, 1995).

These findings suggested that glutamate can trigger the release of ATP from neurons which can act to raise intracellular calcium in other neurons via the activation of P<sub>2</sub>-purinergic receptors. It is not currently known how specifically purinergic neurons interact with the well-known glutamatergic circuitry of the hippocampus (Inoue *et al.*, 1995), however it has been suggested that there may be intermembrane coupling between P<sub>2y</sub>-or P<sub>2y</sub>-like purinergic receptors and glutamate receptors in the hippocampal slice (Motin and Bennett, 1995). Glutamate is released during SD, and it is conceivable that this glutamate release may contribute to the release of ATP in much the same way as the interactions in cell culture resulting in increased release of ATP, which activates metabotropic P<sub>2y</sub> purinergic receptors and the release of Ca<sup>2+</sup> from intracellular stores.

#### **4.8 Origin of extracellular ATP: release during spreading depression**

Experiments in this thesis examined ouabain-induced spreading depression in the absence of extracellular Ca<sup>2+</sup> and the presence of 100 μM EGTA. The affect of low

calcium conditions on SD was an increase in the onset phase, or time to peak. The falling phase, and the one implicated in the volume recovery of *st. radiatum* was unaffected by extracellular  $\text{Ca}^{2-}$  removal.

Previous studies examining RVD in cortical astrocytes determined that astrocyte swelling causes an increase in intracellular  $\text{Ca}^{2-}$  both by an increased influx from the extracellular space and release from intracellular stores (Churchwell *et al.*, 1996). In addition, it was shown that RVD in cortical astrocytes after hypotonic swelling is a  $\text{Ca}^{2-}$  dependent process (O'Conner and Kimelberg, 1993; Bender and Norenberg, 1994), and the removal of extracellular  $\text{Ca}^{2+}$  was shown to inhibit RVD and swelling activated  $\text{K}^+$  and  $\text{Cl}^-$  efflux (Churchwell *et al.*, 1996).

The cytoplasmic level of ATP in most mammalian cells exceeds 5 mM (Zhang *et al.*, 1995), so extracellular levels of ATP during stimulation could rise to a high micromolar range (Gordon, 1986). The findings of this thesis have suggested that the release of ATP is not dependent on either synaptic transmission or an influx of extracellular calcium, suggesting a mechanism of release independent of the findings of Wieraszko *et al.* (1989).

One of the objectives, therefore, was to determine how ATP is being released during ouabain-induced SD. In a similar study in HTC cells, it was suggested that ATP efflux occurs through the opening of a channel, however the molecular identity of the channel is not known (Wang *et al.*, 1996). It may be that a similar mechanism of ATP release occurs in the hippocampus. It has been suggested that ATP-sensitive  $\text{K}^+$  channels, observed in cardiac and other tissues (Ashcroft, 1988; Cook and Hales, 1984; Spruce *et al.*, 1985), may play a role in SD (Aitken *et al.*, 1991). It was also suggested that sulfonylurea receptors, members of ATP binding cassette proteins, may also be permeable to ATP (Al-Awqati, 1995).

Sulfonylurea receptors sensitive to glibenclamide have been found throughout the hippocampus, including the CA1 region (Zini *et al.*, 1993). Glibenclamide was observed to have an effect on the falling phase of spreading depression, but not to the same extent as

suramin. Perhaps glibenclamide did block a component of ATP release during the falling phase of ouabain-induced SD, but did not inhibit the release completely. However, tolbutamide, also a sulfonylurea antagonist (Krnjevic, 1990) failed to have an effect on either the onset or falling phases of spreading depression (Fig. 25). This suggests that ATP-sensitive  $K^+$  channels sensitive to tolbutamide may not play a role in SD in the hippocampus. Alternatively, glibenclamide blocks ATP-sensitive potassium channels, and may have an effect independent of the postulated release of ATP through the channel. Glibenclamide blockade of these channels would inhibit the efflux of potassium, slowing the process of volume recovery, and resulting in a slowing of the falling phase of ouabain-induced SD.

#### **4.9 Activation of purinergic receptors and regulatory volume decrease**

Consistent with previous studies (Andrew and MacVicar, 1994), the application of a hypo-osmotic solution resulted in a reversible increase in tissue transmittance in all regions of the hippocampal slice, particularly in the radiatum of the CA1. This increase in tissue transmittance is correlated with an increase in cell volume (Andrew and MacVicar, 1994) which remained at a stable level until the hypo-osmotic saline was washed off with normosmotic aCSF.

These findings suggest that cell volume regulation in the hippocampal slice does not occur over the short term (minutes) (Andrew and MacVicar, 1994). It was proposed, therefore, that cells in the CA1 region behave passively during osmotic stress lasting several minutes (McGann *et al.*, 1988; White *et al.*, 1992), and over the longer term (hours or days), mechanisms of volume regulation may become activated (Andrew, 1991; Andrew and MacVicar, 1994).

During the falling phase of ouabain-induced spreading depression, there is a rapid increase and then compensatory decay of the tissue transmittance which is associated with the rapid recovery of cell volume in st. radiatum of the CA1. This is also consistent with

the finding that a brief application of NMDA (100  $\mu$ M) results in a similar increase and then decay in the tissue transmittance in st. radiatum of the CA1 (Polischuk and Andrew, 1996a). Results of this thesis have indicated that suramin and RB-2, P<sub>2y</sub> purinergic antagonists, inhibit this volume recovery phase of spreading depression. This provides circumstantial evidence for a release of ATP which mediates the regulatory volume decrease response (Fig. 30).

The release of ATP and activation of P<sub>2</sub> purinergic receptors resulting in a process of regulatory volume decrease by the subsequent activation of chloride channels has been shown in rat hepatoma cells in culture (Wang *et al.*, 1996). Furthermore, RVD was blocked by the purinergic antagonists suramin and RB-2 (Wang *et al.*, 1996). I propose that a similar, novel mechanism of volume recovery occurs in the rat hippocampus during the falling phase of spreading depression as presented in Fig. 30.

At present, there is uncertainty as to which cell type (neuronal, glial, or both) is responsible for the changes in IOS of st. radiatum of the CA1, as there is swelling in both astrocytes (Chebabo *et al.*, 1995) and neurons (Van Harreveld, 1958; Van Harreveld and Khattab, 1967) during SD. It has been suggested that in tissue slices it would be difficult, if not impossible, to determine which cell type contributes to the volume regulation (Huang and Somjen, 1995) during processes such as SD. Quantitative studies of hippocampal cytoarchitecture are scarce, however, there are hints that glia are more abundant in st. radiatum than in st. pyramidale (Herreras and Somjen, 1993), and conceivably may generate a greater proportion of the signal. Additionally, it was demonstrated that exposure to a high K<sup>+</sup> solution resulted in a nearly 40% volume increase in astrocytes (Walz, 1987), which during ouabain-induced SD may contribute to the change in IOS observed in the glia-abundant st. radiatum.

Extracellular field potentials have been measured during a high K<sup>+</sup> induced-SD in st. radiatum, demonstrating initially a rapid shift to a negative peak, followed by a brief plateau, a second larger peak, followed by repolarization, and frequently a positive

overshoot (Somjen *et al.*, 1992), a result confirmed in our laboratory (Basarsky, personal communication). This neuronal and glial repolarization in st. radiatum of the CA1 has been demonstrated in conditions where ATP supply dropped considerably (Olson *et al.*, 1986), and was not altered when external  $\text{Ca}^{2+}$  was removed (Harold and Walz, 1992). This suggests that an elevation of intracellular  $\text{Ca}^{2+}$  could lead to activation of  $\text{Ca}^{2+}$ -activated  $\text{K}^+$  channels (Miller, 1991; Harold and Walz, 1992), as such channels are known to be expressed in astrocytes (Quandt and MacVicar, 1986) or  $\text{Cl}^-$  channels (Bender *et al.*, 1993). Furthermore, it was suggested that this pattern may be compatible with the presence of ATP-sensitive  $\text{K}^+$  channels, whose  $\text{K}^+$  efflux is activated by a drop in ATP concentration (Noma, 1983). However, cytosolic ATP levels must fall to approximately 1 mM before ATP-sensitive channels will open (Noma, 1983; Ashcroft, 1988).

Consistent with this hypothesis, a recent study demonstrated that activation of  $\text{P}_{2y}$  purinoceptors with 2-methylthioATP activates a potassium channel in cultured rat hippocampal neurons (Ikeuchi *et al.*, 1996), and stimulates  $\text{Ca}^{2+}$  release from intracellular stores regulated by a G-protein-mediated signaling pathway (Ikeuchi *et al.*, 1996). The activation of  $\text{K}^+$  channels directly or through the activation of  $\text{Ca}^{2+}$ -activated  $\text{K}^+$  channels may contribute to the regulatory volume decrease during the falling phase of SD. Alternatively,  $\text{P}_2$ -purinergic activation by ATP may result in activation of chloride channels leading to a cell volume decrease (Wang *et al.*, 1996). Evidence from another study in our laboratory provides support for the chloride channel hypothesis. It has been determined that NPPB, a chloride channel inhibitor, has an effect similar to suramin, by slowing the falling phase of ouabain-induced SD. This suggests that chloride channel activation may play a role in the volume-recovery falling phase of ouabain-induced SD (Basarsky and MacVicar, 1996; Basarsky, personal communication).

#### 4.10 Role of sodium influx in spreading depression: Implication of $\text{Na}^+/\text{Ca}^{2+}$ exchanger in the onset phase

The results of this thesis have shown that the propagation and falling phases of ouabain-induced SD as measured in *st. radiatum* of the CA1 are not dependent on the presence of extracellular calcium. The influx of  $\text{Na}^+$  and  $\text{Ca}^{2+}$  has been demonstrated during SD, although the contribution of various  $\text{Na}^+$  channels has not been described. There are several possible pathways for  $\text{Na}^+$  influx: through a  $\text{P}_{2x}$  purinoceptor non-selective cation channel, a  $\text{Na}^+/\text{Ca}^{2+}$  exchanger, a voltage-sensitive  $\text{Na}^+$  channel or perhaps an ATP-induced membrane pore.

Replacement of the bath-applied  $\text{Na}^+$ -containing aCSF with NMDG<sup>+</sup> resulted in a process similar to SD, although the propagation was at a much slower rate (Table 1). The effect of 26mM  $\text{Na}^+$  was not the same throughout all regions of the hippocampus. In the dentate gyrus, propagation of SD occurred at a similar rate as in control slices (data not shown), and in *st. oriens* was measured at a rate not statistically significant relative to control (Table 1). In *st. radiatum* propagation occurred at a significantly slower rate than in control (Table 1), although reaching the same peak level of tissue transmittance as controls. In other words, in a  $\text{Na}^+$ -free (26 mM) medium, ouabain induces a process which looks much like a slowly propagating wave of SD. It has been shown previously that the IOS generated during ouabain-induced SD in the hippocampal slice do not occur in the presence of TTX (Duffy and MacVicar, 1995, unpublished results), suggesting the involvement of TTX-sensitive  $\text{Na}^+$  channels in SD. Furthermore, it was demonstrated that IOS themselves are not blocked by the application of TTX (Andrew and MacVicar, 1994). When these results are taken together, they indicate that perhaps  $\text{Na}^+$  entry during ouabain-induced SD is via TTX-sensitive  $\text{Na}^+$  channels.

Another possibility is that the influx of  $\text{Na}^+$  may occur through channels sensitive to amiloride. Amiloride has been used in the investigation of several  $\text{Na}^+$  transport systems (Garty and Benos, 1988). It is known to block epithelial  $\text{Na}^+$  channels and inhibit  $\text{Na}^+/\text{H}^+$  and  $\text{Na}^+/\text{Ca}^{2+}$  exchange in preparations from various tissues (Luciania *et al.*, 1988). In the

presence of amiloride, the onset phase including the onset to peak time (Fig. 28) and propagation rate in *st. radiatum* (Table 1) of spreading depression is inhibited, suggesting an effect specific to the  $\text{Na}^+$  transport system, or blockade of a subset of amiloride-sensitive  $\text{Na}^+$  channels.

There is a possibility that the  $\text{Na}^+/\text{Ca}^{2+}$  exchanger may be involved in the transport of  $\text{Na}^+$  during the onset phase of SD. Benzamil, a derivative of amiloride, blocks the  $\text{Na}^+/\text{Ca}^{2+}$  exchanger (Kaczorowski *et al.*, 1985; Markram *et al.*, 1995), but does not inhibit the  $\text{Na}^+/\text{H}^+$  exchange (Ong and Kerr, 1994). The onset to peak time of ouabain-induced SD is significantly increased by the application of benzamil (500  $\mu\text{M}$ ) (Fig. 29). In addition, the propagation rate in *st. radiatum* is significantly increased relative to control (Table 1). This suggests that the  $\text{Na}^+/\text{Ca}^{2+}$  exchange may play a role in the onset phase of SD, although at these concentrations benzamil can inhibit other  $\text{Na}^+$  channels resistant to inhibition by amiloride.

In physiological conditions, the importance of the sodium/calcium exchange has been questioned (DiPolo and Beaugé, 1979, 1983). Sodium/calcium exchange becomes much more important during pathological conditions where intracellular calcium levels are far higher than normal (Lees, 1991), such as spreading depression. During application of the glutamate agonist quisqualate, there is increased involvement of the sodium/calcium exchange mechanism to extrude  $\text{Ca}^{2+}$  (Stabel *et al.*, 1990). In cerebellar granule cell cultures, it has been shown that inhibitors of the  $\text{Na}^+/\text{Ca}^{2+}$  exchange exacerbate the degree of neuronal death caused by glutamate (Andreeva *et al.*, 1991).

Benzamil inhibits the onset phase of ouabain-induced SD, suggesting involvement of the  $\text{Na}^+/\text{Ca}^{2+}$  exchange mechanism. Activation of the  $\text{Na}^+/\text{Ca}^{2+}$  exchanger could be a response by the cells to lower the intracellular calcium levels during the massive influx of  $\text{Ca}^{2+}$  during ouabain-induced SD. The high intracellular sodium resulting from SD would also reduce the efficiency of the  $\text{Na}^+/\text{Ca}^{2+}$  exchange (Lees, 1991), decreasing the ability of the cells to cope with the increased calcium influx. The response by the cells to the high

levels of intracellular calcium may be a mechanism during SD to limit the damage caused by the massive influx of  $\text{Ca}^{2+}$  accompanied by the cellular swelling.

#### 4.11 Ouabain-induced spreading depression may lead to cell death

One of the fundamental questions arising from the results of this thesis is whether the wave of spreading depression observed results in cell death. The most obvious observation contributing to this idea is that ouabain-induced SD can only be initiated once in a slice. There are, however, several hypothesized reasons as to why SD can only be initiated once. The first is not necessarily related to cell death. Ouabain binds tightly and nearly irreversibly to the  $\text{Na}^+/\text{K}^+$ -ATPase (Lees and Leong, 1994). Transferring hippocampal slices to a thermo-regulated superfusion bath will allow the slices to be kept alive for a maximum of ten hours. However, washing off ouabain would require a time much greater than ten hours. For this reason, ouabain binds with such efficacy that its effect is nearly irreversible, and this does not necessarily suggest cell death.

Another reason why ouabain-induced SD can be initiated only once in a slice, and for reasons not related to cellular death, stems from other work conducted in our laboratory. In these experiments, an analogue of ouabain, dihydroouabain, was tested to see if spreading depression can be initiated more than once. Dihydroouabain, with one-fifth to one-tenth the potency of ouabain as an inhibitor  $\text{Na}^+/\text{K}^+$  ATPase (Brosemer, 1985; Vyas and Marchbanks, 1981) was tested for its effects in initiating SD, and it was found that it can be washed off in a much shorter time period (within several hours) (Basarsky and MacVicar, unpublished results). Following the wash, SD could be initiated a second time with dihydroouabain in the same slice, although with a much weaker magnitude (Basarsky, personal communication).

Certainly the hypothesis that ouabain-induced spreading depression *does* result in widespread cell death cannot be excluded. Ouabain is one of the most potent neurotoxins in the hippocampus (Lees, 1991), with a toxicity estimated to be at least equivalent to that

of kainic acid and greater than that of NMDA (Lees, 1991). Ouabain, at a dose of 1 nM produces, *in vivo*, neuronal death in all regions of the hippocampus (Lees *et al.*, 1990). Furthermore, injections of ouabain into the brain leads to seizure activity, and neuronal death at the site of injection and other sites in the brain (Bignami and Palladini, 1966; Lowe, 1978). Other studies have demonstrated that ouabain causes the death of cells in cerebellar slices (Garthwaite *et al.*, 1986) and myocardial cells in culture (Liu *et al.*, 1987). For these reasons it is conceivable that if ouabain at 1 nM can result in neuronal death in the hippocampus *in vivo*, surely at a concentration of 100  $\mu$ M, nearly 100,000 times higher, it will have a similar effect in the *in vitro* hippocampal slice.

#### **4.12 Decreased activity of Na<sup>+</sup>,K<sup>+</sup> ATPase by ouabain may result in cell death**

There are several possible mechanisms by which decreased activity of the Na<sup>+</sup>, K<sup>+</sup> -ATPase caused by ouabain may result in a cellular death. The first is that the inhibition of the Na<sup>+</sup>, K<sup>+</sup> -ATPase may induce neuronal death secondarily, by causing the release of toxic concentrations of endogenous glutamate, or a related glutamate agonist. Consistent with this idea, the rate of glutamate release is increased 2-3 fold by infusions of ouabain *in vivo* (Jacobson *et al.*, 1986; Westerink *et al.*, 1989). *In vitro*, glutamate release by a calcium-independent process has been observed (Sánchez-Prieto *et al.*, 1987). Furthermore, cytotoxic potencies of ouabain and dihydroouabain are roughly in the same order as their potency as inhibitors of the enzyme (Brosemer, 1985; Haugar *et al.*, 1985; Vyas and Marchbanks, 1981).

Inhibition by ouabain of Na<sup>+</sup>, K<sup>+</sup> -ATPase results in a slow depolarization of the cellular membrane. The rate of depolarization is dependent on the degree of inhibition by ouabain (Brosemer, 1985; Rugolo *et al.*, 1986). The slow depolarization induced by ouabain would eventually alleviate the magnesium-regulated voltage block of NMDA receptors (Mayer and Westbrook, 1987), and contribute to an increased influx of calcium and sodium. High intracellular concentrations of calcium are toxic to cells (Choi, 1988).

Slices bathed in MK-801 (NMDA receptor antagonist), slowed the onset of spreading depression (Basarsky and MacVicar, 1996), suggesting glutamate release plays a role in the propagation of spreading depression. It is not unreasonable to infer that the application of ouabain triggers a process which results in an increase in extracellular concentrations of glutamate. The ouabain-induced glutamate release may secondarily be responsible for the widespread cell death by glutamate toxicity.

Another observation which contributes to the hypothesis that ouabain results in cell death is the observation that the intrinsic optical signals generated in the cell-body layer, or st. pyramidale, do not decay from peak. There may be several reasons why. A recent study by (Polischuk and Andrew, 1996a) demonstrated that return to baseline of the IOS in st. pyramidale occurs following the treatment of the hippocampal slice with NMDA (100  $\mu$ M). In this study, NMDA (100  $\mu$ M) was perfused for one minute. Following this, a rapid increase in transmittance in both st. radiatum and st. pyramidale of the CA1 was observed. Subsequently, the transmittance levels rapidly returned to baseline in both cellular layers, similar to what is observed only in st. radiatum of the CA1 during ouabain-induced SD. However, if the NMDA (100  $\mu$ M) is perfused for three minutes, there is a similar increase in tissue transmittance in both st. radiatum and st. pyramidale, but no return to baseline of the IOS in st. pyramidale (Polischuk and Andrew, 1996a). Tissue histology was then done forty minutes following treatment and the cells in st. pyramidale appear swollen and dead (Polischuk and Andrew, 1996a).

The infusion of ouabain into brain structures *in vivo* has been demonstrated to release acidic amino acids including glutamate (Jacobson *et al.*, 1986; Westerink *et al.*, 1989), which would have a similar action to the application of NMDA. In addition, the death of neuronal cerebellar granule cells, induced by glutamate and NMDA, is potentiated by non-toxic doses of ouabain (Novelli *et al.*, 1988). This suggests that during ouabain-induced SD, the release of glutamate may secondarily result in cell death by

glutamate toxicity, exacerbated by the presence of ouabain, similar to the swollen and dead cells observed in st. pyramidale following the application of NMDA (Polischuk and Andrew, 1996a).

## 5. SUMMARY CONCLUSIONS

Spreading depression of neuronal activity was first described over 50 years ago (Leão, 1944), and mechanisms describing its propagation have remained elusive. Imaging activity-dependent changes in tissue transmittance in the *in vitro* hippocampal slice preparation has provided a non-invasive method of analyzing the mechanisms underlying the propagation of spreading depression.

This present work suggests a novel mechanism for the recovery of cell volume during the falling phase of ouabain-induced spreading depression. A similar mechanism has been proposed in HTC rat hepatoma cells in culture (Wang *et al.*, 1996) and will be summarized briefly. The swelling-induced release of ATP occurs in a calcium-influx independent manner, activates P<sub>2</sub>-purinergic receptors, and results in the recovery of cell volume. This recovery of cell volume is thought to occur through either Ca<sup>2+</sup>-activated K<sup>+</sup> channels, or as recent work in our laboratory suggests, through the opening of Cl<sup>-</sup> channels (Basarsky, personal communication).

### 5.1 Future Experiments

The swelling-induced release of ATP resulting in volume recovery has not previously, to my knowledge, been suggested during the propagation of spreading depression. Purinergic antagonism with suramin and RB-2 provide circumstantial evidence for ATP release, but the development of more specific purinergic antagonists is necessary

before this can be firmly concluded. A few possible future experiments examining the mechanisms of ATP release during ouabain-induced SD are presented.

1. The most obvious experiment would be to image the release of ATP during ouabain-induced spreading depression and determine if it is correlated with the intrinsic optical wave. In our laboratory, calcium imaging with Fura-2-AM has been combined with imaging the intrinsic optical signals (Duffy and MacVicar, Basarsky and MacVicar, unpublished results), making this a feasible idea. Providing evidence that ATP is released during the falling phase would give the first direct evidence for the involvement of purinergic receptors.
2. Another experiment would be to eliminate ATP from the extracellular space with the presence of phosphatase apyrase (Schwiebert *et al.*, 1995). This would presumably have the same effect as suramin and RB-2, by preventing activation of the P<sub>2</sub> purinergic receptor and inhibiting the recovery of cell volume.
3. ATP stores could be depleted intracellularly before the application of ouabain. If ATP release occurs during the falling phase, then the depletion of ATP stores before SD should inhibit the falling phase similar to suramin and RB-2. Depleting ATP stores may have other devastating non-specific effects on the physiological status of cells, however, further complicating interpretation of these results.

## LITERATURE CITED

- Aitken PG, Jing J, Young J, Somjen GG (1991) Ion channel involvement in hypoxia-induced spreading depression in hippocampal slices. *Brain Res.* **541**: 7-11.
- Al-Awqati Q (1995) Regulation of ion channels by ABC transporters that secrete ATP. *Science* **269**: 805-806.
- Albers RW, Koval GJ, Siegel GJ (1968) Studies on the interactions of ouabain and other cardioactive steroids with sodium potassium-activated adenosine triphosphate. *Mol. Pharmacol.* **4**: 324-336.
- Allsup DJ, Boarder MR (1990) Comparison of P<sub>2</sub>-purinergic receptors of aortic endothelial cells with those of the adrenal medulla: evidence for heterogeneity of receptor subtype and inositol phosphate response. *Mol. Pharmacol.* **38**: 84-91.
- Amaral DG, Witter MP (1995) Hippocampal formation. In *The Rat Nervous System*, 2<sup>nd</sup> edition (ed. Paxinos G). Academic Press, New York.
- Andersen P, Bliss TVP, Skrede KK (1971) Lamellar organization of hippocampal excitatory pathways. *Exp. Brain Res.* **13**: 222-238.
- Andreasen M, Lambert JDC, Jensen MS (1988) Direct demonstration of an N-methyl-D-aspartate receptor mediated component of excitatory synaptic transmission in area CA1 of the rat hippocampus. *Neurosci. Lett.* **93**: 61-66.
- Andreasen M, Lambert JDC, Jensen MS (1989) Effects of new non-N-methyl-D-aspartate antagonists on synaptic transmission in the *in vitro* rat hippocampus. *J. Physiol.* **414**: 317-336.
- Andreeva N, Khodorov B, Stelmashook E, Cragoe E, Victorov I (1991) Inhibition of Na<sup>+</sup>/Ca<sup>2+</sup> exchange enhances delayed neuronal death elicited by glutamate in cerebellar granule cell cultures. *Brain Res.* **548**: 322-325.
- Andrew RD (1991) Seizure and acute osmotic change: Clinical and neurophysiological aspects. *J. Neurol. Sci.* **101**: 7-18.
- Andrew RD, Adams JR, Polischuk TM (1996) Imaging NMDA- and kainate-induced intrinsic optical signals from the hippocampal slice. *J. Neurophysiol.* **76**: 2707-2717.
- Andrew RD, Lobinowich ME, Osehobo EP (1997) Evidence against volume regulation by cortical brain cells during acute osmotic stress. *Exp. Neurol.* **143**: 300-312.

- Andrew RD, MacVicar BA (1994) Imaging cell volume changes and neuronal excitation in the hippocampal slice. *Neurosci.* **62**: 371-383.
- Antonelli MC, Baskin DG, Garland M, Stahl WL (1989) Localization and characterization of binding sites with high affinity for [<sup>3</sup>H]-ouabain in cerebral cortex of rabbit brain using quantitative autoradiography. *J. Neurochem.* **52**: 193-200.
- Archibald JT, White TD (1974) Rapid reversal of internal Na<sup>+</sup> and K<sup>+</sup> contents of synaptosomes by ouabain. *Nature* **252**: 595-596.
- Ashcroft FM (1988) Adenosine 5'-triphosphate-sensitive potassium channels. *Ann. Rev. Neurosci.* **11**: 97-118.
- Ascher P, Large WA, Rang HP (1979) Studies on the mechanism of action of acetylcholine antagonists on rat parasympathetic ganglion cells. *J. Physiol.* **295**: 139-170.
- Ascher P, Marty A, Neild TO (1978) The mode of action of antagonists of the excitatory response to acetylcholine in *Aplysia* neurons. *J. Physiol.* **278**: 207-235.
- Atterwill CK, Cunningham VJ, Balázs R (1984) Characterization of Na<sup>+</sup>,K<sup>+</sup>-ATPase in cultured and separated neuronal and glial cells from rat cerebellum. *J. Neurochem.* **43**: 8-18.
- Avoli M, Drapeau C, Louvel J, Pumain R, Olivier A, Villemure JG (1991) Epileptiform activity induced by low extracellular magnesium in the human cortex maintained *in vitro*. *Ann. Neurol.* **30**: 589-596.
- Balachandran C, Bennett MR (1996) ATP-activated cationic and anionic conductances in cultured rat hippocampal neurons. *Neurosci. Lett.* **204**: 73-76.
- Balcar VJ, Li Y, Killinger S, Bennett MR (1995) Autoradiography of P<sub>2x</sub> ATP receptors in the rat brain. *Br. J. Pharmacol.* **115**: 302-306.
- Ballanyi K, Grafé P (1988) Cell volume regulation in the nervous system. *Renal Physiol. Biochem.* **3-5**: 142-157.
- Barnard EA (1992) Receptor classes and the transmitter-gated ion channels. *Trends. Biochem. Sci.* **17**: 368-374.
- Barnard EA, Burnstock G, Webb TE (1994) G-protein coupled receptors for ATP and other nucleotides: a new receptor family. *Trends Pharmacol. Sci.* **15**: 67-71.

- Basarsky TA, MacVicar BA (1996) Regulation of volume responses during spreading depression in hippocampal slices. *Soc. Neurosci. Abstr.* **22**: 787.
- Bean BP (1992) Pharmacology and electrophysiology of ATP-activated ion channels. *Trends Pharmacol. Sci.* **13**: 87-90.
- Bekkers JM, Stevens CF (1989) NMDA and non-NMDA receptors are co-localized at individual excitatory synapses in cultured rat hippocampus. *Nature* **341**: 230-233.
- Ben-Ari Y (1990) Galanin and glibenclamide modulate the anoxic release of glutamate in rat CA3 hippocampal neurons. *Eur. J. Neurosci.* **2**: 62-68.
- Bender AS, Neary JT, Blicharska J, Norenberg LOB, Norenberg MD (1992) Role of calmodulin and protein kinase C in astrocytic cell volume regulation. *J. Neurochem.* **58**: 1874-1882.
- Bender AS, Neary JT, Norenberg MD (1993) Role of phosphoinositide hydrolysis in astrocyte volume regulation. *J. Neurochem.* **61**: 1506-1514.
- Bender AS, Norenberg MD (1994) Calcium dependence of hypoosmotically induced potassium release in cultured astrocytes. *J. Neurosci.* **14**: 4237-4243.
- Benham CD, Tsien RW (1987) A novel receptor-operated  $\text{Ca}^{2+}$ -permeable channel activated by ATP in smooth muscle. *Nature* **328**: 275-278.
- Berberi-Bertrand I, Maixent JM, Christe G, Lelièvre LG (1990) Two active  $\text{Na}^+/\text{K}^+$ -ATPases of high affinity for ouabain in adult rat brain membranes. *Biochim. Biophys. Acta.* **1021**: 148-156.
- Bignami A, Palladini G (1966) Experimentally produced cerebral status spongiosus and continuous pseudorhythmic electroencephalographic discharges with a membrane-ATPase inhibitor in the rat. *Nature* **209**: 413-414.
- Blackstone CD, Moss SJ, Martin LJ, Levey AI, Price DL, Huganir RL (1992) Biochemical characterization and localization of a non-N-methyl-D-aspartate glutamate receptor in rat brain. *J. Neurochem.* **58**: 1118-1126.
- Blasdel GG, Salama G (1986) Voltage-sensitive dyes reveal a modular organization in monkey striate cortex. *Nature* **321**: 579-585.
- Bo X, Burnstock G (1994) Distribution of [ $^3\text{H}$ ]  $\alpha,\beta$ -methylene ATP binding sites in rat brain and spinal cord. *NeuroReport* **5**: 1601-1604.

- Boyer JL, Zohn IE, Jacobson KA, Harden TK (1994) Differential effects of P<sub>2</sub>-purinoceptor antagonists on phospholipase C- and adenylyl cyclase-coupled P<sub>2Y</sub>-purinoceptors. *Br. J. Pharmacol.* **113**: 614-620.
- Brake AJ, Wagenbach MJ, Julius D (1994) New structural motif for ligand-gated ion channels defined by an ionotropic ATP receptor. *Nature* **371**: 519-523.
- Brosemer RW (1985) Effect of inhibitors of Na<sup>+</sup>, K<sup>+</sup>-ATPase on the membrane potentials and neurotransmitter efflux in rat brain slices. *Brain Res.* **334**: 125-137.
- Bültmann R, Starke K (1994) P<sub>2</sub>-purinoceptor antagonists discriminate three contraction-mediating receptors for ATP in rat vas deferens. *Naunyn-Schmiedeberg's Arch. Pharmacol.* **349**: 74-80.
- Bures J, Buresová O, Krivanek J (1974) The mechanisms and applications of Leão's spreading depression of electroencephalographic activity. Prague: Academia.
- Burnstock G, Kennedy C (1985) Is there a basis for distinguishing two types of P<sub>2</sub>-purinoceptors? *Gen. Pharmacol.* **16**: 433-440.
- Burnstock G (1990) Overview. Purinergic mechanisms. *Ann. NY Acad. Sci.* **603**: 1-17.
- Chang K, Hanaoka K, Kumada M, Takuwa Y (1995) Molecular cloning and functional analysis of a novel P<sub>2</sub> nucleotide receptor. *J. Biol. Chem.* **270**: 26152-26159.
- Charles A, Merrill J, Dirksen E, Sanderson M (1990) Elevation and oscillation of [Ca<sup>2+</sup>]<sub>i</sub> and intercellular communication in glial cells in response to trauma and glutamate. *Soc. Neurosci. Abstr.* **16**: 190.
- Chebabo SR, Hester MA, Aitken PG, Somjen GG (1995) Hypotonic exposure enhances synaptic transmission and triggers spreading depression in rat hippocampal tissue slices. *Brain Res.* **695**: 203-216.
- Chen ZP, Levy A, Lightman SL (1994) Activation of specific ATP receptors induces a rapid increase in intracellular calcium ions in rat hypothalamic neurons. *Brain Res.* **641**: 249-256.
- Choi DW (1988) Calcium-mediated neurotoxicity: relationship to specific channel types and role in ischemic damage. *Trends. Neurosci.* **11**: 465-469.
- Choi DW, Rothman SM (1990) The role of glutamate neurotoxicity in hypoxic-ischemic neuronal death. *Annu. Rev. Neurosci.* **13**: 171-182.

- Choo LK (1981) The effect of reactive blue, an antagonist of ATP, on the isolated urinary bladders of guinea-pig and rat. *J. Pharm. Pharmacol.* **33**: 248-250.
- Christie A, Sharma VK, Sheu SS (1992) Mechanism of extracellular ATP-induced increase of cytosolic  $\text{Ca}^{2+}$  concentration in isolated rat ventricular myocytes. *J. Physiol.* **445**: 369-388.
- Churchwell KB, Wright SH, Emma F, Rosenberg PA, Strange K (1996) NMDA receptor activation inhibits neuronal volume regulation after swelling induced veratridine-stimulated  $\text{Na}^+$  influx in rat cortical cultures. *J. Neurosci.* **16**: 7447-7457.
- Cohen LB (1973) Changes in neuron structure during action potential propagation and synaptic transmission. *Physiol. Rev.* **53**: 373-418.
- Collewijn H, Van Harreveld AV (1966) Membrane potential of cerebral cortical cells during spreading depression and asphyxia. *Exp. Neurol.* **15**: 425-436.
- Cook DL, Hales CN (1984) Intracellular ATP directly blocks  $\text{K}^+$  channels in pancreatic B-cells. *Nature* **311**: 271-273.
- Cook NS (1988) The pharmacology of potassium channels and their therapeutic potential. *Trends Pharmacol. Sci.* **9**: 21-28.
- Cornell-Bell AH, Finkbeiner SM, Cooper MS, Smith SJ (1990) Glutamate induces calcium waves in cultured astrocytes: long-range glial signaling. *Science* **247**: 470-473.
- Cotman CW, Monaghan DT, Ottersen OP, Storm-Mathisen J (1987) Anatomical organization of excitatory amino acid receptors and their pathways. *Trends Neurosci.* **10**: 273-281.
- Cowen DS, Sanders M, Dubyak G (1990)  $\text{P}_2$ -purinergic receptors activate a guanine nucleotide-dependent phospholipase C in membranes from HL-60 cells. *Biochim. Biophys. Acta.* **1053**: 195-203.
- Curtis DR, Watkins JC (1963) Acidic amino acids with strong excitatory actions on mammalian neurones. *J. Physiol.* **166**: 1-14.
- Czéh G, Somjen GG (1990) Hypoxic failure of synaptic transmission in the isolated spinal cord, and the effects of divalent cations. *Brain Res.* **527**: 224-233.

- Dale N, Gilday D (1996) Regulation of rhythmic movements by purinergic neurotransmitters in frog embryos. *Nature* **383**: 259-263.
- Dingledine R, Dodd J, Kelly JS (1977) Intracellular recording from pyramidal neurones in the *in vitro* transverse hippocampal slice. *J. Physiol.* **269**: 13-15P.
- Dingledine R, Dodd J, Kelly JS (1980) The *in vitro* brain slice as a useful neurophysiological preparation for intracellular recording. *J. Neurosci. Met.* **2**: 323-362.
- DiPolo R, Beaugé L (1979) Physiological role of ATP-driven calcium pump in squid axon. *Nature* **278**: 271-273.
- DiPolo R, Beaugé L (1983) The calcium pump and sodium-calcium exchange in squid axons. *Annu. Rev. Physiol.* **45**: 313-324.
- Dubyak GR, el-Moatassim C (1993) Signal transduction via P<sub>2</sub>-purinergic receptors for extracellular ATP and other nucleotides. *Amer. J. Physiol.* **265**: C577-606.
- Dunn PM, Blakeley AGH (1988) Suramin: a reversible P<sub>2</sub>-purinoceptor antagonist in the mouse vas deferens. *Br. J. Pharmacol.* **93**: 243-245.
- Ebner TJ, Chen G (1995) Use of voltage-sensitive dyes and optical recordings in the central nervous system. *Prog. Neurobiol.* **46**: 463-506.
- Edwards FA, Gibb AJ, Colquhoun D (1992) ATP receptor-mediated synaptic currents in the central nervous system. *Nature* **359**: 144-147.
- Ehrlich Y, Davis T, Bock E, Kornecki E, Lenox RH (1986) Ecto-protein kinase activity on the external surface of neural cells. *Nature* **320**: 67-69.
- El-Moatassim C, Dornand J, Mani JC (1992) Extracellular ATP and cell signalling. *Biochim. Biophys. Acta.* **1134**: 31-45.
- Evans R, Derkach V, Surprenant A (1992) ATP mediates fast synaptic transmission in mammalian neurons. *Nature* **357**: 503-505.
- Fabricius M, Jensen LH, Lauritzen M (1993) Microdialysis of interstitial amino acids during spreading depression and anoxic depolarization in rat neocortex. *Brain Res.* **612**: 61-69.

- Federico P, Borg SG, Salkauskus AG, MacVicar BA (1994) Mapping patterns of neuronal activity and seizure propagation by imaging intrinsic optical signals in the isolated whole brain of the guinea-pig. *Neurosci.* **58**: 461-480.
- Ferrari MD, Odink J, Bos KD, Malessy MJA, Bruyn GW (1990) Neuroexcitatory plasma amino acids are elevated in migraine. *Neurol.* **40**: 1582-1586.
- Fortes PAG, Ellory JC, Lew VL (1973) Suramin: a potent ATPase inhibitor which acts on the inside surface of the sodium pump. *Biochim. Biophys. Acta.* **318**: 262-272.
- Fredholm BB, Abbracchio MP, Burnstock G, Daly JW, Harden T, Jacobson KA, Leff P, Williams M (1994) Nomenclature and classification of purinoceptors. *Pharmacol. Rev.* **46**: 143-156.
- Frostig RD, Lieke EE, Ts'o DY, Grinvald A (1990) Cortical functional architecture and local coupling between neuronal activity and the microcirculation revealed by *in vivo* high-resolution optical imaging of intrinsic signals. *Proc. Natl. Acad. Sci.* **87**: 6082-6086.
- Fujii T (1991) Profiles of percent reduction of cytochromes in guinea-pig hippocampal brain slices *in vitro*. *Brain Res.* **540**: 224-228.
- Gainer H, Wolfe SAJ, Obaid AL, Salzberg BM (1986) Action potentials and frequency-dependent secretion in the mouse neurohypophysis. *Neuroendocrinol.* **43**: 557-563.
- Garthwaite J, Garthwaite G, Hajós F (1986) Amino acid neurotoxicity: relationship to neuronal depolarization in rat cerebellar slices. *Neurosci.* **18**: 449-460.
- Garty H, Benos DJ (1988) Characteristics and regulatory mechanisms of the amiloride-blockable Na<sup>+</sup> channel. *Physiol. Rev.* **68**: 309-373.
- Goddard GA, Robinson JD (1976) Uptake and release of calcium by rat brain synaptosomes. *Brain Res.* **110**: 331-350.
- Gordon JL (1986) Extracellular ATP: effects, sources and fate. *Biochem. J.* **233**: 309-319.
- Grinvald A, Manker A, Segal N (1982) Visualization of the spread of electrical activity in rat hippocampal slices by voltage sensitive optical probes. *J. Physiol.* **333**: 269-291.

- Grinvald A, Lieke EE, Frostig RD, Gilbert CD, Wiesel TN (1986) Functional architecture of cortex revealed by optical imaging of intrinsic signals. *Nature* **324**: 361-364.
- Guillaume D, Grisar T, Delgado-Escueta AV, Laschet J, Bureau-Hereen, M (1990) Two isoenzymes of Na<sup>+</sup>,K<sup>+</sup>-ATPase have different kinetics of K<sup>+</sup> dephosphorylation in normal cat and human brain cortex. *J. Neurochem.* **54**: 130-134.
- Hablitz JJ, Heinemann U (1989) Alterations in the microenvironment during spreading depression associated with epileptiform activity in the immature cortex. *Dev. Brain Res.* **46**: 243-252.
- Haglund MM, Ojemann GA, Hochman DW (1992) Optical imaging of epileptiform and functional activity in human cerebral cortex. *Nature* **358**: 668-671.
- Haglund MM, Schwartzkroin PA (1984) Seizure-like spreading depression in the immature rabbit hippocampus *in vitro*. *Dev. Brain Res.* **14**: 51-59.
- Haglund MM, Schwartzkroin PA (1990) Role of Na-K pump potassium regulation and IPSPs in seizures and spreading depression in immature rabbit hippocampal slices. *J. Neurophysiol.* **63**: 225-239.
- Haglund MM, Stahl WL, Kunkel DD, Schwartzkroin PA (1985) Developmental and regional differences in the localization of Na-K-ATPase activity in the rabbit hippocampus. *Brain Res.* **343**: 198-203.
- Hamlyn JM, Blaustein MP, Bova S, DuCharme DW, Harris DW, Mandel F, Mathews WR, Ludens JH (1991) Identification and characterization of a ouabain-like compound from human plasma. *Proc. Natl. Acad. Sci.* **88**: 6259-6263.
- Hansen AJ (1985) Effect of anoxia on ion distribution in the brain. *Physiol. Rev.* **65**: 101-148.
- Hansen AJ, Olsen CE (1980) Brain extracellular space during spreading depression and ischemia. *Acta Physiol. Scand.* **108**: 355-365.
- Hansen AJ, Quistorff B, Gjedde A (1980) Relationship between local changes in cortical blood flow and extracellular K<sup>+</sup> during spreading depression. *Acta Physiol. Scand.* **109**: 1-6.
- Hansen AJ, Zeuthen T (1981) Extracellular ion concentrations during spreading depression and ischemia in the rat brain cortex. *Acta Physiol. Scand.* **113**: 437-445.

- Harden TK, Boyer JL, Nicholas RA (1995) P<sub>2</sub>-purinergic receptors: subtype-associated signaling responses and structure. *Ann. Rev. Pharmacol. Toxicol.* **35**: 541-579.
- Harold DE, Walz W (1992) Metabolic inhibition and electrical properties of type-I-like cortical astrocytes. *Neurosci.* **47**: 203-211.
- Hasséssian H, Bodin P, Burnstock G (1993) Blockade by glibenclamide of the flow-evoked endothelial release of ATP that contributes to vasodilation in the pulmonary vascular bed of the rat. *Br. J. Pharmacol.* **109**: 466-472.
- Hauger R, Luu HMD, Meyer DK, Goodwin FK, Paul SM (1985) Characterization of the "high-affinity" [<sup>3</sup>H]ouabain binding in the rat central nervous system. *J. Neurochem.* **44**: 1709-1715.
- Hawkins LM, Beaver KM, Jane DE, Taylor PM, Sunter DC, Roberts PJ (1995) Characterization of the pharmacology and regional distribution of (S)-[<sup>3</sup>H]-5-fluorowillardiine binding in rat brain. *Br. J. Pharmacol.* **116**: 2033-2039.
- Hernández-Cáceres J, Macias-González R, Brozek G, Bures J (1987) Systemic ketamine blocks cortical spreading depression but does not delay the onset of terminal anoxic depolarization in rats. *Brain Res.* **437**: 360-364.
- Herreras O, Somjen GG (1993) Propagation of spreading depression among dendrites and somata of the same cell population. *Brain Res.* **610**: 276-282.
- Higashida H, Mitarai G, Watanabe S (1974) A comparative study of membrane potential changes in neurons and neuroglial cells during spreading depression in the rabbit. *Brain Res.* **65**: 411-425.
- Hill DK, Keyens RD (1949) Opacity changes in stimulated nerve. *J. Physiol.* **108**: 278-81.
- Hoffmann EK, Dunham PB (1995) Membrane mechanisms and intracellular signalling in cell volume regulation. *Int. Rev. Cyt.* **161**: 173-264.
- Holthoff K, Dodt HU, Witte OW (1994) Changes in intrinsic optical signal of rat neocortical slices following afferent stimulation. *Neurosci. Lett.* **180**: 227-230.
- Holthoff K, Witte OW (1996) Intrinsic optical signals in rat neocortical slices measured with near-infrared dark-field microscopy reveal changes in extracellular space. *J. Neurosci.* **16**: 2740-2749.

- Horisberger JD, Lemas V, Kraehenbühl JP, Rossier BC (1991) Structure-function relationship of Na,K-ATPase. *Annu. Rev. Physiol.* **53**: 565-584.
- Hoyle CHV, Knight GE, Burnstock G (1990) Suramin antagonizes responses to P<sub>2</sub>-purinoceptor agonists and purinergic nerve stimulation in the guinea-pig urinary bladder and taenia coli. *Br. J. Pharmacol.* **99**: 617-621.
- Huang R, Somjen GG (1995) The effect of graded hypertonia on interstitial volume, tissue resistance and synaptic transmission in rat hippocampal tissue slices. *Brain Res.* **702**: 181-187.
- Huston JP (1971) Yawning and penile erection induced in rats by cortical spreading depression. *Nature* **232**: 274-275.
- Huston JP, Bures J (1970) Drinking and eating elicited by cortical spreading depression. *Science* **169**: 702-704.
- Huston JP, Siegfried B, Ornstein K, Waser PG, Borbély A (1974) Eating elicited by spreading depression or electrical stimulation of the hippocampus and neocortex: a common cause. *Brain Res.* **78**: 164-168.
- Ikeuchi Y, Nishizaki T, Mori M, Okada Y (1996) Regulation of the potassium current and cytosolic Ca<sup>2+</sup> release induced by 2-methylthio ATP in hippocampal neurons. *Biochem. Biophys. Res. Comm.* **218**: 428-433.
- Illes P, Nörenberg W (1993) Neuronal ATP receptors and their mechanism of action. *Trends Pharmacol. Sci.* **14**: 50-54.
- Inoue K, Koizumi S, Nakazawa K (1995) Glutamate-evoked release of adenosine 5'-triphosphate causing an increase in intracellular calcium in hippocampal neurones. *NeuroReport* **6**: 437-440.
- Iredale PA, Martin KF, Alexander SPH, Hill SJ, Kendall DA (1992) Inositol 1,4,5-triphosphate generation and calcium mobilisation via activation of an atypical P<sub>2</sub> receptor in the neuronal cell line, N1E-115. *Br. J. Pharmacol.* **107**: 1083-1087.
- Ishizuka N, Weber J, Amaral DG (1990) Organization of intrahippocampal projections originating from CA3 pyramidal cells in the rat. *J. Comp. Neurol.* **295**: 580-623.
- Jacobson KLR, Hagberg H, Sandberg M, Hamberger A (1986) Ouabain-induced changes in extracellular aspartate, glutamate and GABA levels in the rabbit olfactory bulb *in vivo*. *Neurosci. Lett.* **64**: 211-215.

- Jansen KLR, Dragunow M, Faull RLM (1989) [<sup>3</sup>H]-Glycine binding sites, NMDA and PCP receptors have similar distributions in the human hippocampus: an autoradiographic study. *Brain Res.* **482**: 174-178.
- Jöbsis FF (1977) Noninvasive, infrared monitoring of cerebral and myocardial oxygen sufficiency and circulatory parameters. *Science* **198**: 1264-1267.
- Jöbsis FF, Keizer JH, La Manna JC, Rosenthal M (1977) Reflectance spectrophotometry of cytochrome aa<sub>3</sub> *in vivo*. *J. Appl. Physiol.* **43**: 858-872.
- Johnson KM, Jones SM (1990) Neuropharmacology of phencyclidine: Basic mechanisms and therapeutic potential. *Ann. Rev. Pharmacol. Toxicol.* **30**: 707-750.
- Kaczorowski GJ, Barros F, Dethmers JK, Trumble MJ (1985) Inhibition of Na<sup>+</sup>/Ca<sup>2+</sup> exchange in pituitary plasma membrane vesicles by analogues of amiloride. *Biochem.* **24**: 1394-1403.
- Kanzaki A, Akiyama K, Otsuki S (1992) Subchronic methamphetamine treatment enhances ouabain-induced striatal dopamine efflux *in vivo*. *Brain Res.* **569**: 181-188.
- Kastritsis CHC, Salm AK, McCarthy K (1992) Stimulation of the P<sub>2y</sub> purinergic receptor on type I astroglia results in inositol phosphate formation and calcium mobilization. *J. Neurochem.* **58**: 1277-1284.
- Kauer JS (1991) Contributions of topography and parallel processing to odor coding in the vertebrate olfactory pathway. *Trends Neurosci.* **14**: 79-85.
- Kawasaki K, Czéh G, Somjen GG (1988) Prolonged exposure to high potassium concentration results in irreversible loss of synaptic transmission in hippocampal tissue slices. *Brain Res.* **457**: 322-329.
- Kawasaki K, Traynelis SF, Dingledine R (1990) Different responses of CA1 and CA3 regions to hypoxia in rat hippocampal slice. *J. Neurophysiol.* **63**: 385-394.
- Khakh BS, Surprenant A, Humphrey PPA (1995) A study on P<sub>2x</sub>-purinoceptors mediating the electrophysiological and contractile effects of purine nucleotides in rat vas deferens. *Br. J. Pharmacol.* **115**: 177-185.
- Kidd EJ, Grahames CBA, Simon J, Michel AD, Barnard EA, Humphrey PPA (1995) Localization of P<sub>2x</sub> purinoceptor transcripts in the rat nervous system. *Mol. Pharmacol.* **48**: 569-573.

- Kimelberg HK, Goderie SK, Higman S, Pang S, Waniewski RA (1990) Swelling-induced release of glutamate, aspartate, and taurine from astrocyte cultures. *J. Neurosci.* **10**: 1583-1591.
- Koroleva VI, Bures J (1993) Rats do not experience cortical or hippocampal spreading depression as aversive. *Neurosci. Lett.* **149**: 153-56.
- Kraig RP, Nicholson C (1978) Extracellular ionic variations during spreading depression. *Neurosci.* **3**: 1045-1059.
- Kreisman NR, Smith ML (1993) Potassium-induced changes in excitability in the hippocampal CA1 region of immature and adult rats. *Dev. Brain Res.* **76**: 67-73.
- Kreisman NR, LaManna JC, Liao SC, Yeh ER, Alcalá JR (1995) Light transmittance as an index of cell volume in hippocampal slices: optical differences of interfaced and submerged positions. *Brain Res.* **693**: 179-186.
- Krivanek J, Koroleva VI (1996) Protein kinase C in the rat cerebral cortex during spreading depression. *Neurosci. Lett.* **210**: 79-82.
- Krnjević K (1990) Adenosine triphosphate-sensitive potassium channels in anoxia. *Stroke* **21**: 190-193.
- Kuptiz Y, Atlas D (1993) A putative ATP-activated Na<sup>+</sup> channel involved in sperm-induced fertilization. *Science* **261**: 484-486.
- Lambrecht G, Friebe T, Grimm U, Windscheif U, Bungardt E, Hildebrandt C, Bäumert HG, Spatz-Kümbel G, Mutschler E (1992) PPADs, a novel functionally selective antagonist of P<sub>2</sub> purinoceptor-mediated responses. *Eur. J. Pharmacol.* **217**: 217-219.
- La Manna JC, Sick TJ, Pikarsky SM, Rosenthal M (1987) Detection of an oxidizable fraction of cytochrome oxidase in intact rat brain. *Am. J. Physiol.* **253**: C477-C483.
- Larsson O, Ammälä C, Bokvist K, Fredholm B, Rorsman P (1993) Stimulation of the K<sub>ATP</sub> channel by ADP and diazoxide requires nucleotide hydrolysis in mouse pancreatic  $\beta$ -cells. *J. Physiol.* **463**: 349-365.
- Lauritzen M (1987) Cortical spreading depression as a putative migraine mechanism. *Trends Neurosci.* **10**: 8-13.

- Lauritzen M, Hansen AJ (1992) The effect of glutamate receptor blockade on anoxic depolarization and cortical spreading depression. *J. Cereb. Blood Flow Metab.* **12**: 223-229.
- Lauritzen M, Rice ME, Okada YC, Nicholson C (1988) Quisqualate, kainate and NMDA can initiate spreading depression in the turtle cerebellum. *Brain Res.* **475**: 317-327.
- Lauritzen M (1994) Pathophysiology of the migraine aura. The spreading depression theory. *Brain* **117**: 199-210.
- Leão AAP (1944) Spreading depression of activity in the cerebral cortex. *J. Neurophysiol.* **7**: 359-390.
- Leão AAP (1947) Further observations on the spreading depression of activity in the cerebral cortex. *J. Neurophysiol.* **10**: 409-414.
- Leão AAP, Morison RS (1945) Propagation of spreading cortical depression. *J. Neurophysiol.* **8**: 33-45.
- Lees GJ (1991) Inhibition of sodium-potassium-ATPase: a potentially ubiquitous mechanism contributing to central nervous system neuropathology. *Brain Res. Rev.* **16**: 283-300.
- Lees GJ (1993) Contributory mechanisms in the causation of neurodegenerative disorders. *Neurosci.* **54**: 287-322.
- Lees GJ, Lehmann A, Sandberg M, Hamberger A (1990) The neurotoxicity of ouabain, a sodium-potassium ATPase inhibitor, in the rat hippocampus. *Neurosci. Lett.* **120**: 159-162.
- Lees GJ, Leong W (1994) Brain lesions induced by specific and non-specific inhibitors of sodium-potassium ATPase. *Brain Res.* **649**: 225-233.
- Lieke EE, Frostig RD, Arieli A, Ts'o DY, Hildeshiem R, Grinvald A (1989) Optical imaging of cortical activity: real-time imaging using extrinsic dye-signals and high resolution imaging based on slow intrinsic signals. *Ann. Rev. Physiol.* **51**: 543-559.
- Lipton P (1973) Effects of membrane depolarization on light scattering by cerebral cortical slices. *J. Physiol.* **231**: 365-383.

- Liu J, Yang Y, Tan S (1987) Three correlations between extracellular calcium concentration and myocardial cell injury induced by drugs. *Life Sci.* **40**: 2175-2185.
- Lowe DA (1978) Morphological changes in the cat cerebral cortex produced by superfusion of ouabain. *Brain Res.* **148**: 347-363.
- Luciania S, Bova S, Cargnelli G, Debetto P (1988) Effects of amiloride on the cardiovascular system: role of  $\text{Na}^+/\text{Ca}^{2+}$  exchange. *Pharmacol. Res.* **25**: 303.
- Lyons SA, Morell P, McCarthy KD (1995) Schwann cell ATP-mediated calcium increases *in vitro* and *in situ* are dependent on contact with neurons. *Glia* **13**: 27-38.
- MacVicar BA (1984) Infrared video microscopy to visualize neurons in the *in vitro* brain slice preparation. *J. Neurosci. Met.* **12**: 133-139.
- MacVicar BA, Hochman D (1991) Imaging of synaptically evoked intrinsic optical signals in hippocampal slices. *J. Neurosci.* **11**: 1458-1469.
- MacVicar BA, Hochman D, LeBlanc F, Watson T (1990) Stimulation evoked changes in intrinsic optical signals in the human brain. *Soc. Neurosci. Abstr.* **16**: 309.
- Mahoney CW, Azzi A, Huang KP (1990) Effects of suramin, an anti-human immunodeficiency virus reverse transcriptase agent, on protein kinase C. *J. Biol. Chem.* **265**: 5424-5428.
- Manzini S, Hoyle CH, Burnstock G (1986) An electrophysiological analysis of the effect of reactive blue 2, a putative  $\text{P}_2$ -purinoceptor antagonist, on inhibitory junction potentials of rat caecum. *Eur. J. Pharmacol.* **127**: 197-204.
- Markram H, Helm PJ, Sakmann B (1995) Dendritic calcium transients evoked by single back-propagating action potentials in rat neocortical pyramidal neurons. *J. Physiol.* **485**: 1-20.
- Marks MJ, Seeds NW (1978) A heterogeneous ouabain-ATPase interaction in mouse brain. *Life Sci.* **23**: 2735-2744.
- Marrannes R, Willems R, De Prins E, Wauquier A (1988) Evidence for a role of the N-methyl-D-aspartate (NMDA) receptor in cortical spreading depression in the rat. *Brain Res.* **457**: 226-240.
- Marshall WH (1959) Spreading cortical depression of Leão. *Physiol. Rev.* **39**: 239-279.

- Martins-Ferreira H, de Oliveira Castro G (1966) Light-scattering changes accompanying spreading depression in isolated retina. *J. Neurophysiol.* **29**: 715-726.
- Mayer ML, Westbrook GL (1987) The physiology of excitatory amino acids in the vertebrate central nervous system. *Prog. Neurobiol.* **28**: 197-276.
- McGann LE, Walterson ML, Hogg LM (1988) Light scattering and cell volumes in osmotically stressed and frozen-thawed cells. *Cytometry* **9**: 33-38.
- McGrail KM, Phillips JM, Sweadner KJ (1991) Immunofluorescent localization of three Na,K-ATPase isozymes in the rat central nervous system: both neurons and glia can express more than one Na,K-ATPase. *J. Neurosci.* **11**: 381-391.
- McManus M, Fischbarg J, Sun A, Hebert S, Strange K (1993) Laser light-scattering system for studying cell volume regulation and membrane transport processes. *Am. J. Physiol.* **265**: C562-C570.
- Michel AD, Humphrey PPA (1993) Distribution and characterisation of [<sup>3</sup>H]α,β-methylene ATP binding sites in the rat. *Naunyn-Schmiedeberg's Arch. Pharmacol.* **348**: 608-617.
- Miller RJ (1991) The control of neuronal Ca<sup>2+</sup> homeostasis. *Prog. Neurobiol.* **37**: 255-285.
- Milner PM (1958) Note on a possible correspondence between the scotomas of migraine and spreading depression of Leão. *Electroencephalogr. Clin. Neurophysiol* **10**: 705.
- Mironov SL (1993) Metabotropic ATP receptor in hippocampal and thalamic neurones: pharmacology and modulation of Ca<sup>2+</sup> mobilizing mechanisms. *Neuropharmacol.* **33**: 1-13.
- Mitsuya H, Popovic M, Yarchoan R, Matsuchita S, Gallo RC, Broder S (1984) Suramin protection of T cells *in vitro* against infectivity and cytopathic effect of HTLV-III. *Science* **226**: 172-174.
- Mody I, Lambert JD, Heinemann U (1987) Low extracellular magnesium induces epileptiform activity and spreading depression in rat hippocampal slices. *J. Neurophysiol.* **57**: 869-888.
- Monaghan DT, Cotman CW (1985) Distribution of N-methyl-D-aspartate-sensitive L-[<sup>3</sup>H]glutamate-binding sites in rat brain. *J. Neurosci.* **5**: 2909-2919.

- Monaghan DT, Bridges RJ, Cotman CW (1989) The excitatory amino acid receptors: their classes, pharmacology, and distinct properties in the function of the central nervous system. *Ann. Rev. Pharmacol. Toxicol.* **29**: 365-402
- Moskowitz MA (1984) The neurobiology of vascular head pain. *Annal. Neurol.* **16**: 157-168.
- Moskowitz MA (1992) Neurogenic versus vascular mechanisms of sumatriptan and ergot alkaloids in migraine. *Trends Pharmacol. Sci.* **13**: 307-311.
- Motin L, Bennett MR (1995) Effect of P<sub>2</sub>-purinoceptor antagonists on glutamatergic transmission in the rat hippocampus. *Br. J. Pharmacol.* **115**: 1276-1280.
- Nagy AK, Shuster TA, Delgado-Escueta AV (1986) Ecto-ATPase of mammalian synaptosomes: identification and enzymic characterization. *J. Neurochem.* **47**: 976-986.
- Nakazawa K, Fujimori K, Takanaka A, Inoue K (1990a) An ATP-activated conductance in phaeochromocytoma cells and its suppression by extracellular calcium. *J. Physiol.* **428**: 257-272.
- Nakazawa K, Fujimori K, Takanaka A, Inoue K (1990b) Reversible and selective antagonism by suramin of ATP-activated inward current in PC 12 phaeochromocytoma cells. *Br. J. Pharmacol.* **101**: 224-226.
- Nakazawa K, Inoue K, Ito K, Koizumi S, Inoue K (1995) Inhibition by suramin and reactive blue 2 of GABA and glutamate receptor channels in rat hippocampal neurons. *Nauyn-Schmiedeberg's Arch. Pharmacol.* **351**: 202-208.
- Nakazawa K, Inoue K, Fujimori K, Takanaka A (1991) Effects of ATP antagonists on purinoceptor-operated inward currents in rat phaeochromocytoma cells. *Pflügers Arch.* **418**: 214-219.
- Nedergaard M, Cooper AJL, Goldman SA (1995) Gap junctions are required for the propagation of spreading depression. *J. Neurobiol.* **28**: 433-444.
- Nielsen EO, Johansen TH, Wätjen F, Dreger J (1995) Characterization of the binding of [<sup>3</sup>H]NS 257, a novel competitive AMPA receptor antagonist, to rat brain membranes and brain sections. *J. Neurochem.* **65**: 1264-1273.
- Noma A (1983) ATP-regulated K<sup>+</sup> channels in cardiac muscle. *Nature* **305**: 147-148.

- Novelli A, Reilly JA, Lysko PG, Henneberry RC (1988) Glutamate becomes neurotoxic via the N-methyl-D-aspartate receptor when intracellular energy levels are reduced. *Brain Res.* **451**: 205-212.
- O'Connor SE, Dainty LA, Leff P (1991) Further subclassification of ATP receptors based on agonist studies. *Trends Pharmacol. Sci.* **12**: 137-141.
- O'Connor ER, Kimelberg HK (1993) Role of calcium in astrocyte volume regulation and in the release of ions and amino acids. *J. Neurosci.* **13**: 2638-2650.
- Obaid AL, Flores R, Salzberg BM (1989) Calcium channels that are required for secretion from intact nerve terminals of vertebrates are sensitive to  $\omega$ -conotoxin and relatively insensitive to dihydropyridines. *J. Gen. Physiol.* **93**: 715-729.
- Obrenovitch TP, Zilkha E (1996) Inhibition of cortical spreading depression by L-701,324, a novel antagonist at the glycine site of the N-methyl-D-aspartate receptor complex. *Br. J. Pharmacol.* **117**: 931-937.
- Olesen J, Larsen B, Lauritzen M (1981) Focal hyperemia followed by spreading oligemia and impaired activation of rCBF in classic migraine. *Ann. Neurol.* **9**: 344-352.
- Olson JE, Sankar R, Holtzman D, James A, Fleischhacker D (1986) Energy-dependent volume regulation in primary cultured cerebral astrocytes. *J. Cell. Physiol.* **128**: 209-215.
- O'Mara (1995) Spatially selective firing properties of hippocampal formation neurons in rodents and primates. *Prog. Neurobiol.* **45**: 253-274.
- Ong J, Kerr DIB (1994) Suppression of GABA<sub>B</sub> receptor function in rat neocortical slices by amiloride. *Eur. J. Pharmacol.* **260**: 73-77.
- Pasantes-Morales H, Maar TE, Morán J (1993) Cell volume regulation in cultured cerebellar granule neurons. *J. Neurosci. Res.* **34**: 219-224.
- Pasantes-Morales H, Schousboe A (1988) Volume regulation in astrocytes: A role for taurine as an osmoeffector. *J. Neurosci. Res.* **20**: 505-509.
- Paternain AV, Morales M, Lerma J (1995) Selective antagonism of AMPA receptors unmasks kainate receptor-mediated responses in hippocampal neurons. *Neuron* **14**: 185-189.

- Phillips JM, Nicholson C (1979) Anion permeability in spreading depression investigated with ion-sensitive microelectrodes. *Brain Res.* **173**: 567-571.
- Pintor J, Miras-Portugal MT (1995) P<sub>2</sub>-purinergic receptors for diadenosine polyphosphates in the nervous system. *Gen. Pharmacol.* **26**: 229-235.
- Polischuk TM, Andrew RD (1996a) Imaging excitotoxic cell swelling and neuronal death in the hippocampal slice: confirmation with spectrometry and electrophysiology. *Soc. Neurosci. Abstr.* **22**: 804.
- Polischuk TM, Andrew RD (1996b) Real-time imaging of intrinsic optical signals during early excitotoxicity evoked by domoic acid in the rat hippocampal slice. *Can. J. Physiol. Pharmacol.* **74**: 712-722.
- Porter JT, McCarthy KD (1995) Adenosine receptors modulate [Ca<sup>2+</sup>]<sub>i</sub> in hippocampal astrocytes *in situ*. *J. Neurochem.* **65**: 1515-1523.
- Quandt FN, MacVicar BA (1986) Calcium-activated potassium channels in cultured astrocytes. *Neurosci.* **19**: 29-41.
- Quast U, Cook NS (1989) Moving together: K<sup>+</sup> channel openers and ATP-sensitive K<sup>+</sup> channels. *Trends Pharmacol. Sci.* **10**: 431-435.
- Ralevic V, Mathie RT, Alexander B, Burnstock G (1991) Characterization of P<sub>2X</sub>- and P<sub>2Y</sub>-purinoceptors in the rabbit hepatic arterial vasculature. *Br. J. Pharmacol.* **103**: 1108-1113.
- Ramadan NM, Halvorson H, Vande-Linde A, Levine SR, Helpert JA, Welch KMA (1989) Low brain magnesium in migraine. *Headache* **29**: 590-593.
- Reilly WM, Saville VL, Burnstock G (1987) An assessment of the antagonistic activity of reactive blue 2 at P<sub>1</sub>- and P<sub>2</sub>-purinoceptors: supporting evidence for purinergic innervation of the rabbit portal vein. *Eur. J. Pharmacol.* **140**: 47-53.
- Rice WR, Singleton FM (1989) Reactive blue 2 selectively inhibits P<sub>2Y</sub>-purinoceptor-stimulated surfactant phospholipid secretion from rat isolated alveolar type II cells. *Br. J. Pharmacol.* **97**: 158-162.
- Rosene DL, Van Hoesen GW (1987) The hippocampal formation of the primate brain. Cerebral Cortex. Eds. A. Peters and E.G. Jones. Plenum Press: New York.

- Rugolo M, Dolly JO, Nicholls DG (1986) The mechanism of action of  $\beta$ -bungarotoxin at the presynaptic plasma membrane. *Biochem. J.* **233**: 519-523.
- Salter MW, Hicks JL (1994) ATP-evoked increases in intracellular calcium in neurons and glia from the dorsal spinal cord. *J. Neurosci.* **14**: 1563-1575.
- Salter MW, Hicks JL (1995) ATP causes release of intracellular  $\text{Ca}^{2+}$  via the phospholipase  $\text{C}\beta/\text{IP}_3$  pathway in astrocytes from the dorsal spinal cord. *J. Neurosci.* **15**: 2961-2971.
- Salzberg BM, Obaid AL, Gainer H (1985) Large and rapid changes in light scattering accompany secretion by nerve terminals in the mammalian neurohypophysis. *J. Gen. Physiol.* **86**: 395-411.
- Sánchez-Prieto J, Sihra TS, Nicholls DG (1987) Characterization of excitotoxic release of glutamate from guinea-pig cerebral cortical synaptosomes. *J. Neurochem.* **49**: 58-64.
- Schwiebert EM, Egan ME, Hwang TH, Fulmer SB, Allen SS, Cutting GR, Guggino WB (1995) CFTR regulates outwardly rectifying chloride channels through an autocrine mechanism involving ATP. *Cell* **81**: 1063-1073.
- Séguéla P, Haghghi A, Soghomonian JJ, Cooper E (1996) A novel neuronal  $\text{P}_{2\text{x}}$  ATP receptor ion channel with widespread distribution in the brain. *J. Neurosci.* **16**: 448-455.
- Sheardown M (1993) The triggering of spreading depression in the chicken retina: a pharmacological study. *Brain Res.* **607**: 189-194.
- Silinsky EM, Gerzanich V (1993) On the excitatory effects of ATP and its role as a neurotransmitter in coeliac neurons of the guinea-pig. *J. Physiol.* **464**: 197-212.
- Silinsky EM, Hunt JM, Solsona CS, Hirsh JK (1990) Prejunctional adenosine and ATP receptors. *Ann. NY Acad. Sci.* **603**: 324-334.
- Skrede KK, Westgaard RH (1971) The transverse hippocampal slice: a well-defined cortical structure maintained *in vitro*. *Brain Res.* **35**: 589-593.
- Snow RW, Taylor CP, Dudek FE (1983) Electrophysiological and optical changes in slices of rat hippocampus during spreading depression. *J. Neurophysiol.* **50**: 561-572.

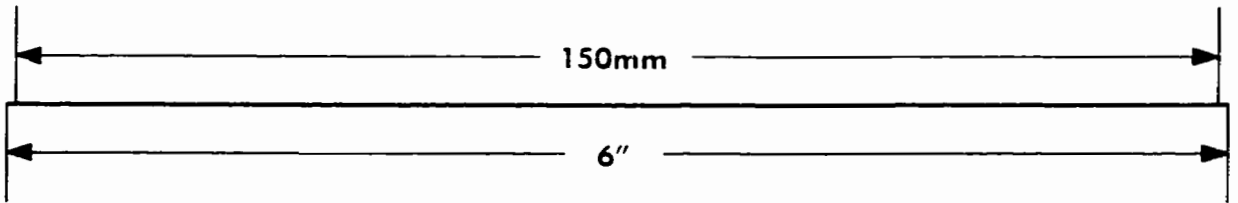
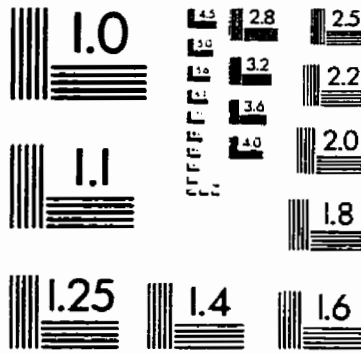
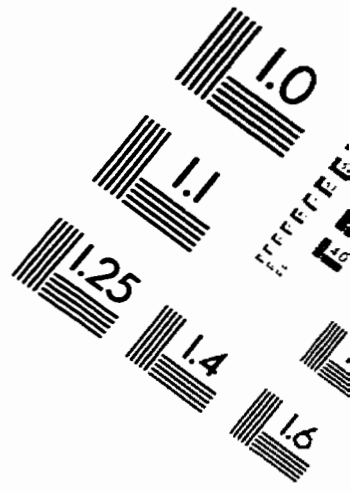
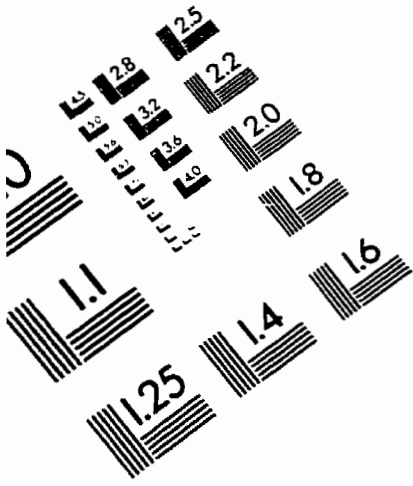
- Somjen GG, Aitken PG, Czéh GL, Herreras O, Jing J, Young JN (1992) Mechanisms of spreading depression: a review of recent findings and a hypothesis. *Can. J. Physiol. Pharmacol.* **70**: S248-54.
- Spruce AE, Standen NB, Standfield PR (1985) Voltage-dependent ATP-sensitive potassium channels of skeletal muscle membrane. *Nature* **316**: 736-738.
- Spruston N, Jonas P, Sakmann B (1995) Dendritic glutamate receptor channels in rat hippocampal CA3 and CA1 pyramidal neurons. *J. Neurophysiol.* **482**: 325-352.
- Stabel J, Arens J, Lambert JDC, Heinemann U (1990) Effects of lowering  $[Na^+]_o$  and  $[K^+]_o$  and of ouabain on quisqualate-induced ionic changes in area CA1 of rat hippocampal slices. *Neurosci. Lett.* **110**: 60-65.
- Stahl WL (1986) The Na, K-ATPase of nervous tissue. *Neurochem. Int.* **8**: 449-476.
- Stepnoski RA, La Porta A, Raccuia-Behling F, Blonder GE, Slusher RE, Kleinfeld D (1991) Noninvasive detection of changes in membrane potential in cultured neurons by light scattering. *Proc. Natl. Acad. Sci. USA* **88**: 9382-9386.
- Sugaya E, Takato M, Noda Y (1975) Neuronal and glial activity during spreading depression in cerebral cortex of cat. *J. Neurophysiol.* **38**: 822-841.
- Swann AC (1983) Brain (Na<sup>+</sup>-K<sup>+</sup>)-ATPase. Opposite effects of ethanol and dimethyl sulfoxide on temperature dependence of enzyme conformation and univalent cation binding. *J. Biol. Chem.* **258**: 11780-11786.
- Swann JW, Smith KL, Brady RJ (1986) Extracellular K<sup>+</sup> accumulation during penicillin-induced epileptogenesis in the CA3 region of immature rat hippocampus. *Dev. Brain Res.* **30**: 243-255.
- Swanson LW, Köhler C (1986) Anatomical evidence for direct projections from the entorhinal area to the entire cortical mantle in the rat. *J. Neurosci.* **6**: 3010-3023.
- Sweadner, KJ (1979) Two molecular forms of (Na<sup>+</sup>-K<sup>+</sup>)-stimulated ATPase in brain. Separation and difference in affinity for strophanthidin. *J. Biol. Chem.* **254**: 6060-6067.
- Sweeney MI, Yager JY, Walz W, Juurlink BHJ (1995) Cellular mechanisms involved in brain ischemia. *Can. J. Physiol. Pharmacol.* **73**: 1525-1535.

- Traynelis SF, Dingledine R (1988) Potassium-induced spontaneous electrographic seizures in the rat hippocampal slice. *J. Neurophysiol.* **59**: 259-276.
- Tremblay E, Zini S, Ben-Ari Y (1991) Autoradiographic study of the cellular localization of [<sup>3</sup>H]glibenclamide binding sites in the rat hippocampus. *Neurosci. Lett.* **127**: 21-24.
- Valera S, Hussy N, Evans RJ, Adami N, North RA, Surprenant A, Buell G (1994) A new class of ligand-gated ion channel defined by P<sub>2x</sub> receptor for extracellular ATP. *Nature* **371**: 516-519.
- Van Calker D, Muller M, Hamprecht B (1979) Adenosine regulates via two different types of receptors, the accumulation of cyclic AMP in cultured brain cells. *J. Neurochem.* **33**: 999-1005.
- Van Harreveld A (1958) Changes in the diameter of apical dendrites during spreading depression. *Am. J. Physiol.* **192**: 457-463.
- Van Harreveld A (1959) Compounds in brain extracts causing spreading depression of cerebral cortical activity and contraction of crustacean muscle. *J. Neurochem.* **3**: 300-315.
- Van Harreveld A (1978) Two mechanisms for spreading depression in the chicken retina. *J. Neurobiol.* **9**: 419-431.
- Van Harreveld A, Fifková E (1971) Glutamate release from the retina during spreading depression. *J. Neurobiol.* **2**: 13-29
- Van Harreveld A, Khattab FI (1967) Changes in cortical extracellular space during spreading depression investigated with the electron microscope. *J. Neurophysiol.* **30**: 911-929.
- Van Harreveld A, Kooiman M (1965) Amino acid release from the cerebral cortex during spreading depression and asphyxiation. *J. Neurochem.* **12**: 431-439.
- Van Harreveld A, Ochs S (1957) Electrical and vascular concomitants of spreading depression. *Am. J. Physiol.* **189**: 159-166.
- Voogd TE, Vansterkenburg ELM, Wilting J, Janssen LHM (1993) Recent research on the biological activity of suramin. *Pharmacol. Rev.* **45**: 177-203.

- Vyas S, Marchbanks RM (1981) The effect of ouabain on the release of [<sup>14</sup>C] acetylcholine and other substances from synaptosomes. *J. Neurochem.* **37**: 1467-1474.
- Walz W (1987) Swelling and potassium uptake in cultured astrocytes. *Can. J. Physiol. Pharmacol.* **65**: 1051-1057.
- Wang Y, Roman R, Lidofsky SD, Fitz JG (1996) Autocrine signalling through ATP release represents a novel mechanism for cell volume regulation. *Proc. Natl. Acad. Sci. USA* **93**: 12020-12025.
- Welford LA, Cusack NJ, Hourani SM (1987) The structure-activity relationships of ectonucleotidases and of excitatory P<sub>2</sub>-purinoceptors: evidence that dephosphorylation of ATP analogues reduces pharmacological potency. *Eur. J. Pharmacol.* **141**: 123-130.
- Westerink BH, Damsma G, De Vries JB (1989) Effect of ouabain applied by intrastriatal microdialysis on the *in vivo* release of dopamine, acetylcholine, and amino acids in the brain of conscious rats. *J. Neurochem.* **52**:705-712.
- White HS, Chow SY, Yen-Chow YC, Woodbury DM (1992) Effect of elevated potassium on the ion content of mouse astrocytes and neurons. *Can. J. Physiol. Pharmacol.* **70**: S263-268.
- Wieraszko A (1995) Facilitation of hippocampal potentials by suramin. *J. Neurochem.* **64**: 1097-1101.
- Wieraszko A, Ehrlich YH (1994) On the role of extracellular ATP in the induction of long-term potentiation in the hippocampus. *J. Neurochem.* **63**: 1731-1738.
- Wieraszko A, Goldsmith G, Seyfried TN (1989) Stimulation-dependent release of adenosine triphosphate from hippocampal slices. *Brain Res.* **485**: 244-250.
- Wilding TJ, Huettner JE (1995) Differential antagonism of  $\alpha$ -amino-3-hydroxy-5-methyl-4-isoxazolepropionic acid-preferring and kainate-preferring receptors by 2,3-benzodiazepines. *Mol. Pharmacol.* **47**: 582-587.
- Wilding TJ, Huettner JE (1997) Activation and desensitization of hippocampal kainate receptors. *J. Neurosci.* **17**: 2713-2721.
- Williams M (1987) Purine receptors in mammalian tissues: pharmacology and functional significance. *Ann. Rev. Pharmacol. Toxicol.* **27**: 315-345.

- Wilson ED, Wormall A (1950) Studies on suramin 9. The action of the drug on some enzymes. *Biochem. J.* **47**: 158-170.
- Wong EH, Knight AR, Woodruff GN (1988) [<sup>3</sup>H]MK-801 labels a site on the N-methyl-D-aspartate receptor channel complex in rat brain membranes. *J. Neurochem.* **50**: 274-281.
- Yamamoto C, McIlwain H (1966) Potentials evoked *in vitro* in preparations from the mammalian brain. *Nature* **210**:1055-56.
- Yoda A, Yoda S (1982) Interaction between ouabain and the phosphorylated intermediate of Na, K-ATPase. *Mol. Pharmacol.* **22**: 700-705.
- Young AB, Fagg GE (1990) Excitatory amino acid receptors in the brain: membrane binding and receptor autoradiographic approaches. *Trends Pharmacol. Sci.* **11**: 126-133.
- Zhang YX, Yamashita H, Ohshita T, Sawamoto N, Nakamura S (1995) ATP increases extracellular dopamine levels through stimulation of P<sub>2y</sub> purinoceptors in the rat striatum. *Brain Res.* **691**: 205-212.
- Zhou QY, Li C, Olah ME, Johnson RA, Stiles GL, Civelli O (1992) Molecular cloning and characterization of an adenosine receptor: the A<sub>3</sub> adenosine receptor. *Proc. Natl. Acad. Sci. USA* **89**: 7432-7436.
- Ziganshin AU, Ziganshina LE, King BF, Pintor J, Burnstock G (1996) Effects of P<sub>2</sub>-purinoceptor antagonists on degradation of adenine nucleotides by ectonucleotidases in folliculated oocytes of *Xenopus laevis*. *Biochem. Pharmacol.* **51**: 897-901.
- Zimmermann H (1994) Signalling via ATP in the nervous system. *Trends Neurosci.* **17**: 420-426.
- Zini S, Tremblay E, Pollard H, Moreau J, Ben-Ari Y (1993) Regional distribution of sulfonyleurea receptors in the brain of rodent and primate. *Neurosci.* **55**: 1085-1091.

# IMAGE EVALUATION TEST TARGET (QA-3)



**APPLIED IMAGE, Inc**  
1653 East Main Street  
Rochester, NY 14609 USA  
Phone: 716/482-0300  
Fax: 716/288-5989

© 1993, Applied Image, Inc.. All Rights Reserved

